MEDITVETJ

MAKÜ DECEMBER 2024 VOLUME 9 ISSUE 3

MEDITERRANEAN
VETERINARY JOURNAL

e - ISSN: 3023-8447

Mediterranean Veterinary Journal
Volume: 09 . *Number:* 03 . 2024
Published tri-annual
Former name
Veterinary Journal of Mehmet Akif Ersoy University

Publisher
On behalf of Budur Mehmet Akif Ersoy University
Faculty of Veterinary Medicine
Prof. Dr. Hüseyin DALGAR
Rector

Address
Burdur Mehmet Akif Ersoy University
Faculty of Veterinary Medicine
Degirmenler, 15030, BURDUR

'This Journal is indexed and abstracted by TUBİTAK-ULAKBİM TR-Dizin, Zoological Record, EBSCO, CAB Abstract, CiteFactor, Google Scholar, Science Library Index, International Institute of Organized Research, Researchbib, SciLit, SJIFactor, COSMOS IF and SOBIAD.'

E-mail: meditvetj@mehmetakif.edu.tr

Web Adress: https://dergipark.org.tr/en/pub/meditvetj

Online Submission

https://dergipark.org.tr/en/journal/4407/submission/step/manuscript/new

The iThenticate/Turnitin plagiarism analysis program is used to check submitted articles for originality before they are accepted for publication.

The reviewers of MEDIVETJ, 2024, 9 (3)*

Ahmed Ibrar, Veterinary and Animal Sciences University, College of Veterinary and Animal Sciences, Department of Animal Nutrition, Punjab, Pakistan

Akçakavak Gökhan, Aksaray University, Faculty of Veterinary Medicine, Department of Pathology, Aksaray, Türkiye

Bozukluhan Kadir, Kafkas University, Ataturk Vocational School, Kars, Türkiye

Dikici Abdullah, Uşak University, Faculty of Engineering, Department of Food Engineering, Uşak, Türkiye

Filikci Kürşat, Harran University, Faculty of Veterinary Medicine, Department of Pathology, Şanlıurfa, Türkiye

Kabak Murat, Ondokuz Mayıs University, Faculty of Veterinary Medicine, Department of Anatomy, Samsun, Türkiye

Kabu Mustafa, Afyon Kocatepe University, Faculty of Veterinary Medicine, Department of Biochemistry, Afyonkarahisar, Türkiye Kanat Özgür, Necmettin Erbakan University, Faculty of Veterinary Medicine, Department of Pathology, Konya, Türkiye

Kök Filiz, Aydın Adnan Menderes University, Faculty of Veterinary Medicine, Department of Department of Food Hygiene and Technology, Aydın, Türkiye

Kutlu Tuncer, Hatay Mustafa Kemal University, Faculty of Veterinary Medicine, Department of Pathology, Hatay, Türkiye

Küçükaslan Özgül, Dicle University, Faculty of Veterinary Medicine, Department of Veterinary Medicine History and Deontology, Diyarbakır, Türkiye

Monsef Yanad Abou, School of National Veterinary, Department of Anatomic Pathology, Toulouse, France

Rahman Abdur, Veterinary and Animal Sciences University, College of Veterinary and Animal Sciences, Department of Animal Nutrition, Punjab, Pakistan

Raza Sanan, Veterinary and Animal Sciences University, Department of Animal Reproduction, Pakistan

Sefergil Şamil, Muğla Sıtkı Koçman University, Faculty of Veterinary Medicine, Department of Anatomy, Muğla, Türkiye

Yılmaz Emre, Ataturk University, Faculty of Veterinary Medicine, Department of Animal Feeding and Nutrition Diseases, Erzurum, Türkiye

Yiğit Ali, Kafkas University, Faculty of Veterinary Medicine, Department of Surgery, Kars, Türkiye

Yücel Tenekeci Gözde, Ankara University, Faculty of Veterinary Medicine, Department of Pathology, Ankara, Türkiye

** Volume 9, Issue 3 of 2024 has an alphabetical list of the editorial board and reviewers.*

CONTENTS

Research Articles

Medit Vet J, 9(3): 337-344, 2024
DOI: 10.24880/meditvetj.1611142

Research Article

The effect of potassium sorbate on the survival of *Brucella melitensis* during ripening of Tulum cheese

Ahmet Hulusi Dinçoğlu[1], Bahri Patır[2]

[1]Department of Nutrition and Dietetics, Faculty of Health Sciences, Burdur Mehmet Akif Ersoy University, Burdur, Türkiye
[2]Department of Food Hygiene and Technology, Faculty of Veterinary Medicine, Bingöl University, Bingöl, Türkiye

Key Words:
Brucella melitensis
chemical quality
microbiological quality
potassium sorbate
tulum cheese

Received. : 13 February 2024
Revised. : 15 October2024
Accepted : 21 October 2024
Published : 31 December2024
Article Code : 1611142

Correspondence:
AH. DİNÇOĞLU
(adincoglu@mehmetakif.edu.tr)

ORCID
AH. DİNÇOĞLU : 0000-0002-9669-5964
B. PATIR : 0000-0001-5933-9971

The abstract of this study was presented as a poster presentation at the 12th World Congress on Public Health. İstanbul, Türkiye, April 27-May 1, 2009

ABSTRACT

The objective of this study was to evaluate the antimicrobial effect of potassium sorbate on the viability of *Brucella melitensis* in Tulum cheese, as well as the resulting microbiological and physicochemical changes during ripening. Five groups were formed, with group A serving as the control and group B inoculated with *B. melitensis*. Groups C, D, and E were also inoculated with *B. melitensis* and treated with potassium sorbate at concentrations of 0.05%, 0.10%, and 0.20%, respectively. During the ripening process, the total number of mesophilic aerobic bacteria, fecal streptococci, staphylococci-micrococci, coliforms, and yeasts and molds in the samples varied depending on the amount and presence of sorbate. The presence of potassium sorbate affected *B. melitensis* at different rates during ripening. The level of *B. melitensis* was found to be higher in group B compared to groups C, D, and E. There were no significant differences in the acidity of the treatment groups. During ripening, the pH values of the samples with sorbate were lower than those without sorbate. No significant differences in salt amounts and moisture levels were observed between the groups with sorbate and those without sorbate. The addition of definite concentrations of potassium sorbate to the formulation of Tulum cheese revealed a shortened lifespan of *B. melitensis* and a significant reduction in the number of other harmful microorganisms. This suggests that the use of sorbate in Tulum cheese manufacturing has the potential to improve microbial safety in this type of product.

INTRODUCTION

Brucellosis is a zoonotic disease that was clinically defined by Morston in 1859 and has been known since ancient times. It remains the most common zoonotic disease worldwide, with over 500,000 new cases reported annually, despite its low mortality rate. Brucellosis is associated with significant permanent disability and is a major cause of travel-related morbidity (Pappas et al., 2006). Brucella has been reported as a possible type B biological weapon (Shakir, 2020).

Eleven species of the *Brucella* genus have been identified to date. However, only *B. abortus*, *B. melitensis*, *B. suis*, and *B. canis* affect humans (Seleem et al., 2010; Shakir, 2020). Brucellosis remains a neglected disease in many developing countries. Based on data published between 1983 and 2019, it has been reported that the prevalence of brucellosis is high in Kosovo, Kuwait, Qatar, Venezuela, Syria, and Iraq (Franc et al., 2018). In endemic areas, humans can contract brucellosis by coming into contact with infected animals or consuming dairy products, particularly unpasteurized cheeses made from ewe and goat milk (Seleem et al., 2010). *Brucella melitensis* infections are more common in the general population than other *Brucella* species, while *B. abortus* and *B. suis* infections typically affect occupational groups. In some countries, including Italy, 99% of human brucellosis was caused by *B. melitensis* (De Massis et al., 2005).

According to the report, *B. melitensis* (29.48%) is the most prevalent *Brucella* species found in dairy products. This is attributed to the unregulated raising and transportation of numerous ewe and goat herds, as well as the production of milk and dairy products without processing in small-scale goat and ewe farms (Capparelli et al., 2009). Research results show that in regions where the disease is endemic, raw milk has a higher level of *Brucella* contamination (16.97%) compared to cheese (7.1%). This is due to the role of fermenting bacteria in reducing the growth of *Brucella* species in cheese, as well as ambient pH and nutrient competition (De Massis et al., 2005; Dadar et al., 2020).

Tulum cheese is a traditional cheese made from raw ewe milk in Turkey. It can also be made from goat's milk, a combination of ewe and goat's milk, or cow's milk. The cheese has a granular or open texture, is semi-hard, and is white or cream-colored with a sharp aroma (Tekin and Güler, 2019). Microorganisms, particularly yeasts present in the milk and ripening medium, play a crucial role in the ripening process of cheese. Tulum cheese is produced locally from raw milk without the use of a starter culture, which means that its mi-

To cite this article:
Dinçoğlu AH, Patır B. The effect of potassium sorbate on the survival of *Brucella melitensis* during ripening of Tulum cheese. Medit Vet J. 2024; 9(3): 337-344.

crobial content is solely derived from the natural microbiota of raw milk (Tomar et al., 2020). This poses a potential public health risk to individuals who consume Tulum cheese made from raw milk. Studies have reported different levels of bacterial isolation in commercially available Tulum cheeses when testing for the presence of *Brucella* species (Patır and Dinçoğlu, 2001). According to Öztürk and Nazlı's (1996) report, the number of bacteria in Tulum cheese produced with cow and ewe milk inoculated with *B. melitensis* was $1.5x10^9$ and $2.0x10^9$ cfu/g at the beginning of ripening. However, on the 20th day of ripening, the number of bacteria decreased significantly to $1x10^2$ and $2.8x10^2$ cfu/g, and bacteria could not be isolated in the subsequent days.

As a result of studies examining the effects of many antibacterial components against *Brucella* spp., both in vivo and in vitro, have obtained results at different levels (Ijaz et al., 2021). Many antimicrobial additives are used alone or in combination in foods, including sorbic acid and its salts as a preservative. Potassium sorbate is an antimicrobial compound widely used in the food industry since the mid-1950s. It is a salt of sorbic acid and has many advantages over other preservatives. Potassium sorbate is considered a substance 'generally recognized as safe' (GRAS) and its usage should not exceed 0.2%. (Alzate et al., 2017; Palou et al., 2016). As per the United States Code of Federal Regulations, specifically Title 21 and Section 182.3640, potassium sorbate is a recommended general-purpose preservative when used by good manufacturing practices (Lungu and Johnson, 2005). Sorbic acid and its salts are primarily used in the milk and dairy industry and are commonly employed in cheese production. Although antifungal effects are primarily used in dairy products, research has also been conducted on their inhibitory effects against pathogens in various foods (Mohammadzadeh-Aghdash et al., 2018).

This study investigates the survival of *B. melitensis* and the microbiological and physicochemical changes in Tulum cheeses produced from raw ewe milk by adding *B. melitensis* and potassium sorbate at different concentrations during the ripening process.

MATERIALS and METHODS

Milk samples

Tulum cheese was produced using commercially obtained ewe milk samples. The milk was collected in the early morning and transported to the laboratory under cold chain conditions. Two hundred milliliters of the milk were analyzed for microbiological and physicochemical properties as well as antibiotic residues and kept at 4°C.

B. melitensis strain used in inoculation

The study utilized the B. melitensis biotype 3 strain, which was previously isolated and identified by Patır and Dinçoğlu (2001) from Tulum cheese sold in Elazığ. Before inoculation, the strain was incubated in Mueller-Hinton Broth (MHB, Merck) at 37°C for 22 hours. The final inoculum contained 10^5 CFU/ml of bacteria.

Preparation of experimental Tulum cheese samples

Raw ewe milk, free of antibiotics and inhibitory substances, was divided into five groups (A-E) as shown in Table 1. Group A served as the control, while the other groups (B-E) were inoculated with fresh *B. melitensis* strain. The milk was heated to 32°C and rennet at the strength of 1/6000 was added to coagulate the milk within approximately 90 min. The coagulum was cut into pieces 4 cm × 4 cm × 4 cm cubes and the curd pieces were transferred into cotton bags for whey drainage and then pressed for 24 hours using metal weights (first press). After the first press, the curd was broken into pea-size pieces by hand and potassium sorbate at the concentrations indicated in Table 1 and 2% (w/w) salt was added, mixed, and transferred into the bags for the second press (24 h). At the end of the period, the steps of the previous press were repeated for the final press, except for the addition of potassium sorbate. Following the third press, the curds were broken into small pieces and air-dried for 24 hours at ambient temperature. Subsequently, the plastic containers were tightly filled with curd using a wooden stick, and the packaged samples were ripened at 4 ± 1°C for 90 days (Tekinşen et al., 2002). The study was conducted in four replicates.

Table 1. Presence of *B. melitensis* and potassium sorbate concentrations in Tulum cheese samples.

Groups	*B. melitensis*	Potassium sorbate (%)
A	-	-
B	+	-
C	+	0.05
D	+	0.10
E	+	0.20

Microbiological analyses

Isolation and identification of Brucella spp. from Tulum cheese samples

Each cheese sample (10 g) was homogenized with a Stomacher in 90 ml of Brucella broth (Himedia, M348). Then, a 0.1 ml aliquot of each homogenate was inoculated in duplicate using the spread plating technique onto the Brucella Medium Base (Oxoid CM169) with 5% inactivated horse serum (Oxoid SR35), 10 g/l glucose (Merck 1.08346.1000), and 1 vial/500 ml of Brucella selective supplement (Oxoid SR83). The first set of plates was incubated aerobically, while the second set was incubated in 10% CO^2 for 5 days at 37°C. Petri dishes without colony formation were incubated until the 10th day (Alton et al., 1988).

Identification of *Brucella* species was performed together with colonial morphology, Gram staining properties, and biochemical tests including H_2S formation, urease, and catalase activities, CO_2 requirement, growth in thionine and basic fuchsine, and serological screening, and Brucella phage test.

Detection of other microorganism groups

Samples of 10 g were taken aseptically from the Tulum cheese. A sterilized ringer solution with a dilution of 1:9 (w/v)

was added, and the samples were homogenized for 3 minutes in a stomacher. Bacterial counts were determined by plating serial decimal dilutions.

Plate count agar (PCA-Oxoid CM0325B) was used to determine total mesophilic aerobic microorganisms after incubation at 30±1°C for 72 h (ISO, 2003). The detection of coliform bacteria was performed using Violet Red Bile Agar (VRBA-Oxoid CM0968) and incubated for 24 hours at 30±1°C (ISO, 2006). Fecal streptococci were grown on Barnes' Thallous Acetate Tetrazolium Glucose Agar (TTTA) and incubated for 48 hours at 45±1°C (Barnes, 1959). *Staphylococcus-Micrococcus* were enumerated by plating on Mannitol Salt Agar (MSA-Difco) at 37°C for 48 hours (ISO, 2015). Yeast and molds were quantified on Potato Dextrose Agar (PDA) using the surface plate method. The samples were incubated at 22±1°C for 5-7 days, following ISO (2008) guidelines. All determinations were performed in duplicate and expressed as $\log_{10}$ cfu/g.

Physicochemical analyses

Analysis of milk samples

The milk samples' pH was measured using a digital pH meter (EDT, GP353). The titratable acidity was determined by the titration method and the results were expressed as % lactic acid. The fat content in the samples was determined by the Gerber method (AOAC, 1984). In the determination of antibiotic residues in milk, 50 ml of milk was pasteurized and cooled to 42°C. At this temperature, 3% of the yogurt culture was added to the milk and incubated for one hour. The acidity level was measured every 15 minutes, and changes in acidity were monitored. Decisions were made based on the recorded values (APHA, 2004).

Analysis of cheese samples

The samples were analyzed for pH, acidity, and dry matter content following AOAC (2019) guidelines. The salt content of the cheese was determined using the Mohr method (ISO, 2007).

Statistical Analysis

All analyses were conducted in quadruplicate. The effect of potassium sorbate and time on the microbiological and physicochemical profile of the Tulum cheeses during ripening was determined using analysis of variance (ANOVA), followed by the Tukey test. The results were expressed as mean±standard deviation (SD). Statistical analysis was performed using SPSS version 17.0 (SPSS Inc., Chicago, IL, USA). Significant differences were compared using the Mann-Whitney U test at a significance level of $P<0.05$.

RESULTS

Microbiological and chemical properties of raw milk used in making cheese samples

Total mesophilic aerobic bacteria, fecal streptococci, *Staphylococcus-Micrococcus*, coliforms, and yeast and mold counts of raw milk used in production were determined as 8.33, 5.97, 5.57, 7.08, and 7.75 log cfu/ml, respectively. *Brucella* was not detected in any of the milk samples. The acidity, pH, fat content, and dry matter content of the raw milk used in making experimental Tulum cheese were found to be 0.20, 6.48, 7.00%, and 17.51%, respectively.

Changes in Tulum Cheese during ripening

Microbiological changes

Table 2 presents the microbiological changes that occur during ripening. The total mesophilic aerobic bacteria count in Tulum cheese samples was highest at the beginning of ripening and tended to decrease over time. Throughout the ripening period, groups C, D, and E, which contained varying amounts of potassium sorbate, had lower TMAB counts than groups A and B, which did not contain potassium sorbate. As the concentration of potassium sorbate increased to the highest level (0.20%), the TMAB counts decreased, and a statistical difference was observed between the A and B groups during the period up to the 60th day of ripening ($P<0.05$).

Throughout the ripening process, fecal streptococci counts were consistently lower in the groups that contained potassium sorbate compared to those that did not. By the end of maturation, groups C, D, and E showed no presence of bacteria. The decrease in bacterial presence observed during ripening was highly significant between the first and last days of ripening ($P<0.05$).

The *Staphylococcus-Micrococcus* counts were determined on the first and last days of ripening in all groups, with the highest and lowest counts recorded ($P<0.05$). The number of bacteria decreased steadily in all samples until the end of ripening, except for a small increase on the 15th day in group A. Throughout the ripening process, the samples with sorbate had lower *Staphylococcus-Micrococcus* counts compared to those without sorbate, with counts below <10 $\log_{10}$ cfu/g on the 90th day.

The count of coliforms generally decreased during ripening, with the most significant change observed in groups D and E. Tulum cheeses with sorbate had lower bacteria counts during ripening compared to those without sorbate ($P<0.05$). Bacteria were not isolated from groups D and E after the 45th day, and from group C after the 60th day.

Cheeses containing sorbate exhibited lower yeast and mold counts, as demonstrated in Table 2 ($P<0.05$). The number of yeast and mold decreased during ripening in groups with sorbate. Similar to coliforms, and yeast and mold were not detected in the analyses after the 45th day in groups D and E and the 60th day in group C.

Changes in the survival of Brucella melitensis

Table 3 shows the mean levels of *B. melitensis* detected in the experimental Tulum cheese samples as $\log_{10}$ cfu/g. The samples in group B, which did not contain potassium sorbate, had the highest number of *B. melitensis* at the beginning of ripening. The counts of *B. melitensis* in this group remained constant until the 15th day, after which they rapidly decreased and reached their lowest level ($P<0.05$) by the 30th day. By the 45th day of ripening, *B. melitensis* could not be isolated. In contrast, the

Table 2. Microbiological changes observed in Tulum cheese samples during ripening (log10 cfu/g).

Groups	Ripening period (day)					
	0	15	30	45	60	90
TMAB						
A	7.08±0.09^{Aa}	6.45±0.07^{ABb}	6.40±0.09^{Ab}	5.94±0.07^{Ac}	6.00±0.06^{Ac}	5.72±0.06^{Bd}
B	6.67±0.08^{Ba}	6.48±0.09^{Aab}	6.34±0.08^{Ab}	6.04±0.08^{Ac}	5.93±0.04^{ABc}	5.92±0.05^{Ac}
C	6.45±0.08^{Ca}	5.95±0.08^{Db}	5.95±0.08^{Bb}	5.56±0.07^{Bc}	5.83±0.09^{ABCb}	5.52±0.05^{Cc}
D	6.26±0.06^{Ca}	6.26±0.07^{BCa}	6.23±0.07^{Aa}	5.580.08^{Bc}	5.79±0.07^{BCb}	5.51±0.07^{Cc}
E	6.20±0.07^{Da}	6.11±0.09^{CDa}	5.69±0.95^{Cb}	5.26±0.06^{Cc}	5.69±0.04^{Cb}	5.59±0.09^{BCb}
Fecal streptococci						
A	4.63±0.08^{Aa}	4.34±0.07^{Ab}	3.76±0.08^{Bc}	3.81±0.09^{Ac}	3.76±0.07^{Ac}	1.23±0.08^{Ad}
B	4.58±0.04^{Aa}	4.28±0.07^{Ab}	3.96±0.08^{Ac}	3.88±0.05^{Ac}	3.89±0.09^{Ac}	1.08±0.06^{Bd}
C	4.26±0.04^{Ba}	3.76±0.09^{Bb}	3.63±0.04^{Bb}	3.30±0.06^{Bc}	3.26±0.06^{Bc}	0
D	4.08±0.09^{Ca}	3.64±0.07^{Bb}	3.36±0.08^{Ccd}	3.42±0.09^{Bc}	3.20±0.05^{Bd}	0
E	4.23±0.05^{BCa}	3.23±0.09^{Cb}	3.30±0.08^{Cb}	3.20±0.07^{Cb}	3.18±0.06^{Bb}	0
Staphylococcus-Micrococcus						
A	4.69±0.05^{BCa}	4.81±0.05^{Aa}	4.34±0.05^{Ab}	4.26±0.07^{Ab}	3.17±00.8^{Bc}	0.85±0.07^{Bd}
B	4.91±0.09^{Aa}	4.54±0.09^{Bb}	4.48±0.07^{Ab}	4.23±0.08^{Ac}	3.49±0.05^{Ad}	1.15±0.08^{Ae}
C	4.32±0.08^{Da}	3.93±0.07^{Db}	3.71±0.04^{Bc}	3.26±0.06^{Bd}	2.45±0.09^{Ce}	0
D	4.84±0.07^{ABa}	4.20±0.08^{Cb}	3.54±0.09^{Cc}	3.11±0.04^{Bd}	1.36±0.07^{De}	0
E	4.56±0.06^{Ca}	4.40±0.09^{BCa}	3.40±0.04^{Cb}	3.11±0.07^{Bc}	2.49±0.08^{Cd}	0
Coliform						
A	5.23±0.04^{Aa}	4.75±0.07^{Ab}	4.76±0.04^{Ab}	3.23±0.08^{Bc}	3.00±0.04^{Bd}	0.78±0.08^{Ae}
B	5.32±0.07^{Aa}	4.88±0.08^{Ab}	4.83±0.09^{Ab}	3.74±0.06^{Ac}	3.65±0.08^{Ac}	0.60±0.07^{Bd}
C	4.40±0.06^{Da}	4.08±0.09^{Bb}	3.32±0.08^{Bc}	2.23±0.06^{Cd}	0.48±0.06^{Ce}	0
D	5.04±0.06^{Ba}	4.15±0.06^{Bb}	2.98±0.06^{Cc}	1.23±0.04^{Ed}	0	0
E	4.61±0.05^{Ca}	4.00±0.09^{Bb}	2.99±0.07^{Cc}	1.43±0.08^{Dd}	0	0
Yeast and molds						
A	6.62±0.10^{Aa}	6.81±0.08^{Aa}	5.72±0.06^{Ab}	5.89±0.05^{Bb}	4.08±0.06^{Bc}	3.72±0.08^{Bd}
B	6.32±0.07^{Ba}	5.96±0.09^{Bb}	5.85±0.08^{Ab}	6.43±0.09^{Aa}	4.53±0.07^{Ac}	4.30±0.09^{Ad}
C	4.97±0.09^{Ca}	4.83±0.09^{Ca}	3.66±0.08^{Bb}	1.43±0.05^{Cc}	0.70±0.07^{Cd}	0
D	4.79±0.08^{Ca}	4.26±0.09^{Db}	2.52±0.08^{Cc}	1.23±0.06^{Dd}	0	0
E	4.82±0.07^{Ca}	4.78±0.04^{Ca}	2.70±0.07^{Cb}	1.04±0.09^{Ec}	0	0

Values are expressed as means ± standard deviation (SD)
A-F: Values with different superscripts in the same column are significantly different (P<0.05)
a-g: Values with different superscripts in the same line are significantly different (P<0.05)

samples in group C, which contained 0.05% sorbate, exhibited a significant decrease (P<0.05) in *B. melitensis* counts compared to group B on the 15th and 30th days. The bacteria were undetectable in subsequent analyses. The counts of bacteria in groups D and E, which contained 0.10% and 0.20% sorbate, respectively, showed a statistically insignificant decrease on the 15th day (P>0.05). *B. melitensis* was not detected in the E group samples on the 30th day or the D group samples on the 45th day (P<0.05). Figure 1 shows that the bacterial counts were similar among all groups at the beginning of ripening and significantly decreased in the following days. After the 15th day of ripening, all groups containing potassium sorbate showed a statistically significant decrease compared to group B without sorbate (P<0.05).

Physicochemical changes

Table 4 presents the physicochemical changes that occur in Tulum cheeses during ripening. Throughout the ripening process, acidity levels increased in all groups, reaching their peak on the 90th day. Groups A and B, which had the lowest acidity values at the beginning of storage, maintained the same characteristics until the end. The highest acidity value was observed in group E, with 1.52% on the first day, while groups C and D reached 1.83% on the 90th day. There were no statisti-

Table 3. *B. melitensis* counts during ripening of Tulum cheese samples (log10 cfu/g)

Groups	Ripening period (day)		
	0	15	30
B	3.76±0.15^{Aa}	3.75±0.05^{Aa}	1.58±0.06^{Ab}
C	3.54±0.54^{ABa}	3.57±0.06^{Ba}	0.70±0.04^{Bb}
D	2.62±0.10^{Ba}	2.58±0.06^{Ca}	0.30±0.07^{Cb}
E	2.61±0.08^{Ba}	2.59±0.05^{Ca}	0.00±0.01^{Db}

Values are expressed as means ± standard deviation (SD)
A-F: Values with different superscripts in the same column are significantly different (P<0.05)
a-g: Values with different superscripts in the same line are significantly different (P<0.05)

Table 4. Physicochemical changes observed in Tulum cheese samples during ripening.

Groups	Ripening period (day)					
	0	15	30	45	60	90
Acidity (%la)						
A	1.47±0.09^{Ac}	1.52±0.06^{ABbc}	1.61±0.07^{Aabc}	1.68±0.07^{Aab}	1.73±0.06^{Aa}	1.77±0.01^{Aa}
B	1.41±0.08^{Ad}	1.48±0.08^{Bcd}	1.55±0.08^{Abcd}	1.62±0.05^{Aabc}	1.73±0.09^{Aab}	1.75±0.01^{Aa}
C	1.42±0.04^{Ac}	1.58±0.06^{ABb}	1.57±0.08^{Ab}	1.62±0.06^{Ab}	1.80±0.05^{Aa}	1.83±0.01^{Aa}
D	1.47±0.08^{Ac}	1.65±0.04^{Ab}	1.65±0.08^{Ab}	1.65±0.07^{Ab}	1.72±0.06^{Aab}	1.83±0.01^{Aa}
E	1.52±0.08^{Ab}	1.57±0.08^{ABb}	1.61±0.06^{Ab}	1.61±0.08^{Ab}	1.80±0.08^{Aa}	1.80±0.01^{Aa}
pH						
A	4.94±0.06^{Aa}	4.89±0.05^{Aa}	4.62±0.05^{Ab}	4.47±0.06^{Ab}	4.58±0.07^{Ab}	4.54±0.07^{Ab}
B	4.64±0.09^{Ba}	4.64±0.09^{Ba}	4.55±0.06^{Aab}	4.47±0.06^{Aab}	4.42±0.05^{ABc}	4.43±0.08^{Ac}
C	4.76±0.08^{ABa}	4.62±0.07^{Bab}	4.55±0.04^{Abc}	4.44±0.05^{Abcd}	4.35±0.09^{Bd}	4.38±0.08^{Acd}
D	4.66±0.06^{Ba}	4.50±0.07^{Babc}	4.52±0.08^{Aab}	4.38±0.04^{Abc}	4.33±0.06^{Bd}	4.37±0.07^{Acd}
E	4.63±0.06^{Ba}	4.60±0.09^{Bab}	4.54±0.04^{Aabc}	4.43±0.07^{Abc}	4.44±0.08^{ABbc}	4.40±0.08^{Ac}
Salt (%)						
A	5.67±0.08^{Be}	5.77±0.04^{Bde}	5.90±0.07^{Bcd}	6.03±0.07^{Cc}	6.25±0.09^{Bb}	6.61±0.06^{Ba}
B	5.73±0.04^{ABc}	5.86±0.07^{ABc}	6.11±0.08^{Ab}	6.04±0.06^{Cb}	6.63±0.09^{Aa}	6.64±0.07^{Ba}
C	5.88±0.08^{Ab}	5.96±0.08^{Ab}	6.26±0.04^{Aa}	6.27±0.08^{ABa}	6.29±0.08^{Ba}	6.44±0.07^{Ca}
D	5.67±0.06^{Bf}	5.82±0.08^{ABe}	6.17±0.06^{Ad}	6.37±0.06^{Ac}	6.77±0.05^{Ab}	6.93±0.04^{Aa}
E	5.61±0.06^{Bc}	5.70±0.09^{Bc}	6.12±0.08^{Ab}	6.12±0.07^{BCb}	6.30±0.06^{Ba}	6.44±0.04^{Ca}
Moisture (%)						
A	32.66±0.08^{Da}	32.54±0.04^{Da}	31.15±0.09^{Cb}	29.56±0.07^{Dc}	29.02±0.08^{Dd}	28.75±0.08^{Ce}
B	33.39±0.08^{Ca}	33.16±0.07^{Bb}	32.07±0.06^{Bc}	31.33±0.10^{Bd}	30.65±0.08^{Be}	30.30±0.06^{Bf}
C	34.56±0.04^{Ba}	32.85±0.07^{Cb}	32.19±0.08^{Dc}	30.88±0.08^{Cd}	30.41±0.06^{Ce}	30.23±0.08^{Be}
D	31.20±0.04^{Ea}	30.55±0.08^{Eb}	28.91±0.07^{Dc}	28.09±0.08^{Ed}	27.04±0.07^{Ee}	26.82±0.08^{Df}
E	36.61±0.09^{Aa}	35.24±0.08^{Ab}	33.86±0.04^{Ac}	32.64±0.08^{Ad}	32.28±0.05^{Ae}	32.26±0.09^{Ae}

Values are expressed as means ± standard deviation (SD)
A-F: Values with different superscripts in the same column are significantly different (P<0.05)
a-g: Values with different superscripts in the same line are significantly different (P<0.05)

cally significant differences between the groups, except for the values of groups B and D on the 15th day of ripening (P<0.05).

The pH values of Tulum cheese samples were highest at the beginning of ripening and lowest at the 60th day in groups B, C, and D, and at the 90th day in group E. After a decrease in all groups until the 45th day of ripening, these values generally continued to decrease, except for an increase in group A. However, no major changes occurred. The pH values in groups A and B without potassium sorbate were higher on the first day of ripening than in groups with sorbate. The ripening process showed statistically significant differences between the first and last-day values in all groups (P<0.05). The addition of sorbate resulted in no differences between the groups on

any day of maturation (P>0.05). Differences were observed between groups A and B, D and E on day 0, between group A and all other groups on day 15, and between group A and groups C, D, and E on day 60 (P<0.05), depending on whether the samples contained sorbate.

In all groups, the lowest and highest salt values were determined on the 0th and 90th days of ripening, respectively (P<0.05). Table 4 shows that the salt values detected in the cheese samples varied between the groups with and without sorbate on different days, but the addition of sorbate did not result in a significant difference overall. At the end of the ripening process, group C had the highest initial salt content and group E had the lowest, but their values had reversed, with group D having the highest salt content.

Regarding moisture content, all groups decreased almost in parallel during ripening. The highest and lowest moisture contents were recorded on the first and last days of ripening, respectively (P<0.05). Group E samples showed the highest values during ripening (P<0.05), while group D samples showed the lowest values (P<0.05). Moisture values decreased continuously during ripening in all groups.

DISCUSSION

In this study, the survival of *Brucella melitensis* and the microbiological and physicochemical changes in the product during ripening of Tulum cheese produced by adding different concentrations of potassium sorbate to raw ewe's milk and inoculating *Brucella melitensis* were investigated. TMAB levels were compared to those of Tulum cheese without sorbate, as determined in previous studies (Morul ve İşleyici, 2012; Öztürk and Nazlı, 1996). The addition of sorbate to cheese leads to a decrease in TMAB counts. A study conducted on vacuum-packaged Tulum cheeses, where sorbate was added at the same concentrations as in our study, showed higher TMAB counts throughout storage. However, an increase in sorbate concentration resulted in a decrease in bacterial counts, as observed in our study (Demir et al., 2017). The lower TMAB counts observed in the sorbate-added groups in this study can be attributed to the stronger antibacterial effect of sorbates, which is due to their high acidity and low moisture content (Liewen and Marth, 1985). Similar results were reported by Doğruer et al. (1996) regarding fecal streptococci numbers in cheese groups with sorbate. While some researchers have found consistent reduction and inhibition of fecal streptococci during ripening (Patır et al., 2001; Yerlikaya and Akbulut, 2019), others have reported irregular patterns (Boyd, 1995). In this study, the decrease and inhibition of fecal streptococci in cheeses with sorbate is attributed to the antibacterial effect of potassium sorbate and starter cultures. Studies on cheese types containing sorbate have shown that potassium sorbate has an antibacterial effect on *Staphylococcus-Micrococcus* (Doğruer et al., 1996; Demir et al., 2017). The counts of *Staphylococcus-Micrococcus* detected in both sorbate and non-sorbate groups remained at lower levels than those in the other study (Patır et al., 2000). The variation in outcomes could be because the experimental production in the present study was carried out under rigorous hygienic conditions to prevent contamination of raw milk and products with environmental bacteria. Furthermore, the increased acidity level in the product may have played a role in the observed difference. Similar to the present study, previous research has shown that coliform group bacteria decrease at higher rates in sorbate-containing cheeses compared to the control group and are inhibited at various storage periods (Doğruer et al., 1996; Demir et al., 2017). Additionally, potassium sorbate has been found to have the highest inhibitory effect on yeast and molds among microorganism groups (Liewen and Marth, 1985). Our study confirms this finding, which is consistent with previous research (Demir et al., 2017; Khorshidian et al., 2021).

Studies have been conducted on the effects of sorbates on food pathogens in cheeses. For example, Benítez-Azaola et al. (2017) reported that the combination of plant extracts and potassium sorbate can inhibit the growth of *L. monocytogenes* in Panela cheese. Pérez et al. (2011) found that the growth of Shiga toxin-producing *Escherichia coli* can be inhibited in edible film-coated cheeses with potassium sorbate. Similarly, Demir et al. (2017) also reported a similar effect. One study examined the survival of *Brucella* species in cheeses without antimicrobial substances. The study found that the amount of *B. melitensis* decreased from 9-log at the beginning of ripening to below detectable levels by the 30th day (Öztürk and Nazlı, 1996). Cosseddu and Pisanu (1985) reported that they could not isolate the bacteria after the 45th and 50th days of ripening in goat milk cheese inoculated with *B. melitensis*. The physicochemical structure of the product may vary depending on the quality of the milk used in cheese making, the type and inoculation level of *Brucella*, the ripening process, and production technologies. These factors are the main reasons for the observed differences.

CONCLUSION

The microbiological properties of Tulum cheese are affected by several factors, such as the quality of raw milk, production conditions and technology, employee hygiene, and storage conditions. Despite the addition of salt, antimicrobial metabolites, low pH, and moisture levels, the product remains vulnerable to foodborne pathogens that can pose a significant risk to consumers, even after the ripening period. The use of food additives that combat foodborne pathogens posing a risk to public health can yield positive results. Sorbic acid and its salts are commonly used preservatives in the food industry, particularly for their antifungal properties, and are frequently employed in cheese production. The objective of this study was to examine the effect of potassium sorbate on the survival of *B. melitensis* in Tulum cheeses, as well as to determine the microbiological and physicochemical changes that occur during ripening. The results suggest that the use of potassium sorbate, particularly at a concentration of 0.20%, had an antibacterial effect on *B. melitensis* and enhanced the microbiological quality of Tulum cheese. Additionally, it did not have any negative impact on the physicochemical properties of the product. The study found that the use of potassium sorbate in Tulum cheese production is recommended for both product quality and public health.

DECLARATIONS

Ethics Approval

Not applicable.

Conflict of Interest

The authors declare no coflict of interest.

Consent for Publication

Not applicable.

Author contribution

Idea, concept and design: BP

Data collection and analysis: AHD

Drafting of the manuscript: AHD

Critical review: AHD

Data Availability

The data used to prepare this manuscript are available from the corresponding author when requested.

Acknowledgements

Not applicable.

REFERENCES

Alton, G. G., Jones, L. M., Angus, R. D., & Verger, J. M. (1988). Techniques for the brucellosis laboratory. Institut National de la recherche Agronomique (INRA).

Alzate, P., Miramont, S., Flores, S., & Gerschenson, L. N. (2017). Effect of the potassium sorbate and carvacrol addition on the properties and antimicrobial activity of tapioca starch–Hydroxypropyl methylcellulose edible films. Starch□ St*ä*rke, 69(5-6), 1600261. https://doi.org/10.1002/star.201600261

American Public Health Association-APHA. (2004). Standard methods for the examination of dairy products. American Public Health Association. Washington, USA.

Association of Official Analytical Chemists-AOAC. (1984). Official methods of analysis of AOAC International (14th ed). Washington, DC., USA.

Association of Official Analytical Chemists-AOAC. (2019). Official methods of analysis of AOAC International (21st ed). Arlington, VA, USA.

Barnes, E. M. (1959). Differential and selective media for the faecal streptococci. Journal of the Science of Food and Agriculture, 10(12), 656-662. https://doi.org/10.1002/jsfa.2740101204

Benítez-Azaola, R., García-Varela, R., García-García, R. M., Suárez-Jacobo, A., Cardineau, G. A., Altamirano, J., & Serna-Saldívar, S. O. (2017). Listeria monocytogenes growth inhibition in inoculated fresh panela cheese by the addition of Rhoeo discolor aqueous extracts combined with potassium sorbate. Revista Mexicana de Ingeniería Química, 16(2), 425-434.

Boyd, R. F. (1995). Basic medical microbiology. In Basic medical microbiology (5th ed.). Little Brown Publishing.

Capparelli, R., Parlato, M., Iannaccone, M., Roperto, S., Marabelli, R., Roperto, F., & Iannelli, D. (2009). Heterogeneous shedding of Brucella abortus in milk and its effect on the control of animal brucellosis. Journal of Applied Microbiology, 106(6), 2041-2047. https://doi.org/10.1111/j.1365-2672.2009.04177.x

Cosseddu, A.M. and Pisanu, S. (1985). Survival of Brucella melitensis of goats's milk cheese. Atti della Societa Italiana delle Scieneze Veterinarie, 39(11), 624-626.

Dadar, M., Fakhri, Y., Shahali, Y., & Khaneghah, A. M. (2020). Contamination of milk and dairy products by Brucella species: A global systematic review and meta-analysis. Food Research International, 128, 108775. https://doi.org/10.1016/j.foodres.2019.108775

De Massis, F., Di Girolamo, A., Petrini, A., Pizzigallo, E., & Giovannini, A. (2005). Correlation between animal and human brucellosis in Italy during the period 1997–2002. Clinical Microbiology and Infection, 11(8), 632-636. https://doi.org/10.1111/j.1469-0691.2005.01204.x

Demir, P., Öksüztepe, G., İncili, G.K. ve İlhak, O.İ. (2017). Vakum paketli Şavak Tulum peynirlerinde potasyum sorbatın kullanımı. Kafkas Üniversitesi Veteriner Fakültesi Dergisi, 23(1), 23-30. https://doi.org/10.9775 /kvfd.2016.15707

Doğruer, Y., Gürbüz, Ü., & Nizamlhoğlu, M. (1996). Potasyum sorbatın beyaz peynirin kimyasal ve mikrobiyolojik kalitesine etkisi. Selçuk *Üniversitesi* Veteriner Bilimleri Dergisi, 12(1), 109-116.

Franc, K. A., Krecek, R. C., Häsler, B. N., & Arenas-Gamboa, A. M. (2018). Brucellosis remains a neglected disease in the developing world: a call for interdisciplinary action. BMC Public Health, 18(1), 1-9. https://doi.org/10.1186/s12889-017-5016-y

International Organization for Standardization-ISO. (1999). Microbiology of food and animal feeding stuffs — Horizontal method for the enumeration of coagulase-positive staphylococci (Staphylococcus aureus and other species) — Part 2: Technique using rabbit plasma fibrinogen agar medium. ISO 6888-2, 2015. ISO 6888-2:1999. International Organization for Standardization (ISO), Geneva, Switzerland.

International Organization for Standardization, Türk Standartları Enstitüsü-ISO, TSEN. (2007). Peynir ve eritme peynir ürünleri-Klorür miktarı tayini potansiyometrik titrasyon metodu. ISO 5943:2007. Türk Standartları Enstitüsü, Ankara, Türkiye.

International Organization for Standardization-ISO. (2003). Microbiology of food and animal feeding stuffs- Horizontal method for the enumeration of microorganisms- Colony-count technique at 30 °C. ISO 4833:2003. International Organization for Standardization (ISO), Geneva, Switzerland.

International Organization for Standardization-ISO. (2006). Microbiology of food and animal feeding stuffs — Horizontal method for the enumeration of coliforms — Colony-count technique. ISO 4832:2006. International Organization for Standardization (ISO), Geneva, Switzerland.

International Organization for Standardization-ISO. (2008). Microbiology of food and animal feeding stuffs — Horizontal method for the enumeration of yeasts and moulds — Part 1: Colony count technique in products with water activity greater than or equal to 0,95. ISO 21527-1, 2008. International Organization for Standardization (ISO), Geneva, Switzerland.

Khorshidian, N., Yousefi, M., & Mortazavian, A. M. (2021). Comparıson of antıfungal properties of lactobacıllus rhamnosus and lactobacıllus reuterı wıth potassıum sorbate ın the Iranıan uf-feta cheese. Journal of Microbiology, Biotechnology and Food Sciences, e3318-e3318. https://doi.org/10.55251/jmbfs.3318

Liewen, M. B., & Marth, E. H. (1985). Growth and inhibition of microorganisms in the presence of sorbic acid: a review. Journal of Food Protection, 48(4), 364-375. https://doi.org/10.4315/0362-028x-48.4.364

Lungu, B. and Johnson, M. G. (2005). Potassium sorbate does not increase control of Listeria monocytogenes when added to zein coatings with nisin on the surface of full fat turkey frankfurter pieces in a model system at 4 °C. Journal of Food Science, 70(2), M95-M99. https://doi.org/10.1111/j.1365-2621.2005.tb07109.x

Mohammadzadeh-Aghdash, H., Sohrabi, Y., Mohammadi, A., Shanehbandi, D., Dehghan, P., & Dolatabadi, J. E. N. (2018). Safety assessment of sodium acetate, sodium diacetate and potassium sorbate food additives. Food Chemistry, 257, 211-215. https://doi.org/10.1016/j.foodchem.2018.03.020

Morul, F., & İşleyici, Ö. (2012). Divle tulum peynirinin kimyasal ve mikrobiyolojik özellikleri. Yüzüncü Yıl Üniversitesi Veteriner Fakültesi Dergisi, 23(2), 71-76.

Muhammad, I., Niaz, S., Nayab, G. E., Hussain, A., Ahmad, S., Rahman, N., & Ali, A. (2021). Molecular Docking and In vitro Analysis of Fagonia Cretica and Berberis Lyceum Extracts Against Brucella Melitensis. Current Computer-Aided Drug Design, 17(7), 946-956. https://doi.org/10.2174/1573409916666200612145712

Öztürk, G. Y., & Nazlı, B. (1996). Deneysel olarak enfekte edilen sütte yapılan tulum peynirlerinde Brucella melitensis' in mevcudiyeti üzerine araştırmalar. Pendik Veteriner Mikrobiyolojisi Dergisi, 27, 123-142.

Palou, L., Ali, A., Fallik, E., & Romanazzi, G. (2016). GRAS, plant-and animal-derived compounds as alternatives to conventional fungicides for the control of postharvest diseases of fresh horticultural produce. Postharvest Biology and Technology, 122, 41-52. https://doi.org/10.1016/j.postharvbio.2016.04.017

Pappas, G., Papadimitriou, P., Akritidis, N., Christou, L., & Tsianos, E. V. (2006). The new global map of human brucellosis. The Lancet Infectious Diseases, 6(2), 91-99. https://doi.org/10.1016/S1473-3099(06)70382-6

Patır, B., & Dinçoğlu, A. H. (2001). Elazığ'da tüketime sunulan taze beyaz peynirler ile tulum peynirlerinde Brucella spp.'nin varlığı üzerine araştırmalar. Fırat *Üniv*ersitesi Sağlık Bilimleri Veteriner Dergisi, 15(1), 15-22.

Patır, B., Ateş, G., & Dinçoğlu, A. H. (2001). Geleneksel yöntemle üretilen tulum peynirinin olgunlaşması sırasında meydana gelen mikrobiyolojik ve kimyasal değişimler üzerine araştırmalar. F*ırat Üniversitesi* Sağlık Bilimleri Dergisi, 15(1), 1-8.

Patır, B., Ateş, G., Dinçoğlu, A. H., & Kök, F. (2000). Elazığ'da tüketime sunulan tulum peynirinin mikrobiyolojik ve kimyasal kalitesi ile laktik asit bakterileri üzerine araştırmalar. Fırat *Üniversitesi* Sağlık Bilimleri Dergisi, 14, 75-83.

Pérez, L. M., Balagué, C. E., Rubiolo, A. C., & Verdini, R. A. (2011). Evaluation of the biocide properties of whey-protein edible films with potassium sorbate to control non-O157 shiga toxinproducing Escherichia coli. Procedia Food Science, 1, 203-209. https://doi.org/10.1016/j.profoo.2011.09.032

Seleem, M. N., Boyle, S. M., & Sriranganathan, N. (2010). Brucellosis: a re-emerging zoonosis. Veterinary Microbiology, 140(3-4), 392-398.

Shakir, R. (2021). Brucellosis. Journal of the Neurological Sciences, 420, 117280. https://doi.org/10.1016/j.jns.2020.117280.

Tekin, A., & Güler, Z. (2019). Glycolysis, lipolysis and proteolysis in raw sheep milk Tulum cheese during production and ripening: Effect of ripening materials. Food Chemistry, 286, 160-169. https://doi.org/10.1016/j.foodchem.2019.01.190

Tekinşen, O. C., Atasever, M., Keleş, A., & Tekinşen, K. K. (2002). Süt, Yoğurt, Tereyağı, Peynir Üretim ve Kontrol (Birinci basım). Selçuk Üniversitesi Basımevi.

Tomar, O., Akarca, G., GÖk, V., & Çağlar, M. Y. (2020). The effects of packaging materials on the fatty acid composition, organic acid content, and texture profiles of Tulum cheese. Journal of Food Science, 85(10), 3134-3140. https://doi.org/10.1111/1750-3841.15404

Yerlikaya, O., & Akbulut, N. (2019). Potential use of probiotic Enterococcus faecium and Enterococcus durans strains in Izmir Tulum cheese as adjunct culture. Journal of Food Science and Technology, 56(4), 2175-2185. https://doi.org/10.1007/s13197-019-03699-5

Medit Vet J, 9(3): 345-353, 2024
DOI: 10.24880/meditvetj.1611151

Research Article

Research on beliefs about animals in Balıkesir folklore

Nigar Yerlikaya[1]

[1]Department of Veterinary History and Deontology, Faculty of Veterinary Medicine, Ankara University, Ankara, Türkiye

Key Words:
animals
Balıkesir
beliefs
folklore

Received : 28 February 2024
Revised : 17 August 2024
Accepted : 21 August 2024
Published : 31 December 2024
Article Code : 1611151

Correspondence:
N. YERLİKAYA
(nigaryerlikaya@gmail.com)

ORCID
N. YERLİKAYA: 0000-0002-7106-1367

ABSTRACT

In the research, it was aimed to contribute to folklore research by identifying various beliefs about animals among the people in Balıkesir region. For this purpose, face-to-face interviews were conducted with 50 resource persons living in the region between January 1 and February 1, 2023, through the "information collection form" prepared for this purpose. The data obtained from the sources was evaluated with the "content analysis" technique. The study identified 144 folk beliefs about animals among the people. The findings obtained from the study were classified under six headings, namely,"beliefs about good luck and abundance ", "beliefs about bad luck", "beliefs about the evil eye", "religious beliefs", "beliefs about illness and treatment, " and "other beliefs". As a result, in this study carried out in the Balıkesir region, rich folkloric practices were identified, and when compared with the studies conducted in other regions, it was determined that they have both similarities and differences Furthermore, it was found that people interact with animals in cultural and social settings and have integrated their beliefs into their everyday lives.

INTRODUCTION

The dictionary definition of belief is given as "the act of believing, the thing that is believed" (TDK, 2023). "Veterinary medicine folklore" refers to the distinctive practices, customs, and diverse beliefs that are specific to the veterinary medical profession (Salman, 1948; Dinçer, 1967; Dinçer, 1980; Doğanay, 1982; Boratav, 1994; Yüksel, 2021). Because of their nomadic culture, Turks have had close bonds with animals since the beginning of history, and they have always lived a life intermingled with animals due to their geography (Yeşildal, 2007). Over time, this background has led the Turkish people to develop a spiritual bond with animals, and they have incorporated into their everyday lives and folklore a variety of beliefs that have arisen from these close bonds (Yeşildal, 2007; Mollaibrahimoğlu, 2008). Animal-related beliefs and behaviors, which hold a significant place in folk beliefs, have also been studied within the scope of folklore research in veterinary medicine. Studies on folk beliefs in veterinary medicine have been authored in various regions of Türkiye (Örnek, 1966; Doğanay, 1982; Mollaibrahimoğlu, 2008; Özen and Yüksel, 2014; Küçükaslan and Uçar, 2016; Sinmez and Aslım, 2017; Yüksel and Özen, 2021). Nevertheless, the results of the literature review revealed that no relevant study had been conducted in the Balıkesir region.

Balıkesir's favorable soil, climate, and location on the coast of the Marmara and Aegean seas have made it the home of numerous civilizations throughout history. Research revealed that the Balıkesir region was the site of the prehistoric settlement of Balkan immigrants, particularly towards the end of the Chalcolithic period (Veli, 2003). During the Bronze Age, life in this area was influenced by the Trojan civilization (Sevgi, 1994). Balıkesir, earlier referred to as Mysia and Karesi, has been ruled by the Roman, Byzantine, Anatolian Seljuk, Karasid Dynasty, and Ottoman Empires (Kahyaoğlu, 2021). The purpose of the study was to determine the folk beliefs that the people in the Balıkesir region had about the animals, to assess these beliefs by tracing their origins, and to make a contribution to the field of folk science research.

MATERIALS and METHODS

The primary data sources for the study were in written and spoken form, collected from residents in the Balıkesir area. For written data, a *"data collection form"* with six questions total about knowledge and beliefs about animals from the Balıkesir region was prepared, in addition to questions about demographic data like *"name-surname, year of birth, profession, name of the district, and village."* The oral data were recorded once the source individuals gave consent to it. The methodology of *"informant interviews"* has been employed as one of the qualitative research methods in the social sciences. In the selection of informants, factors like having been born in Balıkesir and its districts or having resided in the area were taken into consideration. At the end of the study, the sociodemographic details of the informants who either have beliefs or attest to their presence are provided. The data collected through face-to-face interviews with 50 informants in January and February 2023 was processed and analyzed individually using the content analysis method. In a qualitative sense, content analysis uncovers the cultural structure of the area under consideration as opposed

To cite this article:
Yerlikaya N. Research on beliefs about animals in Balıkesir folklore. Medit Vet J. 2024; 9(3): 345-353.

to making generalizations The ethics committee's permission was obtained to conduct the study. The list of informants is provided at the end of the article.

The results of the study were categorized under several headings, *namely, "Beliefs regarding good luck and abundance", "Beliefs regarding jinx," "Beliefs regarding the evil eye," "Religious beliefs," "Beliefs regarding illness and treatment,"* and *"Other beliefs."*

RESULTS

Table 1. Beliefs regarding good luck and abundance.

Category	Resource Persons	Category	Resource Persons
The stork brings blessings, and good luck	(KK.1, KK.19, KK.38)	The cat is auspicious, it increases energy and fertility	(KK.26)
It is believed that storks are lucky	(KK.27)	It is auspicious to feed bees	(KK.40)
The squirrel is auspicious and fertile	(KK.2, KK.3, KK.5, KK.16, KK.18, KK.19, KK.29, KK.31, KK.45)	Bees are fertile	(KK.36)
The ant brings abundance	(KK.2, KK.3, KK.15, KK.14, KK.21, KK.24, KK.25, KK.23, KK.27, KK.31, KK.34)	The lamb and the sheep are like angels	(KK.20, KK.36)
It will be fortunate if the ant gets into the home	(KK.39, KK.50)	The hummingbird hawk-moth brings good luck	(KK.37, KK.47)
The lamb is a blessing	(KK.4, KK.13, KK.22, KK.29)	The goat is an auspicious animal	(KK.40)
The sheep is a blessing	(KK.32, KK.33, KK.39, KK.40, KK.41, KK.42, KK.43, KK.48, KK.50)	When a sheep comes in, it makes the household wealthy	(KK.41)
The lamb is an auspicious, fertile, blessed, and lucky animal	(KK.9, KK.17, KK.20, KK.30, KK.32, KK.33, KK.40, KK.41, KK.42, KK.43, KK.48)	The weasel is a lucky animal	(KK.46)
The lamb and the goat are blessed animals	(KK.6)	On summer evenings, a swift approaching the house's chimney indicates good fortune	(KK.46)
The swallow is an auspicious and fertile animal	(KK.5, KK.9, KK.10, KK.12, KK.13, KK.19, KK.38)	The pigeon is a lucky animal	(KK.46)
You will find success if the snake runs away before you	(KK.11)	The cow is fertile	(KK.48)
The ladybug brings good luck, it is a lucky animal	(KK.15, KK.24, KK.25, KK.35)	The horseshoe represents luck	(KK.48)
The ladybug is a blessing	(KK.22)	Feeding a dog or cat at home is beneficial	(KK.48)
The ladybug brings good news	(KK.47)	When the ant comes inside the home, blessings will follow	(KK.49)
The elephant brings abundance, serenity, and luck	(KK.31)	The birth of a pied sheep is auspicious	(KK.49)
The camel is a blessed animal	(KK.19)		

Table 2. Beliefs regarding jinx.

Category	Resource Persons	Category	Resource Persons
A dog's howl is not lucky; rather, it's an unlucky sign	(KK.1, KK.14, KK.26, KK.28, KK.48)	The crow brings bad luck	(KK.4, KK.7, KK.10, KK.44, KK.49)
A dog's howl indicates that someone is about to pass away	(KK.3, KK.45, KK.35)	The crow is a disliked animal	(KK.15)
Feeding a dog at home is bad and regarded as filthy	(KK.37)	Crowing brings bad luck	(KK.37)
Killing weasels is not a good thing	(KK.16, KK.17)	The raven symbolizes evil omens	(KK.15)
Getting into trouble with a weasel brings bad luck; it is unlucky	(KK.5, KK.9, KK.11, KK.12, KK.13, KK.19, KK.20)	The raven is ominous	(KK.7, KK.44)
Dove flesh is regarded as ominous	(KK.13)	The pig is ominous	(KK.22)
For whoever kills the spider, bad fortune will follow	(KK.6)	Seeing a pig is not a good thing	(KK.30)
Shooting a deer brings bad luck	(KK.7, KK.17, KK.18, KK.21)	The pig is filthy	(KK.37)
The owl is ominous	(KK.4, KK.15, KK.24, KK.28, KK.29, KK.39)	Feeding a pig is not a good thing	(KK.45)
A dead body will exit a house if an owl sits on its chimney of it	(KK.9)	There will be stealing if there are too many mice	(KK.26)
If an owl sits on the chimney of a house, it is ominous	(KK.8, KK.46, KK.48)	A black cat crossing the street brings misfortune	(KK.26, KK.27, KK.31)
Seeing an owl is associated with death	(KK.23, KK.25, KK.34)	Things will not go well if a black cat is spotted on the road	(KK.33, KK.38, KK.47)
Seeing an owl means that things will go wrong	(KK.30)	The cat is a filthy animal	(KK.41)
The owl's crowing brings bad luck	(KK.8, KK.36)	The rabbit is ominous	(KK.38)
Seeing an owl brings death to the household	(KK.43)	Seeing a rabbit go by is thought to be unlucky	(KK.41)
When an owl stares directly into one's eyes, it's ominous	(KK.28, KK.32)		

Table 3. Beliefs regarding the evil eye

Category	Resource Persons	Category	Resource Persons
A dry animal head is hung at a cropland's entrance	(KK.4, KK.14, KK.40, KK.48, KK.49)	The "ant prayer" is hung on the door of houses against the evil eye	(KK.31)
Horseshoes are hung on the doors of houses	(KK.5, KK.8, KK.15, KK.17, KK.22, KK.25, KK.32, KK.34, KK.32, KK.50)	A cow's head is hung against the evil eye in a bee yard	(KK.37)
A horseshoe and a rabbit's foot are hung over the door at the entrance	(KK.46)	Animal heads are hung on the door against the evil eye	(KK.38, KK.50)
A camel is good for the evil eye; it is an auspicious animal	(KK.13)	Sap is taken from trees and fed to children to ward off the evil eye if they hear the rusty sound of a rooster	(KK.39)
Anyone who comes eye to eye with a black cat will get the evil eye	(KK.29)	The animal collar is adorned with bells and beads to keep off the evil eye	(KK.42)
An evil eye will come upon someone who comes eye to eye with an owl	(KK.31)	The evil eye will stay away if the turtle skin is dried and hung	(KK.48)

Table 4. Religious beliefs.

Category	Resource Persons	Category	Resource Persons
Alevis eat fox meat	(KK.44)	The lamb is an angel	(KK.16, KK.19)
Rabbit meat is forbidden for Alevis, they do not eat it	(KK.1, KK.3, KK.6, KK.9, KK.10, KK.13, KK.17, KK.18, KK.44)	Fox (çatal tilki) is forbidden	(KK.40)
Dove flesh is inedible; it is forbidden	(KK.13)	Owls allude to Allah	(KK.46)
Rabbit cannot be eaten	(KK.44)	Venison is forbidden	(KK.47)
Pork cannot be eaten	(KK.21)	Because the prophet rubbed the cat's back, they refer to it as prayed	(KK.49)
Pigs are forbidden; they are not loved	(KK.2, KK.4, KK.5, KK.11, KK.12, KK.14, KK.15, KK.16, KK.29, KK.30, KK.32, KK.35, KK.44, KK.50)	The ant is regarded as sacred	(KK.49)
The lamb is a blessed animal	(KK.6, KK.23, KK.24, KK.34, KK.43)	Camel meat breaks the spell	(KK.16)

Table 5. Beliefs regarding illness and treatment.

Category	Resource Persons	Category	Resource Persons
Alcoholics are given the foam from a camel's mouth to help them quit drinking	(KK.1, KK.6, KK.11, KK.12, KK.16, KK.18, KK.36)	Boiled badger flesh is beneficial for sheep with sulaz and foot-and-mouth diseases	(KK.38)
Goat's milk is beneficial for children	(KK.4)	Sour black mulberry is beneficial for rams	(KK.38)
Goat milk helps children with bronchitis	(KK.20, KK.46)	Shark meat is good for back pain	(KK.29)
The fat and fleece from the lamb's tail are wrapped around the bodies of children with bronchitis	(KK.5, KK.17, KK.22, KK.34, KK.43)	Spiny juniper is beneficial if it is mixed with salt and fed to animals	(KK.38)
The water that the lovebird sips is given to the child who is unable to speak	(KK.6, KK.25, KK.34)	Patients with bronchitis are fed raw, mashed village chicken flesh	(KK.38)
Pressing flesh on the skin helps to heal painful bruises	(KK.30)	Ticks and moths from horses can be removed with the help of olive oil	(KK.38)
The foam from the camel's mouth is beneficial for children who are unable to speak	(KK.1, KK.8, KK.9, KK.10, KK.14, KK.15, KK.45)	Olive oil causes sheep and goats to shed their hair, feathers, and internal parasites	(KK.50)
When the galyak[1] is still warm, it is wrapped around the child who has bronchitis	(KK.15)	Animal spleen is good for anemia	(KK.26)
Lambskin is good for bronchitis	(KK.19)	The wounded area of the body is covered in tail fat	(KK.39)
Partridge meat is beneficial for children	(KK.21)	There will be suffering if the pig gets into the garden	(KK.40)
The tail fat of animals is medicinal	(KK.23)	Animal bone is beneficial against the human evil eye	(K.41)
The lamb's tail fat is tied around the waist to relieve low back pain	(KK.28)	At a push, the horse's right foot can be eaten	(KK.41)
Three stones in the head of brown meagre are beneficial for kidney stones	(KK.28)	Turtle blood is good for hemorrhoids	(KK.42)
Leeches are used medicinally	(KK.31)	Veal is applied to the region that was bruised during the fall	(KK.46)
Lamb tail fat is applied to the sore area	(KK.32)	When a scorpion stings, it is crushed and applied to the wound	(KK.48, KK.46)
Leech therapy is good for both humans and animals	(KK.35)	The newborn baby is fed with the milk from the animal that has just given birth	(KK.46)
Consuming a wolf heart would be beneficial for epilepsy patients	(KK.37)	Galyak is good for bronchitis	(KK.48)
When a person has bronchitis, animal skin is adhered to the body in a moist condition	(KK.38)	The frog is good for warts	(KK.48)

[1]A flat, glossy kind of fur obtained from a newborn or stillborn lamb or kid (goat).

Table 6. Other beliefs.

Category	Resource Persons	Category	Resource Persons
Winter begins in a week or ten days if the animals from the dispersed plateau return to the village on their own	(KK.39)	When cats show the back of their heads, it means it's going to rain	(KK.37)
Dog howling is believed to be an allusion to the call to prayer	(KK.3, KK.21, KK.42)	Winter begins in a week or ten days if the animals from the plateau return to the village	(KK.39)
The wolf is an animal that is feared and considered a monster	(KK.45)	Seeing a slithering snake on your way to work indicates that things will go smoothly	(KK.39)
The wolf is a respected animal	(KK.18)	Winter will pass well if the animals lie scattered when they go to sleep; summer will pass smoothly if they remain together	(KK.39)
The wolf is a symbol of power; it is called a monster; people respect it and are also afraid of it	(KK.4, KK.5, KK.11, KK.14)	If one messes up with the weasel or the marten, it will ruin even the house's owner	(KK.46)
Turkmens do not eat rabbit meat	(KK.7)	The arrival of the Aegean-native Sülümancık Mediterranean house gecko will be accompanied by blessings	(KK.46)
Whoever spots the stork in the sky goes off on a journey	(KK.2, KK.12, KK.14)	If it flies, the hummingbird hawk-moth will welcome guests into your home	(KK.48)
Seeing a snake indicates that things will go smoothly	(KK.24)	The hummingbird hawk-moth is ungrateful	(KK.49)
It is not good to ruin a bird's nest; if one does, he will not have peace at home; grief will follow	(KK.28)	The cat is ungrateful	(KK.49)
If a person sees a snake on the road, his affairs will flow like water	(KK.33)	An animal sleeping in the shade develops illness in its lungs	(KK.50)

DISCUSSION

Upon a detailed examination of the study's findings, it is observed that for the belief related to animals in the Balıkesir-region, sheep, lambs, goats, cows, horses, camels, elephants, storks, swifts, pigeons, swallows, cats, dogs, weasels, squirrels, ladybugs, bees, ants, geckos, and snakes are associated with good fortune and prosperity (Table 1). According to the findings of the study, the Balıkesir region has diverse beliefs about animals with rich elements (Table 1, Table 2, Table 3, Table 4, Table 5, Table 6). The finding that the stork and dove are auspicious, while the sheep and lamb are both blessed and auspicious, is consistent with the findings of previous research on beliefs in Anatolian folklore about animals (Olgunsoy, 2007; Yüksel, 2012; Küçükaslan and Uçar, 2016; Sinmez and Aslım, 2017; Yüksel and Özen, 2021).

A study conducted in a different region has also identified the belief that the pigeon brings luck and holiness because it protected the Prophet Muhammad (Danış et al., 2021). The findings of this study, which focuses on the Balıkesir region, regarding the belief that the pigeon is a lucky animal, can also be attributed to the fact that it protected the Prophet.

Again, religious influences are known to play a role in why the pigeon, which is said to bring good luck and blessings, is so beloved in the Balıkesir region (Olgunsoy, 2007). Swallows are not killed in the Balıkesir region. The swallow is believed to be an auspicious and fertile animal (Table 1). The study suggests that religion has a role in the Balıkesir region's reverence for the swallow, who is believed to have saved the Prophet Muhammad (Olgunsoy, 2007). The fact that "horseshoes are hung on the doors of houses" to keep the evil eye away can be explained by the fact that this belief is prevalent across Anatolia (Gezgin, 2007). Although the cat is regarded as an auspicious and fertile animal, it is well known that the belief that a black cat crossing the road brings bad luck originates from the cat's ungratefulness as well as religious factors (Olgunsoy, 2007).

The ancient Turks thought that the evil eye could affect both live and inanimate beings, so they used a horse's head on scarecrows or stakes in yards to protect their vineyards and gardens

from the evil eye (Çıbla, 2004). It has been discovered that the practice of hanging dry animal heads at croplands' entrances in the Balıkesir region as a means of protection from the evil eye is also used in other regions (Dinçer, 1967; Araz, 1991; Arslan, 1998; Yerlikaya, 2002; Kurum, 2008; Mollaibrahimoğlu, 2008; Sinmez, 2011; Özen and Yüksel, 2014; Küçükaslan and Uçar, 2016; Sinmez and Aslım, 2017). The Alevi-Bektashi tradition is primarily responsible for the manifestation of ominousness associated with rabbits in the Balıkesir region and our country as a whole. The results of the research support this theory (Selçuk, 2008; Üçer, 2005; Boratav, 1984; Küçükaslan and Uçar, 2016).

The view that dove flesh is considered ominous and forbidden is dominant in the region (Table 2). Another study in the region determined that the dove is important to the locals. One of the reasons for not killing the dove was that it used to be a human, a bird beloved by Allah, and was close to humans (Olgunsoy, 2007).

The study determined that the belief that the owl brings bad luck and evokes death stems from religious beliefs (Table 2, Table 4). The fact that the owl is regarded as an ominous bird associated with death has also been established in a previous doctoral dissertation study, as well as in other studies (Yüksel, 2012; Küçükaslan and Uçar, 2016; Sinmez and Aslım, 2017). Although the owl is generally regarded as ominous in religious culture, studies have revealed that it is both auspicious and ominous in Turkish culture (Kaman, 2015; Olgunsoy, 2007; Köse, 2019). Furthermore, it was discovered that the participants' expression "Owls allude to Allah" was very similar to the expression "They say it is ominous for an owl, but it always says the name of Allah, so it cannot be ominous" as mentioned in a doctoral dissertation study conducted in the same region earlier. Despite the association between owls and death and ominousness, the data collected in the Balıkesir region indicates that owls have a positive reputation (Olgunsoy 2007). Moreover, it is possible to believe that Allah sees the owl as having a place.

Although the study findings state that eating venison is prohibited in a religious understanding, the Directorate of Religious Affairs has declared that, by Islamic law, there are provisions that allow it (Din İşleri Yüksek Kurulu, 2024a, 2024b). It could lead us to believe that this is just a local superstition with no connection to religion.

The study suggests that in terms of illnesses and treatments, alcoholics should be given camel's mouth foam to help them quit drinking (Table 5), and that children who are unable to speak can benefit from camel's mouth foam because camels are said to have a protective charm against the evil eye. In a previous survey in the Balıkesir region, the informants stated in their responses to a question regarding camels that the devil can be disguised as anything other than a camel or sacrificial sheep (Olgunsoy, 2007). There is a very large collection of folklore regarding the camel, which is particularly important, especially in the Aegean region (Seyirci, 1987).

Research has revealed that there is scientific support for the claim that goat's milk can help children with bronchitis (Table 5). According to certain studies, goat's milk can help treat eczema, asthma, digestive issues, and some allergy symptoms. Children who drink goat's milk also tend to be heavier, and taller and have better skeletal systems and blood serum content values (such as calcium and vitamin A) than children who drink cow's milk (Coşkun and Öndül, 2004; Demirhan and Şahinler, 2022). We can say that this belief expressed by local people is not only considered a folkloric practice but also has a scientific basis.

The information provided in this study, which was carried out in the Balıkesir region, also indicates to us that camels are highly valued by the local population (Table 1, Table 3). Religious themes provide an explanation for the belief that "it is not good to ruin a bird's nest; if one does, he will not have peace at home; grief will follow," which is featured in the "other beliefs" section. It is well known that touching a bird's nest or young is undesirable in Islam. It's well known that Turks have an intense love for birds of all kinds, including pigeons, storks, and swallows. In fact, during the Ottoman Empire, people were believed to have committed sins if they hurt these animals or disturbed their nests; it was also illegal to take bird eggs or young, and violators faced severe punishments (Sarıcık, 2001).

The wolf, believed to be sacred by the Turks, is known to symbolize enlightenment, valor, power, and the state (Çoruhlu, 2011; Yurdakul, 2023). In addition, the wolf is also seen as a symbol of descent and reproduction in the old Turkish belief system (Çoruhlu, 2019). The wolf is known to have represented the might of the Turks throughout history and to have always been a powerful animal. The wolf embodies the core characteristics of the Turkish people, being a powerful and venturous animal (Sarı, 2017; Altun 2019). The phrase "strong like a wolf" further attests to the strength of wolves (Altun 2019). Therefore, the conclusion that *"the wolf is a symbol of power"* as found in this study is not coincidental. Several studies have suggested that people view wolves as symbols of power, as the examples above have demonstrated, and this study shows that this belief is valid among the people in the analyzed region.

CONCLUSION

Consequently, this study found that the Balıkesir region's medicine is rooted in folklore beliefs about animals, has great potential, and is significant to the local population because animals are a part of human existence from birth to death. This study is also thought to be useful for guiding broader studies in the future.

DECLARATIONS

Ethics Approval

This research was approved by The Ethics Committee of the Ankara University. (AÜEK, Ref No: 160, Tarih: 07/11/2022)

Conflict of Interest

Author declare that there are no conflicts of interest for this study.

Consent for Publication

Not applicable

Author contribution

Idea, concept and design: NY

Data collection and analysis: NY

Drafting of the manuscript: NY

Critical review:NY

Data Availability

The data is available from the corresponding author on reasonable request.

Acknowledgements

Not applicable

REFERENCES

Aktüre, S. (1994). Anadolu bronz çağı kentleri.Tarih Vakfı Yurt Yayınları.

Altun, Z. (2019). Türk kültüründe "kurt kavramı" üzerine bir inceleme.21.yy Eğitim ve Toplum Dergisi, 8(22), 91-108.

Araz, R. (1991). Harput'ta eski türk inançları ve halk hekimliği. Atatürk Kültür Dil ve Tarih Yüksek Kurumu.

Boratav, P.N. (1994). Türk halkbilimi II/100 soruda türk folkloru (İnanışlar, Töre ve Törenler, Oyunlar). Gerçek Yayınevi.

Çıbla, N. (2004). Halk Kültüründe Nazar, Nazarlık İnancı Ve Bunlara Bağlı Uygulamalar. Türklük Bilimi Araştırmaları, 15, 103-125.

Çoruhlu, Y. (2011). Türk mitolojisinin ana hatları. Kabalcı Yayınları.

Çoruhlu, Y. (2019). Türk sanatında hayvan sembolizmi 2. Ötüken Yayınları.

Danış, E.M., Çelik, E., Aslım, G., Yaşar, A. (2021). Konya ili folklorunda güvercin: 3. inanışlar ve uygulamalar. Lokman Hekim Dergisi, 11(3), 472-480. https://doi.org/10.31020/mutftd.902202

Demirhan, S.,& Şahinler N. (2022). Bazı hayvansal ürünlerin beslenme ve sağlık açısından önemi. Türk Tarım Gıda Bilimi ve Teknolojisi Dergisi, 10, 2696-2700. https://doi.org/10.24925/turjaf.v10isp1.2696-2700.5671

Dinçer, F. (1967). Türk Folklorunda Veteriner Hekimliği Üzerine Araştırmalar. Ankara Üniversitesi Veteriner Fakültesi Yayınları, Doktora Tezi.

Dinçer, F. (1980). A report on the Folklore Activites and Folk Veteriner Medicine in Turkey. Ankara Üniversitesi Veteriner Fakültesi Dergisi, 18, 237-245.

Din İşleri Yüksek Kurulu. (2024a). https://kurul.diyanet.gov.tr/Cevap-Ara/985/kara-hayvanlarindan-eti-yenilip-yenilmeyenler-hangileridir

Din İşleri Yüksek Kurulu. (2024b). https://webdosya.diyanet.gov.tr/DiyanetAnasayfa/UserFiles/DiniBilgiler/ilmihal_cilt_2.pdf

Doğanay, S. (1982). Afyon Folklorunda Veteriner Hekimlik Araştırma ve İncelemeleri. II. Milletlerarası Türk Folklor Kongresi Bildirileri, Gazi Üniversitesi Basın-Yayın Yüksekokulu Basımevi, 131-151, Ankara, Türkiye.

Gezgin, D. (2007). Hayvan Mitosları. Sel Yayıncılık.

Örnek, S.V. (1966). Sivas ve Çevresinde Hayatın Çeşitli Safhalarıyla İlgili Batıl İnançların ve Büyüsel İşlemlerin Etnolojik Tetkiki. Ankara Üniversitesi Dil ve Tarih-Coğrafya Fakültesi Yayınları.

Mollaibrahimoğlu, Ç. (2008). Anadolu Halk Kültüründe Hayvanlar Etrafında Oluşan İnanç ve Pratikler (Yüksek Lisans Tezi, Karadeniz Teknik Üniversitesi, Sosyal Bilimler Enstitüsü).

Kahyaoğlu, S. (2021). Edremit Tarihi Uygarlıkların Körfezinde 3500 Yıl. Kafe Kültür Yayıncılık.

Kaman, G.S. (2015). Baykuş Kelimesi ve Baykuşla İlgili İnançlar Üzerine. Turkish Studies. 10(8) , 1137-1154. http://dx.doi.org/10.7827/TurkishStudies.8008

Köse, S. (2019). Türk Kültüründe Baykuş. Kültür Araştırmaları Dergisi, 1(3), 288-301.

Küçükaslan, Ö.,& Uçar, M. (2016). Diyarbakır folklorunda hayvanlarla ilgili inanışlar üzerine bir araştırma. Eurasian Journal of Veterinary Sciences, 32(4), 220-228. https://doi.org10.15312/EurasianJVetSci.2016422392

Olgunsoy, B. (2007). Balıkesir Yöresinden Derlenmiş Bitki ve Hayvanlarla İlgili İnanış ve Uygulamalar Üzerine Bir Araştırma. (Yüksek Lisans Tezi, Balıkesir Üniversitesi, Sosyal Bilimler Enstitüsü).

Özen, R., & Yüksel E. (2014). Kayseri folklorunda hayvanlar ile ilgili inanışlar üzerine bir değerlendirme. Erciyes Üniversitesi Veteriner Fakültesi Dergisi, 11(1), 23-28.

Sari, İ. (2017). Türk tarihinde bozkurt, Nokta E-Book Publishing Yayınları.

Sarıcık, M. (2001). Kültürümüzde Kuş Yuvasına ve Yavrusuna Dokunmama Konusunda Birkaç Örnek. Süleyman Demirel Üniversitesi İlahiyat Fakültesi Dergisi, 8,17-34.

Salman, M. (1948). Halk Hekimliği ve Halk Veterinerliği. Milli Kültür Araştırmaları. Ulus Basımevi.

Selçuk, A. (2008). Ağaçeri Türkmenleri-Tahtacılar. IQ Kültür Sanat Yayınları.

Sevin, V. (2003). Anadolu Arkeolojisi, Der Yayınları.

Sinmez, Ç. (2011). Bozlak kültüründe folklorik veteriner hekimliği ve hayvancılık üzerine araştırma. (Doktora Tezi, Selçuk Üniversitesi,Sağlık Bilimleri Enstitüsü).

Sinmez, Ç. Ç.,& Aslım, G. (2017). İç Anadolu Bölgesindeki hayvanlarla ilgili inanış ve uygulamalar üzerine bir değerlendirme, Bilig, 81, 205-232.

Seyirci, M. (1987). Deve Folkloru ve Güney Göçerlerinde Deve Donanımları. III. Milletlerarası Türk Folklor Kongresi Bildirileri. Başbakanlık Basımevi, 327-336, Ankara, Türkiye.

Üçer, C. (2005). Tokat Yöresinde Geleneksel Alevilik. Ankara Okulu Yayınları.

Yeşildal Ü.Y. (2007). Anadolu Folklorunda Geyik. (Yüksek Lisans Tezi, Selçuk Üniversitesi, Sosyal Bilimler Enstitüsü).

Yurdakul, N.B. (2023). Türk Halk Hekimliğinde Hayvan Sembolizmi. Türk Dünyasi İncelemeleri Dergisi, 23(1), 187-200. https://doi.org/10.32449/egetdid.1280860

Yüksel E. (2012). Aşağı Fırat Havzasında Veteriner Hekimliği Folkloru Üzerine Araştırmalar (Doktora Tezi, Fırat Üniversitesi, Sağlık Bilimleri Enstitüsü).

Yüksel, E.,& Özen, R. (2021). Aşağı Fırat Havzasında Veteriner Hekimliği Folkloru Üzerine Araştırmalar: Hayvanlar ile İlgili İnanışlar ve Uygulamalar. Kocatepe Veterinary Journal, 14(1), 91-100. https://doi.org 10.30607/kvj.841573

Türk Dil Kurumu. (2003, March 10). Güncel Türkçe Sözlük. https://www.sozluk.gov.tr

Resource Persons

KK.1. Kayhan Kuzu, born in 1983-ship captain.

KK. 2-Türker Ayhan, born in 1979-manager.

KK.3. Barış Baykara, born in 1979-architect.

KK4. Cihat Yedikardeşler, born in 1971-farmer.

KK.5-Ayça Nadasbaş, born in 1990-manager.

KK.6-Osman Doğru, born in 1950-chauffeur jobs.

KK.7-Baykal Doğan, born in 1974-official manager.

KK.8-Leyla Kılıç, born in 1984-civil servant.

KK.9-Murat Ersoy, born in 1985-manager.

KK.10-Yiğit Çobankuşu*, born in 1988-manager.*

KK.11-Eren Ocaktürk, born in 1987-basketball player.

KK.12-Onur Canbaz, born in 1989-firefighter.

KK.13-Cenk Yoldaş, born in 1979-manager.

KK.14-Mürvet Yenikardeş, born in 1947-housewife.

KK.15-Kamile Dokuyucu, born in 1975-manager.

KK.16-Rahmi Akkuzu, born in 1977-butcher.

KK.17-Özden Dokuyucu, born in 1971-worker.

KK.18-Bekir Yılmaz, born in 1935-soldier.

KK.19-İbrahim Emir,born in 1973-driver.

KK.20-Arda Topsakal, born in 2004-carpenter.

KK.21-Ziynet Yılmaz, born in 1974-worker.

KK.22-Gürcan Ersoy, born in 1979-manager.

KK.23-Serkan Ocaktürk, born in 1985-driver.

KK.24-Ali Sarıbaş, born in 1992-business man.

KK.25-Mert Kolaşinli, born in 1983-banker.

KK.26-Funda Can, born in 1979-manager.

KK.27-Hatice Yağmur, born in 1981-manager.

KK.28-Ferah Sağduç, born in 1974-manager.

KK.29-Hande Kocabıyık, born in 1988-manager.

KK.30-Fulden Varol, born in 1995-food engineer.

KK.31-Seda Nadasbaş, born in 1983-teacher.

KK.32-Menşure Sarıkız, born in 1959-nurse.

KK.33-Süleyman Özdemir, born in 1989-worker.

KK.34-Cüneyt Nadasbaş, born in 1979-teacher.

KK.35-Burcu Muştu, born in 1956-financier.

KK.36-İsmet Topsakal,born in 1951-driver.

KK.37-Medine Yalazı, born in 1967-hauswife.

KK.38-Şazi Aşık, born in 1979-farmer.

KK.39-Hayrettin Aykut, born in 1963-farmer.

KK.40-Mehmet Yalazı, born in 1969-chef.

KK.41-Hafız Mustafa Aykurt, born in 1933-teacher.

KK.42-Kadir Karaaslan, born in 1957-driver.

KK.43-Arzu Topsakal, born in 1974-accountant.

KK.44-Bora Ceylan, born in 1979-pharmacist.

KK.45-Hakkı Evran, born in 1972-teacher.

KK.46-Behiye Topsakal, born in 1957-hauswife.

KK.47-Meral Çakır, born in 1987-hauswife.

KK.48-Ayşe Yalazık, born in 1946-hauswife.

KK.49-Emine Bayram, born in 1977-hauswife.

KK.50-İlker Topsakal,born in 1979-soldier.

Medit Vet J, 9(3): 354-363, 2024
DOI: 10.24880/meditvetj. 1611156

Research Article

Determination of hypoxia, angiogenesis and tumour microenvironment in feline mammary tumours by immunohistochemical and histopathological methods

Erdinc Guner[1], Fatih Hatipoglu[2,3]

[1]Izmir Bornova Veterinary Control Institute, Pathology Laboratory, Bornova, Izmir, Türkiye
[2]Department of Pathology, Faculty of Veterinary Medicine, Selcuk University, Konya, Türkiye
[3]Department of Pathology, Faculty of Veterinary Medicine, Kyrgyz-Turkish Manas University, Bishkek, Kyrgyzstan

Key Words:
angiogenesis
feline mammary tumors
hypoxia
tumor-associated macrophages
tumor microenvironment

Received : 22 March 2024
Revised : 21 October 2024
Accepted : 23 October 2024
Published : 31 December 2024
Article Code : 1611156

Correspondence:
E. GUNER
(eguner35.5@gmail.com)

ORCID
E. GUNER : 0000-0003-2529-8475
F. HATIPOGLU : 0000-0002-0103-5868

ABSTRACT

This study used immunohistochemical method to investigate the relationship between the tumor microenvironment, hypoxia, and angiogenesis in biopsy samples of feline mammary tumors brought to Selcuk University Faculty of Veterinary Medicine and Bornova Veterinary Control Institute between 2015 and 2019. The staining of paraffin tissue sections was performed with CD31, vascular endothelial growth factor (VEGF), hypoxia-inducible factor-1 (HIF-1a) CD68, and CD163 antibodies, and their correlation with each other and the observed histopathological changes was explored. The study used mature mammary tissue samples from 12 cats of different breeds and ages for diagnostic purposes. The examined biopsy materials with microvessel density (MVD), VEGF, HIF-1a, CD68, and CD163 antibodies showed no significant relationship between benign and malignant tumors ($p>0.05$). Furthermore, the study found no significant relationship between malignant tumors and their histological grade, tumor size, mitotic score, lenfovascular invasion (LVI), and necrosis features ($p>0.05$). It is believed that the low number of materials used in the study prevented the detection of a statistically significant difference between the IHC results of tumors and their histopathological and clinicopathological features. The study concluded that presenting the data would be appropriate to contribute to the fields of veterinary medicine and veterinary oncology.

INTRODUCTION

Mammary tumors rank third in cats, following hematopoietic and skin tumors (Misdorp, 2002). Goldschmidt et al. (2017) have reported that the annual incidence rate in cats is 25.4/100,000. When examined by age, the frequency of occurrence increases in cats over nine years old, with the highest diagnosis rates between 10 and 12 years of age. Despite the incomplete understanding of the breed predisposition for mammary tumors in cats, reports indicate a higher incidence in the Siamese breed (Goldschmidt et al., 2017).

The tumor microenvironment defines the cells and structures surrounding the cancer cells in the tumor, including the tumor's vascular system, lymphatics, fibroblasts, pericytes, and sometimes adipocytes (Balkwill et al., 2012). Various non-tumor cells in the tumor microenvironment also affect the behavior of tumor cells (Sun et al., 2014).

Macrophages make up a significant portion of the infiltrated leukocytes in the tumor tissue (Murdoch et al., 2004). Tumor-associated macrophages (TAMs) classify these cells as either anti-tumoral (M1) or pro-tumoral (M2) macrophages, depending on their activation status in response to microenvironmental changes (Chanmee et al., 2014; Mantovani and Locati, 2013). In the tumor microenvironment, TAMs are very important. They affect the movement of tumor cells, the breakdown and remodeling of the extracellular matrix, the growth of new blood vessels, and the metastasis and invasion of tumor cells (Chanmee et al., 2014; Zhang et al., 2012).

Hypoxia is the most important metabolic change in the tumor microenvironment, and 50–60% of solid tumors have heterogeneously distributed hypoxic and anoxic areas within the tumor mass (Vaupel, 2004; Vaupel and Mayer, 2007). To adapt to hypoxic conditions, cells undergo a series of changes in gene expression and function. Many alterations in gene expression during hypoxia are caused by the activation of hypoxia-inducible factor (HIF) (McNeil et al., 2016). HIF allows tumor cells to adapt to and survive in hypoxic conditions in the tumor microenvironment by reprogramming genes involved in angiogenesis, glycolytic metabolism, oxygen consumption, invasion, and migration (Rapisarda and Melillo, 2009).

The formation of new blood vessels is termed angiogenesis. Tumors require new blood vessels to grow beyond 1-2 mm in size. Angiogenesis facilitates the progression, metastasis, and invasion of tumor tissue, providing the oxygen, growth factors, and nutrients necessary for the tumor's development (McNamara et al., 1998).

Because of the clinicopathological, histological, and epidemiological similarities between feline and human mammary cancers, feline mammary tumors can be used as models for human mammary tumors in cancer research. In addition, studies in feline mammary tumors may provide clues to better understand the mechanisms of cellular response, angiogenesis, and hypoxia in the tumor microenvironment. In this study, it was aimed to determine the relationship of paraffin tissue sections of cat mammary tumor biopsy samples with the tu-

To cite this article:
Guner E, Hatipoglu F. Determination of hypoxia, angiogenesis and tumour microenvironment in feline mammary tumours by immunohistochemical and histopathological methods. Medit Vet J. 2024; 9(3): 354-363.

mor microenvironment, hypoxia, and angiogenesis by immunohistochemical method. For this purpose, we evaluated the immunexpressions of CD31, vascular endothelial growth factor (VEGF), HIF-1a, CD68, and CD163 antibodies used in staining and investigated the relationship between them and the observed histopathological changes.

MATERIALS and METHODS

The material for the study consisted of mature mammary tissue samples from 12 cats of various breeds and ages, brought for diagnostic purposes to Selcuk University Faculty of Veterinary Medicine and Bornova Veterinary Control Institute between 2015 and 2019. After the tissue samples of the mammary tissues obtained by the surgical operation were sent to the pathology laboratories of the above-mentioned departments, they were examined macroscopically and tissue samples were taken from the necessary areas for examination.

Histopathological Examination

Mammary biopsy samples were fixed in 10% buffered formaldehyde solution and embedded in paraffin after routine tissue processing procedures. The tissue samples were sectioned at a thickness of 5 microns on a microtome (Leica RM 2125RT), stained with Haemotoxylene&Eosin (H&E) and examined under a binocular light microscope (Olympus BX51).

The malignancy degree of cat tumors was determined according to the newly reported numerical grading system (Goldschmidt et al. 2017).These grading systems are shown in Table 1. An Olympus BX51 microscope (with a 0.55 mm diameter field of view at x400 magnification) was used for histomorphological assessment.

Immunohistochemistry Staining and Evaluation

All sections from the cases were examined, and paraffin blocks representing the tumor most accurately were selected. The evaluation of hypoxia, angiogenesis, and tumor-associated macrophages in the tumor microenvironment was conducted using CD68, CD163, CD31, VEGF, and HIF-1α antibodies. Immunohistochemistry was done on 4-micron-thick sections obtained from paraffin tissue blocks of these cases and mounted on Poly-L-lysine-coated slides were used and subjected to tissue applications of the Novolink™ Polymer Detection System RE7150-K by Leica Microsystems, following the recommended protocol of the respective company. Clone numbers, dilution rates, and incubation times of the primary antibodies used are summarized in Table 2. Negative controls for each staining were also processed using the same procedure but with TBS instead of the primary antibody. For positive controls, hemangiosarcoma tissue from a dog was used for CD31, healthy liver tissue for VEGF, and lung tissue with pneumonia from another dog for HIF-1a, CD68, and CD163. Following staining using the same procedure for all sections, they were examined under a light microscope (Olympus BX51) and evaluated semi-quantitatively (Choudhury et al., 2010. Hameed et al., 2015; Weidner et al., 1991; Monteiro et al., 2018).

The evaluation of samples labeled with VEGF and HIF-1a was performed according to the Allred scoring method (Choudhury et al., 2010; Hameed et al., 2015; Ates, 2019). This scoring system assessed staining intensity and proportion scores in two categories, similar to standard scoring systems. According to this method, staining intensity (darkness) scores were determined as 0 (no staining), 1 (weak), 2 (moderate), and 3 (intense/dark). Proportion score was determined based on the ratio of stained cells to all cells in the examined area, as follows: 0 (no staining), 1 (>0-1/100), 2 (>1/100-1/10), 3 (>1/10-1/3), 4 (>1/3-2/3), 5 (>2/3-1). The staining intensity score and proportion score were added to determine the Allred score for each case, ranging from 0 to 8 (Hameed et al., 2015; Ates, 2019) (Table 3).

To determine microvessel density (MVD), samples were evaluated immunohistochemically using CD31 staining. Weidner et al. (1991) modified the technique for MVD determination. Initially, sections were scanned at low magnifications (x40 and x100) under a light microscope. Subsequently, areas with the highest vascularization, called 'hot spots,' were selected at x100 magnification. Microvessel counting was performed in five different 'hot spots' areas at ×200 magnification. Endothelial cells or clusters positively stained with CD31 were included in the count. Vessels in normal breast tissue, fibrosis, necrotic

Table 1. Grading of feline mammary carcinomas (Goldschmidt et al. 2017).

Histologic features		**Score**
A. Lymphovascular invasion	Absent	0
	Present	1
B. Nuclear form	< % 5 abnormal	0
	≥ % 5 abnormal	1
C. Mitotic count (10 consecutive HPF)	≤62	0
	>62	1
Total score (A+B+C)	**Grade**	
0	1	Low grade
1	2	Intermediate grade
2-3	3	High grade

(BBA: x40 magnificant; 0,55 mm diamater, Olympus BX51 microscope)

Table 2. Antibody Panel.

Antibody	Clone number	Company	Dilution Rate	Incubation Time	Cellular localization
CD31	H-3 (Mouse Monoclonal)	Santa Cruz	1:400	Room temperature/ 1 hour	Cytoplasmic
CD68	3F103 (Mouse Monoclonal)	Santa Cruz	1:50	+4°C/overnight	Cytoplasmic
CD163	GHI/61 (Mouse Monoclonal)	Santa Cruz	1:50	+4°C/overnight	Cytoplasmic
VEGF	VG-1 (Mouse Monoclonal)	Santa Cruz	1:250	Room temperature/ 1 hour	Cytoplasmic
HİF-1a	28b (Mouse Monoclonal)	Santa Cruz	1:100	+4°C/overnight	Nuclear/ Cytoplasmic

Table 3. Allred scoring method (adapted from Hameed et al (2015).

Proportion score	PS*	Intensity score	IS*
0	0	No staining	0
>0-1/100	1	Weak	1
>1/100-1/10	2	Moderate	2
>1/10-1/3	3	Intense	3
>1/3-2/3	4		
>2/3-1	5	Allred Score= PS+IS	

*PS: Proportion score, IS: Intensity score

regions, areas with inflammation, and vessels with muscle walls were excluded from the count. The average microvessel counts in the five high vascularization areas in the sections were used to calculate MVD.

Macrophages were evaluated immunohistochemically using CD68 and CD163 staining. The technique employed for macrophage counting was adapted from Monteiro et al. (2018). Initially, sections were scanned at low magnifications (x40 and x100) under a light microscope, and five areas with the highest macrophage density, referred to as 'hot spots,' were identified. Macrophage counting was performed at ×400 magnification for each area. Macrophage cells stained with CD68 and CD163 were included in the count for each area.

Statistical analysis

The statistical data analysis was conducted using the SPSS for Windows 25 software package. The Chi-square test was used for comparing groupable clinicopathological data with each other and with immunohistochemical data. The Mann-Whitney U test (for comparison between two groups) and the Kruskal-Wallis test (for comparison among more than two groups) were employed to compare mean values with other clinicopathological data. Quantitative variables were presented as mean ± standard deviation. Results were considered statistically significant at $p< 0.05$.

RESULTS

The histopathological classification of cases was conducted according to Goldschmidt et al. (2017) criteria (Table 4). Tumor types, sizes, and localization of masses, as well as information on animal species, age, and breed, were presented in Table 5 based on this classification.

Out of the 12 examined cases of mammary tumors, nine were malignant and three were benign, all of which were comprised of mastectomy materials. The ages of the cats included in the study ranged from 1 to 14 years (mean: 9.6 years). The highest incidence of mammary tumors was observed in the age range of 9–12 years (Figure 1). When evaluated by breed, the highest number of tumors was detected in the mixed breed (n = 7).

Macroscopic findings

The smallest tumor size among the cases was 2x0.8x1.2 cm, and the largest was 8x3.5x2.5 cm. The cross-sections of some cases appeared grayish-white, moist, and lobulated. In some cases, the outer parts were elastic, while the inner parts had occasional complex foci. The cut sections of these tumors were grayish-white, and areas resembling bone-like calcifications were present (Figure 2).

Histopathological Findings

The lymphovascular invasion status, tumor necrosis, mitot-

Table 4. Histologic classification of feline mammary neoplasms (Goldschmidt et al. 2017).

1. Hyperplasia/dysplasia	**3. Malignant epithelial neoplasms**	**4. Malignant epithelial neoplasms – special types**
Duct ectasia	Carcinoma – *in situ*	Squamous cell carcinoma
Lobular hyperplasia (adenosis)	Carcinoma – simple	Adenosquamous carcinoma
Regular	a. tubular	Mucinous carcinoma
With secretory activity	b. tubulopapillary	Lipid-rich (secretory) carcinoma
With fibrosis	c. cystic-papillary	Spindle cell carcinoma
With atypia	d. cribriform	Squamous cell carcinoma – spindle cell variant
Epitheliosis	Carcinoma – micropapillary invasive	Carcinoma – spindle cell variant
Papillomatosis	Carcinoma – solid	Inflammatory carcinoma
Fibroadenomatous change	Comedocarcinoma	**5. Malignant mesenchymal neoplasms – sarcomas**
Gynecomastia	Carcinoma – anaplastic	Fibrosarcoma
2. Benign neoplasms	Intraductal papillary carcinoma	Other sarcomas
Adenoma – simple	Ductal carcinoma	
Intraductal papillary adenoma		
Ductal adenoma		
Fibroadenoma		

Table 5. Mammary tumors in feline and information about animals.

No	Diagnosis	Race	Age	Localization	Size
1*	Tubular carcinoma	Mixed	14	No information	2x2,7x2,5 cm
2*	Solid carcinoma	Mixed	10	No information	3,5x1,5x1 cm
3*	Ciytic-papillary carcinoma	No information	10	No information	3x1,4x3,1 cm
4*	Solid carcinoma	Mixed	11	No information	2,5x2x1 cm
5*	Mucinous carcinoma	Mixed	11	Cranial mammary lobe	8x3,5x2,5 cm
6*	Tubular carcinoma	Siamese cat	8	No information	3,5x3,2x1 cm
7*	Tubulopapillary carcinoma	Mixed	13	No information	2x2x1,2 cm
8*	Ductal adenoma	No information	11	No information	2x0,8x1,2cm
9*	Simple adenoma	Mixed	9	No information	1,5x2x2,1cm
10*	Comedokarcinoma	Mixed	9	No information	5x3,6x1,1 cm
11**	Anaplastic carcinoma	Siamese cat	8	Inguinal mammary lobe	1,5x2x1,3 cm
12**	Simple adenoma	Persian cat	1	Cranial and caudal thoracic mammary lobe	4x1,2x3 cm

*: Bornova Veterinary Control Institute
**: Selcuk University Faculty of Veterinary Medicine

ic score, and grade information, along with histopathological diagnosis details and IHC results for the cases comprising the study material, are presented in Table 6. In two cases, corpora amylacea of varying sizes were found in ectatic glands and duct lumens (Figure 3).

Immunohistochemical Findings

CD31, HIF-1a, and VEGF antibodies labeled all cases with positive immunoreactivity. CD68 and CD163 labels revealed positive immunoreactivity in 5 and 7 cases, respectively. CD31 expression was observed rarely in endothelial cells of small and large blood vessels and occasionally in macrophages. VEGF expression was modest in endothelial cells and widespread or localized in granular form in the cytoplasm of tumor cells. Tumor cells primarily displayed HIF-1a in their cytoplasm and nucleus, particularly in perinecrotic areas. Macrophages labeled with CD68 and CD163 were observed individually or in clusters in the tumor stroma (Figure 4).

The MVD of benign tumors (40,87±18,79) in cats was lower compared to malignant tumors (49,64±15,22). The mean VEGF IHC staining score in benign tumors was 5.67±0.58, which was higher than in malignant tumors, 5.22±1.56. The mean HIF-1a IHC staining score was higher in benign tumors (5.00±1.73) compared to malignant tumors (3.44±1.42). The density of macrophages labeled with CD68 in benign tumors was 5.00±5.00, while it was 11.11±23.35 in malignant tumors. The density of macrophages labeled with CD163 in benign tumors (3.00±2.65) was higher than in malignant tumors

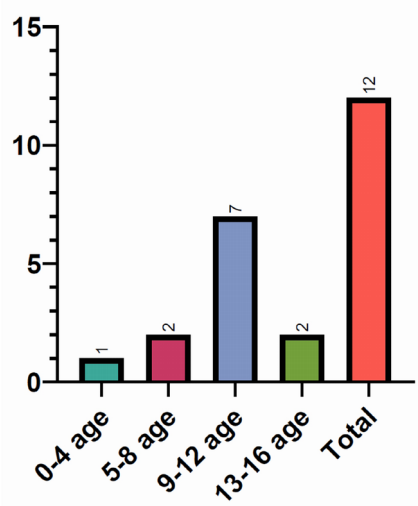

Figure 1. The distribution of mammary tumors of feline according to age.

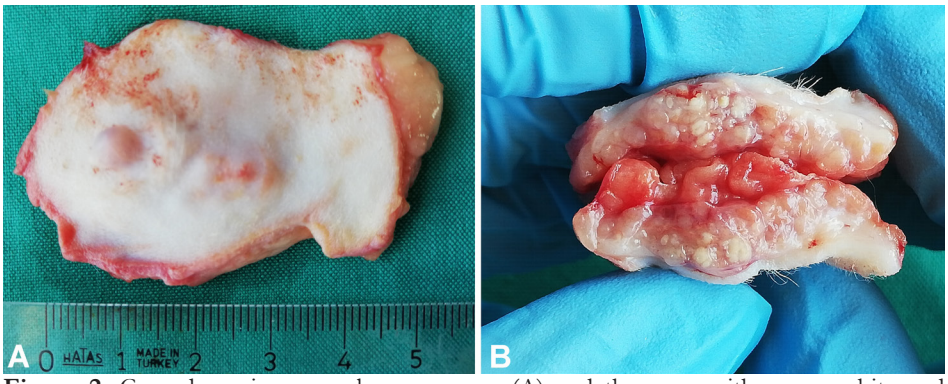

Figure 2. Comedocarcinoma, pale appearance (A) and the mass with a grey-white and lobular appearance on cut-section (B), case number:10.

Table 6. IHC scores and histopathological features of mammary tumors from cats.

No	Diagnosis	MVD (CD31)	VEGF TS	HIF-1A TS	CD68	CD163	LVI	Necrosis	Mitotic score	Grade
1	Tubular carcinoma	51	5	2	0	41	+	+	50	3
2	Solid carcinoma	37.6	6	2	29	75	+	+	82	3
3	Ciytic-papillary carcinoma	34.4	3	3	0	48	-	-	45	1
4	Solid carcinoma	28.2	8	6	0	7	-	-	25	2
5	Mucinous carcinoma	52.2	5	4	68	65	-	+	30	2
6	Tubular carcinoma	64.8	3	3	3	0	+	+	70	3
7	Tubulopapillary carcinoma	73.2	5	6	0	0	-	-	35	2
8	Ductal adenoma	55.2	5	5	0	0	-	-	-	-
9	Simple adenoma	19.6	6	4	10	5	-	-	-	-
10	Comedocarcinoma	62.8	6	6	0	0	+	+	35	3
11	Anaplastic carcinoma	42.6	6	6	0	0	+	+	85	3
12	Simple adenoma	47.8	6	2	5	4	-	-	-	-

LVI: Lenfovascular Invasion +=present, - = absent
Necrosis: + =present, - = absent
Mitotic score (BBA: x40 magnificant; 0,55 mm diamater, Olympus BX51 microscope)
TS: Total Score= Proportion Score (PS)+intensity score (IS)

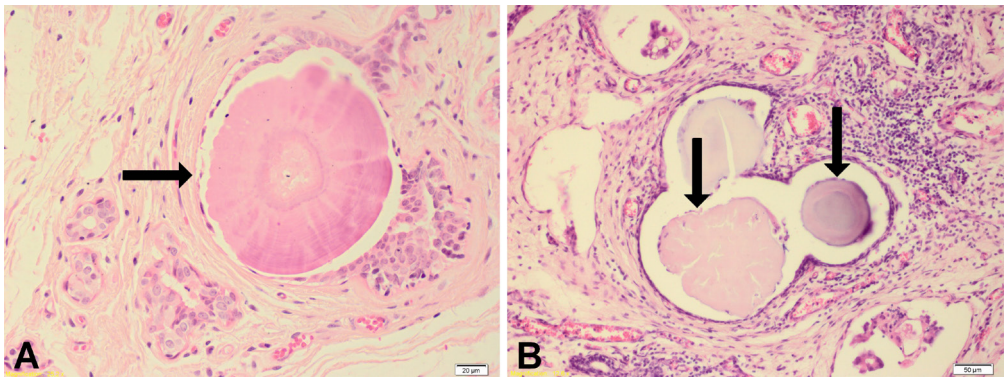

Figure 3. Corpora amylaceae of different sizes (arrows) in ectatic gland and duct lumens. A. Simple adenoma, feline (case no:9), B. Anaplastic carcinoma, feline, (case no:11).

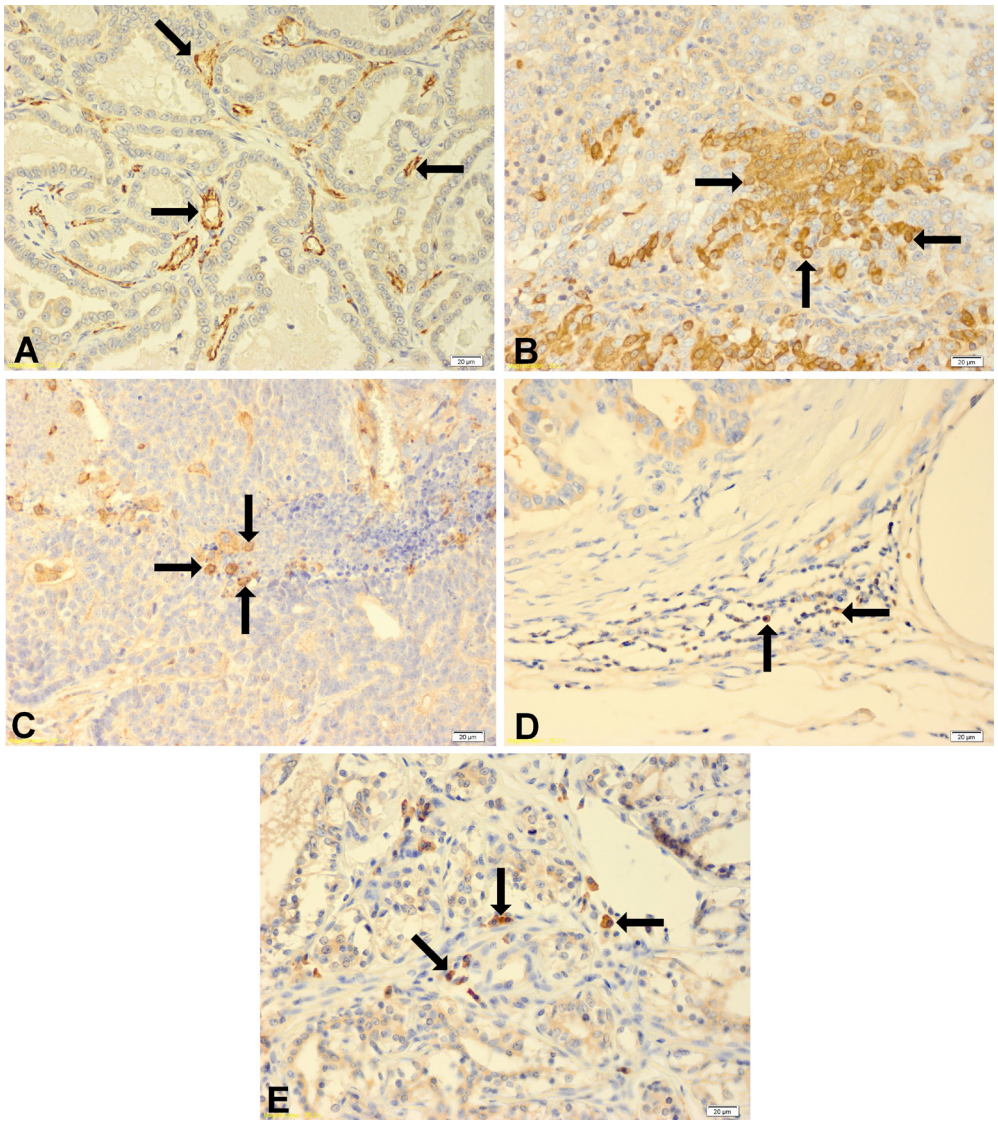

Figure 4. Tubulopapillary carcinoma, (A); Expression of CD31 in vascular endothelium among tubulopapillary structures (arrows); feline, case no:7, Bar=20 µm. Ductal adenoma, (B); Expression of VEGF in tumor cells (arrows) feline, case no:8, Bar=20 µm. Comedocarcinoma, (C);HIF-1a expression in tumor cells (arrows) around the necrotic area; feline, case no:10, Bar=20 µm. Solid carcinoma, (D); Expression of CD163 in macrophage cytoplasms (arrows);feline, case no:2, Bar=20 µm. Tubular carcinoma, (E); Expression of CD68 in macrophage cytoplasms (arrows); feline, case no:6, Bar=20 µm.

(26.22±31.02) and the difference between them was statistically insignificant in all the above-mentioned data. ($p > 0.05$) (Figure 5). In the examined malignant tumors, no statistically significant relationship was found between IHC results and histological grade, tumor size, mitotic score, LVI, and necrosis features ($p > 0.05$) (Table 7).

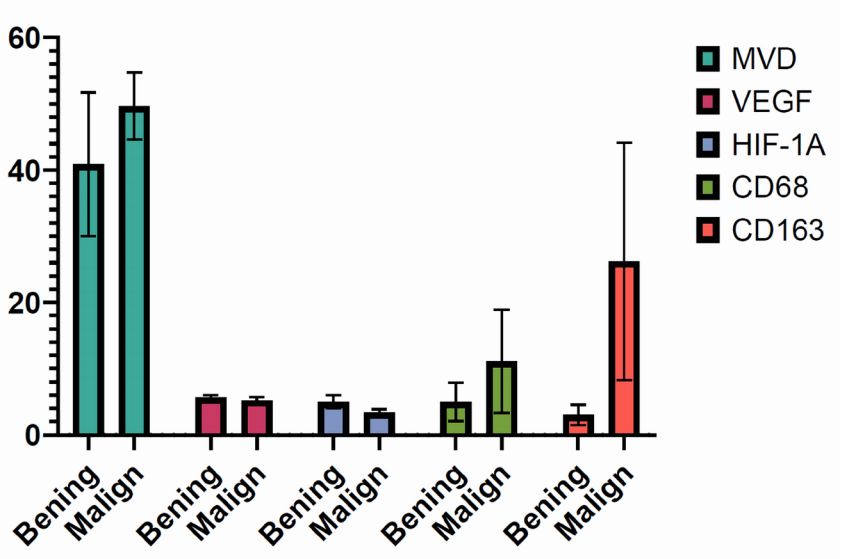

Figure 5. IHC Results in benign and malignant tumors (Mean±sd)

Table 7. Immunohistochemical results and histopathological clinicopathological features of malignant tumors in feline (Mean±sd)

		n	MVD	VEGF	HIF-1A	CD68	CD163
Histological Grade*	1	1	34.40±0.00	3.00±0.00	3.00±0.00	-	48.00±0.00
	2	3	51.20±22.52	6.00±1.73	3.00±1.00	22.67±39.26	24.00±35.68
	3	5	51.76±12.01	5.20±1.30	3.80±1.79	6.40±12.70	23.20±33.97
	p		0.509	0.364	0.820	0.864***	0.678
Tumor size *	2-3 cm	4	48.75±18.82	6.00±1.41	3.00±1.15	-	12.00±19.61
	>3cm	5	50.36±14.00	4.60±1.52	3.80±1.64	20±29.47	37.60±35.66
	p		1.000	0.413	0.556	---	0.413
Mitotic Score**	≤62	6	50.30±16.89	5.33±1.63	3.17±1.17	11.33±27.76	26.83±28.07
	>62	3	48.33±14.48	5.00±1.73	4.00±2.00	10.67±15.95	25.00±43.3
	p		1.000	1.000	0.548	0.381	0.905
LVI**	Present	5	51.76±12.01	5.20±1.30	3.80±1.79	6.40±12.70	23.20±33.97
	Absent	4	47.00±20.21	5.25±2.06	3.00±0.82	17.00±34.00	30.00±31.51
	p		0.730	0.730	0.556	0.905	0.556
Necrosis**	Present	8	46.70±13.25	5.25±1.67	3.38±1.51	12.50±24.56	29.50±31.45
	Absent	1	73.20±0.00	5.00±0.00	4.00±0.00	-	-
	p		0.222	0.889	0.667	---	---

(*) Kruskall Wallis Varyans Analysis, (**) Mann Whitney-U test, (***) Since there is no grade 1 CD68 staining, Mann Whitney-U test was performed.

DISCUSSION

This study aimed to investigate the relationship between CD31, HIF-1a, VEGF, CD68, and CD163 antibodies, which are used to investigate hypoxia, angiogenesis, and malignancy in feline mammary tumors, and their relationship with histopathological changes using immunohistochemical methods.

It has been reported that more than 85% of mammary tumors in felines are malignant (Karabolovski et al., 2020; Murphy, 2008). In the study, out of 12 mammary gland tumors diagnosed in female cats, 9 (75%) were malignant, and 3 (25%) were benign tumors.

Although the occurrence rate of mammary tumors in felines shows a noticeable increase after the age of 9, the highest diagnosis is reported to be between the ages of 10-12 (Goldschmidt et al., 2017; Hayes and Mooney, 1985). In the study, the ages of felines with mammary tumors ranged from 1 to 14 years, with an average age of 9.6 years. As for the age range, it was most commonly observed between 9 and 12 years, consistent with literature data (n=7).

Certain breeds, such as Siamese, Persian, and domestic shorthair cats, are reported to be more prone to mammary tumors (Amorim et al., 2006; Goldschmidt et al., 2017; Hayes et al., 1981; Shida et al., 2010). In the study, the highest incidence of mammary tumors in cats was observed in the mixed breed (n=7). Although this result is not very reliable due to the small number of materials evaluated, it is concluded that it cannot be definite regarding the breed characteristics in Konya and Izmir regions due to the fact that the samples of cats belonging to mixed breeds were more common in the date range in which the samples were examined.

Studies on benign and malignant mammary tumors have reported that MVDs are higher in malignant tumors than benign tumors (Jakab et al., 2008; Raposo et al., 2014; Restucci et al., 2000; Sleeckx et al., 2014). In our study, the MVD in malignant tumors in cats was higher than in benign tumors, in line with the literature data. However, the difference was statistically insignificant in both groups ($p>0.05$).

In studies, VEGF was found to be higher in malignant tumors compared to benign tumors (Qui et al., 2008; Restucci et al., 2002). Unlike these studies, in our study, VEGF was higher in benign tumors than in malignant tumors. This difference may be due to the fact that the studies were conducted on canine mammary tumors or that the number of benign mammary tumors used in our study was lower than the number of malignant tumors. Studies exploring the connection between angiogenesis and VEGF in cats are scarce. Islam et al. (2012) reported a positive correlation between VEGF expression and MVD in feline mammary tumors. Millanta et al. (2002) conducted a different study on feline mammary tumors and reported that, unlike other researchers, they did not detect a significant relationship between VEGF and angiogenesis. In our study, correlation analysis could not be performed due to the low number of materials.

Many studies have presented evidence that HIF-1a is effective in the development of aggressive tumors (Shin et al., 2015; Madej et al., 2013). The mean HIF-1a IHC score was higher in benign tumors than in malignant tumors, and the statistical difference was insignificant ($p > 0.05$). In addition, we couldn't find any relationship between clinicopathological features. Despite studies reporting a relationship between histological grade and HIF-1a, our results underscore the need for large-scale studies on this issue.

Studies reported that the number of tumor-associated macrophages was significantly higher in malignant tumors than in benign tumors. (Raposo et al., 2014; Raposo et al., 2015). Although CD68 and CD163 numbers in feline tumors were statistically insignificant, similar to the studies, they were higher in malignant tumors than benign tumors, and similar to these studies, we could not detect a significant relationship between them and features such as tumor size, histological grade, necrosis and lymph node metastasis in feline mammary tumors ($p>0.05$).

CONCLUSION

No statistically significant difference was found between the IHC results of the tumors used in the study and histopathological and clinicopathological features ($p>0.05$). This may have been due to insufficient sample numbers. Therefore, it would be more accurate to conduct multicenter studies examining histopathological and clinicopathological characteristics with more materials. The study concluded that presenting the data would be appropriate to contribute to the fields of veterinary medicine and veterinary oncology.

DECLARATIONS

Ethics Approval

For the study, Selcuk University, Faculty of Veterinary Medicine Experimental Animal Production and Research Center Ethics Committee (SUVDAMEK) approval was obtained (Date: 31.01.2019, Decision No:2019/04).

Conflict of Interest

The authors declared no potential conflicts of interest with respect to the research, authorship, and/or publication of this article.

Consent for Publication

Not applicable.

Author contribution

Idea, concept and design: EG, FH

Data collection and analysis: EG

Drafting of the manuscript: EG, FH

Critical review: FH

Data Availability

The datasets during and/or analyzed during the current study available from the corresponding author on reasonable request (E. GUNER).

Acknowledgements

This research was supported by Selçuk University Scientific

Research Projects Coordination Office (BAP) with the project number 18202064 and summarised from the part of Erdinç Güner's PhD thesis on feline mammary tumours.

This study encompasses the section on cat mammary tumors from a PhD thesis project that included dog and cat mammary tumors brought to Selçuk University Faculty of Veterinary Medicine and Bornova Veterinary Control Institute between 2015 and 2019 (Guner, 2020). The data obtained from the investigation of dog mammary tumors within the same project have been previously shared to contribute to the field of veterinary oncology (Guner and Hatipoğlu, 2023).

REFERENCES

Amorim, F.V., Souza, H.J.M., Ferreira, A.M.R., & Fonseca, A.B.M. (2006). Clinical, cytological and histopathological evaluation of mammary masses in cats from Rio de Janeiro, Brazil. Journal of Feline Medicine and Surgery, 8(6), 379-388. https://doi.org/10.1016/j.jfms.2006.04.004

Ates, M. B. (2019). Immunohistochemical investigation of effects of Nigella Sativa l. and Thymoquinone on aflatoxin biotransformation in liver in broilers (Publication No: 117O872) [Doctoral thesis, Selcuk Unıversity].

Balkwill, F.R., Capasso M., & Hagemann T. (2012). The tumor microenvironment at a glance. Journal of Cell Science, 125(pt23), 5591-6. https://doi.org/10.1242/jcs.116392

Choudhury, K. R., Yagle, K. J., Swanson, P. E., Krohn, K. A., & Rajendran, J. G. (2010). A robust automated measure of average antibody staining in immunohistochemistry images. The Journal of Histochemistry and Cytochemistry, 58(2), 95–107. https://doi.org/10.1369/jhc.2009.953554

Goldschmidt M.H., Peña L. & Zappulli V. (2017). Tumors of the mammary gland. In: Donald J. Meuten(5th ed.),Tumors in Domestic Animals, (p.723-65). Ames, Iowa: Wiley/Blackwel

Guner, E. (2020). Investigation of tumor microenvironment, hypoxia and angiogenesis by immunohistochemical and histopathological methods in mammary tumors of dogs and cats (Publication No: 648626)[Doctoral thesis, Selcuk Unıversity].

Guner, E. & Hatipoğlu, F. (2023). Investigation of tumor microenvironment, hypoxia and angiogenesis by immunohistochemical and histopathological methods in canine mammary tumors. Veterinarski Arhiv, 93 (6):665-682. https://doi.org/10.24099/vet.arhiv.2007

Hameed, K. A., Banumathi, A., & Ulaganathan, G. (2015). Performance evaluation of maximal separation techniques in immunohistochemical scoring of tissue images. Micron, 79, 29-35. https://doi.org/10.1016/j.micron.2015.07.013

Hayes, A. A., & Mooney, S. (1985). Feline mammary tumors. The Veterinary Clinics of North America. Small Animal Practice, 15(3), 513–520. https://doi.org/10.1016/s0195-5616(85)50054-6

Hayes Jr, H. M., Milne, K. L. & Mandell, C. P. (1981). Epidemiological features of feline mammary carcinoma. The Veterinary Record, 108(22), 476–479. https://doi.org/10.1136/vr.108.22.476

Islam, M. S., Matsumoto, M., Hidaka, R., Miyoshi, N. &Yasuda, N. (2012). Expression of NOS and VEGF in feline mammary tumours and their correlation with angiogenesis. The Veterinary Journal, 192: 338-344. https://doi.org/10.1016/j.tvjl.2011.08.032.

Jakab, C., Halász, J., Kiss, A., Schaff, Z., Szász, A.M., Rusvai, M., Tóth, Z.A., & Kulka, J. (2008). Evaluation of microvessel density (mvd) in canine mammary tumours by quantitative ımmunohistochemistry of the claudin-5 molecule. Acta Veterinaria Hungarica, 56(4), 495-510. https://doi.org/10.1556/AVet.56.2008.4.7.

Karabolovski, N., Pejcinovska, N., Dameski, P., Dodovski, P., Zdraveski, I & Stojanovski, S. (2020). Feline mammary tumors, prevalence and pathohıstologıcal classıfıcatıon. Horizons, 8, 61-68. https:/doi.org/10.20544/HORIZONS.B.03.1.16.P07

Madej, J.A., Madej, J. P., Dziegiel, P., Pula, B. & Nowak, M. (2013): Expression of hypoxia-inducible factor-1α and vascular density in mammary adenomas and adenocarcinomas in bitches. Acta Veterinaria Scandinavica, 55, 73. https://doi.org/10.1186/1751-0147-55-73.

Mantovani, A., & Locati, M. (2013). Tumor-associated macrophages as a paradigm of macrophage plasticity, diversity, and polarization: lessons and open questions. Arteriosclerosis, Thrombosis, and Vascular Biology, 33(7), 1478–1483. https://doi.org/10.1161/ATVBAHA.113.300168.

McNamara, D. A., Harmey, J. H., Walsh, T. N., Redmond, H. P. & Bouchier Hayes, D. J. (1998). Significance of angiogenesis in cancer therapy. British Journal of Surgery, 85(8), 1044-1055.

McNeil, B., Papandreou, I., & Denko, N. C. (2016). Hypoxic reprograming of tumor metabolism, matching environmental supply with biosynthetic demand. Tumor Hypoxia, 147.

Millanta, F., Lazzeri, G., Vannozzi, I., Viacava, P. & Poli, A. (2002). Correlation of vascular endothelial growth factor expression to overall survival in feline invasive mammary carcinomas. Veterinary Pathology, 39, 690-696. https://doi.org/10.1354/vp.39-6-690.

Misdorp, W. (2002). Tumors of the mammary gland. In: Donald J. Meuten(5th ed.),Tumors in Domestic Animals, (p.575-599). Ames, Iowa: Wiley/Blackwell. https://doi.org/10.1002/9780470376928.ch12

Monteiro, L. N., Rodrigues, M. A., Gomes, D. A., Salgado, B. S., & Cassali, G. D. (2018). Tumour-associated macrophages: Relation with progression and invasiveness, and assessment of M1/M2 macrophages in canine mammary tumours. The Veterinary Journal, 234, 119-125. https://doi.org/10.1016/j.tvjl.2018.02.016.

Murdoch, C., Giannoudis, A., & Lewis, C. E. (2004). Mechanisms regulating the recruitment of macrophages into hypoxic areas of tumors and other ischemic tissues. Blood, 104(8),

2224-2234. https://doi.org/10.1182/blood-2004-03-1109

Murphy, S. (2008). Mammary tumours in dogs and cats. In Practice, 30(6), 334-339. https://doi.org/10.1136/inpract.30.6.334

Qiu, C. W., D. G. Lin, J. Q. Wang, C. Y. Li, & Deng, G. Z. (2008). Expression and significance of PTEN and VEGF in canine mammary gland tumours. Veterinary Research Communications, 32, 463. https://doi.org/10.1007/s11259-008-9049-7.

Rapisarda, A., & Melillo, G. (2009). Role of the hypoxic tumor microenvironment in the resistance to anti-angiogenic therapies. Drug Resistance Updates, 12(3), 74-80. https://doi.org/10.1016/j.drup.2009.03.002.

Raposo, T., Gregório, H., Pires, I., Prada, J. & Queiroga, F. L. (2014). Prognostic value of tumour□ associated macrophages in canine mammary tumours. Veterinary and Comparative Oncology, 12(1), 10-19. https://doi.org/10.1111/j.1476-5829.2012.00326.x.

Raposo, T. P., Pires, I., Carvalho, M. I., Prada, J., Argyle, D. J. & Queiroga, F. L. (2015). Tumour-associated macrophages are associated with vascular endothelial growth factor expression in canine mammary tumours. Veterinary and Comparative Oncology, 13, 464-474. https://doi.org/10.1111/vco.12067.

Restucci, B., De Vico ,G., & Maiolino, P. (2000). Evaluation of angiogenesis in canine mammary tumors by quantitative platelet endothelial cell adhesion molecule immunohistochemistry. Veterinary Pathology, 37(4), 297-301. https://doi.org/10.1354/vp.37-4-297

Restucci, B., Papparella, S., Maiolino, P. & De Vico, G. (2002): Expression of vascular endothelial growth factor in canine mammary tumors. Veterinary Pathology, 39, 488-493. https://doi.org/10.1354/vp.39-4-488.

Shin, J. I., Lim, H. Y., Kim, H. W., Seung, B. J. & Sur, J. H. (2015). Analysis of hypoxia-inducible factor-1α expression relative to other key factors in malignant canine mammary tumours. Journal of Comparative Pathology, 153, 101-110. https://doi.org/10.1016/j.jcpa.2015.05.004.

Sleeckx, N., Van Brantegem, L., Van den Eynden, G., Fransen, E., Casteleyn, C., Van Cruchten, S. & Van Ginneken, C. (2014). Angiogenesis in canine mammary tumours: a morphometric and prognostic study. Journal of Comparative Pathology, 150(2-3), 175-183. https://doi.org/10.1016/j.jcpa.2013.09.005.

Sun, Z., Wang, S. & Zhao, R. C. (2014). The roles of mesenchymal stem cells in tumor inflammatory microenvironment. Journal of Hematology & Oncology, 7(1), 1-10.https://doi.org/10.1186/1756-8722-7-14

Vaupel, P. (2004). Tumor microenvironmental physiology and its implications for radiation oncology. In Seminars in Radiation Oncology (Vol. 14, No. 3, pp. 198-206). WB Saunders. https://doi.org/10.1016/j.semradonc.2004.04.008

Vaupel, P. & Mayer, A. (2007). Hypoxia in cancer: significance and impact on clinical outcome. Cancer and Metastasis Reviews, 26, 225-239.https://doi.org/10.1007/s10555-007-9055-1

Weidner, N., Semple, J. P., Welch, W. R. & Folkman, J. (1991). Tumor angiogenesis and metastasis—correlation in invasive breast carcinoma. New England Journal of Medicine, 324(1), 1-8. https://doi.org/10.1056/NEJM199101033240101

Zhang, Q. W., Liu, L., Gong, C. Y., Shi, H. S., Zeng, Y. H., Wang, X. Z. & Wei, Y. Q. (2012). Prognostic significance of tumor-associated macrophages in solid tumor: a meta-analysis of the literature. PloS one, 7(12), e50946. https://doi.org/10.1371/journal.pone.0050946.

Medit Vet J, 9(3): 364-370, 2024
DOI: 10.24880/meditvetj. 1611164

Research Article

Investigations of insulin resistance in obese dogs

Ecenur Esra Sarıkaya[1], Halil İbrahim Gökce[2]

[1]Department of Internal Medicine, Institute of Health, Burdur Mehmet Akif Ersoy Üniversity, Burdur, Türkiye
[2]Department of Internal Medicine, Faculty of Veterinary Medicine, Burdur Mehmet Akif Ersoy University, Burdur, Türkiye

Key Words:
dog
insulin resistance
obese
overweight

Received : 27 March 2024
Revised : 13 May 2024
Accepted : 29 July 2024
Published : 31 December 2024
Article Code : 1611164

Correspondence:
Hİ. GÖKCE
(higokce@mehmetakif.edu.tr)

ORCID
EE. SARIKAYA : 0000-0002-5311-4736
Hİ. GÖKCE : 0000-0002-4458-6671

ABSTRACT

The aim of the study was to investigate insulin resistance in overweight and obese dogs. Obesity is excessive fat accumulation in the body and is defined as being 30% above the ideal body weight. In the study, a total of 30 dogs were divided into 3 equal groups: ideal weight, overweight and obese. Fasting serum samples were collected and used to measure insulin (INS) and asprosin (ASP) levels using dog-specific ELISA kits. Glucose (GLU) and fructosamine (FRU) were also determined using biochemistry analyzer and Idexx test kits, respectively. HOMA-IR (homeostasis model assessment of insulin resistance), HOMA-β% (homeostasis model assessment of β cell function) and insulin-glucose ratio (IGR) were calculated using glucose and insulin values. In the study, ASP ($p<0.05$), INS ($p<0.05$), HOMA-β ($p<0.05$) and IGR ($p<0.05$) values of both overweight and obese dogs were higher than the ideal weight group. Very strong correlations were detected between INS and HOMA-IR ($p<0.01$), HOMA-β ($p<0.01$), IGR ($p<0.01$) in both groups. It was determined that insulin resistance developed in 60% of overweight dogs and 90% of obese dogs. It is thought that HOMA-IR, HOMA-β, IGR, INS, FRU and ASP can be used in the evaluation of insulin resistance in obese dogs.

INTRODUCTION

Obesity is defined as accumulation of excess fat in the body. It is the most common nutrition-related health disorders in dog and cats. It generally occurs as a result of energy imbalance and develops when the energy consumed is more than the energy used (Preet et al., 2021; Ronja and Kölle, 2021). Various predisposing factors contribute to the development of obesity in dogs. These predisposing factors include inactivity, high-energy diet, race, gender, neutering, and the presence of some metabolic disorders including hyperadrenocorticism, hypothyroidism, and insulinoma (Buishand and Kirpensteijn, 2023; Preet et al., 2021; Ronja and Kölle, 2021). Obesity is a growing chronic health problem in dogs that 22-66 percent of dogs are claimed to be obese (Munoz-Prieto et al., 2018; Preet et al., 2021; Ronja and Kölle, 2021). Studies have revealed that cancer, diabetes mellitus (DM), heart diseases, hypertension, joint diseases and skin diseases are more common in obese dogs (Preet et al., 2021; Ramos and Castillo, 2020; Ronja and Kölle, 2021). Therefore, obesity negatively affects the health and welfare of dogs.

Insulin resistance is the phenomenon of tissues such as liver, muscle and fat not responding to insulin. In this case, the pancreas produces more insulin, and on the other hand, blood sugar rises because glucose cannot be used in energy production. Therefore, insulin resistance develops and this ends with the development of type 2 DM. Over time, these animals develop complications such as obesity, high blood pressure, high cholesterol and triglycerides, and low HDLP (Marchi et al., 2022; Preet et al., 2021; Ronja and Kölle, 2021).

Insulin resistance has been shown to be more common in both obese people (Li et al., 2021; Xu et al., 2021) and obese pets (Ramos and Castillo, 2020), and a relationship between type 2 DM and obesity is noted. In studies, increases in parameters such as HOMA-IR (homeostasis model assessment of insulin resistance), HOMA-β% (homeostasis model assessment of β cell function) insulin, glucose, triglyceride, total cholesterol and high density lipoprotein (HDLP) were determined in obese dogs (Imamura et al., 2013; Preet et al., 2021; Ronja and Kölle, 2021; Sung et al., 2010; Villar and Bravo, 2022). Additionally, significant increases in blood asprosin levels have been detected in obese people, and a relationship between asprosin and obesity and insulin resistance has been determined (Li et al., 2021; Naiemian et al., 2020; Silistre and Hatipoglu, 2020; Xu et al., 2021). There are many studies on obesity and insulin resistance in humans, but there are very limited studies on the development of insulin resistance in obese dogs. Asprosin is also suggested as a biomarker to identify insulin resistance in obese adults and children (Naiemian et al., 2020; Romere et al., 2016; Silistre and Hatipoğlu, 2020). However, there is no study on asprosin and insulin resistance in obese cats and dogs

Therefore, the aim of this study was to investigate insulin resistance in overweight and obese dogs. Additionally, the diagnostic value of asprosin in determining insulin resistance in these dogs was also investigated.

To cite this article:
Sarıkaya EE, Gökce Hİ. Investigations of insulin resistance in obese dogs. Medit Vet J. 2024; 9(3): 364-370.

MATERIALS and METHODS

Dogs

A total of 30 owned dogs were used in the research. Dogs were divided into 3 groups: 10 overweight (n=10), obese (n=10), and ideal weight (n=10). The dogs were of different ages, breeds and genders.

This study was approved by the Animal Ethics Committee (AEC), Burdur Mehmet Akif University, Türkiye (No:929/2022).

Evaluation of Obesity

Body condition score (BCS) was used to assess obesity in dogs as described elsewhere (Chun et al., 2019; Williams and Buzhardt, 2022). Thus, BCS in dogs was scored in the range of 1-9. BCS 4-5/9 was considered ideal weight, while BCS 6/9 and 7-9/9 were considered overweight and obese, respectively. Dogs with any systemic disease and those that had surgery within 6 weeks were not included in the study.

Blood Samples

Fasting (8-12 hours) blood samples were taken from each animal into plane tubes and centrifuged at 4000 rpm for 20 minutes to prepare serum samples. These serum samples were then stored at -80°C until used.

Biochemical analysis

In the study, serum concentrations of insulin (SunRed, catalog number: 201-15-0201, Shangai-CHINA) and asprosin (My-Biosource catalog number: MBS2612398, San Diego-USA) were detected by using dog-specific ELISA kits. ELISA tests were applied according to the manufacturer's recommendations. Serum fructosamine values were determined by using dog-specific Idexx test kits (Idexx Catalyst One Chemistry Analyzer, USA). Serum glucose levels were measured by using a biochemistry device (Roche cobas integra 400 Plus, USA). Insulin and glucose values were then used to calculate HOMA-IR, HOMA-β and insulin-glucose ratio (IGR) for each dog. The formulas used in HOMA-IR, HOMA-β and IGR calculations are as shown below.

HOMA-IR: fasting glucose (mg/dl) x fasting insulin (mU/L)/405

HOMA-β: 20 x fasting insulin (µIU/ml)/fasting glucose (mmol/L)-3.5.

IGR: fasting insulin (mU/ml)/fasting glucose (mmol/L).

In the study, 2-fold dilutions were made for standard insulin (80mU/L-6.25mU/L) and asprosin (10ng/ml-0.156ng/ml) and the optical density (OD) of each well for insulin and asprosin was determined with a micro-ELISA plate reader (96A, Minray, CHINA) at a test wave-length of 450 nm. Regression analysis was performed with the OD values of the obtained standard dilutions in the Excel program, and the formulas derived for insulin and asprosin were used to calculate their levels in the test samples as follows.

Insulin in the test samples was calculated using the formulas $y=66.459x-32967$ ($R^2=0.998$) and asprosin $y=4.9091x-1.4838$ ($R^2=0.9992$).

Statistical analysis

The normality of the distribution of the data obtained in the study was determined by the Kolmogorov-Smirnov test. One-Way ANOVA (posthoc Duncan) test was used to analyze

Table 1. Parameters of Ideal weight, Overweight and Obese dogs (mean±standard deviation. SD)

Parameters	Ideal weight (n=10)	Overweight (n=10)	Obese (n=10)	Median (min-max)
ASP (ng/mL)	1.38±0.26 [b]	2.15±0.61 [a]	1.96±0.53 [a]	1.69 (1.14-3.2)
GLU (mg/dL)	74.87±12.00 [a]	74.7±10.49 [a]	86.5±19.39[a]	76.5 (56-126)
INS (mU/L)	13.49±5.19 [b]	34.42±22.6 [a]	43.13±27.75[a]	20.32 (7.3-82.4)
FRU (µmol/L)	273±34.91 [b]	308±42.13[ab]	344.16±42.13 [a]	305 (194-427)
HOMA-IR	2.44±0.88 [b]	6.17±3.86 [ab]	9.44±6.64[a]	3.7 (1.36-19.73)
HOMA-β (%)	64.06±33.62 [b]	171.74±132.6 [a]	178.61±115.88 [a]	108.36 (3-438)
IGR (µU/mL)	0.18±0.09 [b]	0.48±0.36[a]	0.5±0.32 [a]	0.31 (0.09-1.22)

ASP: asprosin. GLU: glucose. INS: insulin. FRU: fructosamine. HOMA-IR: homeostasis model assessment of insulin resistance. HOMA-β: homeostasis model assessment of beta-cell function. IGR: Insulin/glucose ratio. The significance of the deviations between the values of the groups is indicated with superscript letters. and the presence of different letters on the same line indicates the significance between the groups ($p<0.05$).

the significance of data differences between groups. Additionally, the correlation between parameters was analyzed with the Pearson's correlation coefficient (r) test. In the correlation test, negative (-) or positive (+) correlation values (r) were accepted as very weak (-,+ 0-0.19), weak (-,+ 0.2-0.39), moderate (-,+ 0, 4 -0.59), strong (-,+ 0.6-0.79) and very strong (-,+ 0.8-1.00) as defined by Meghanathan (2016). In the study, the cut-off value of each parameter in overweight or obese dogs was determined by ROC analysis and individual increases or decreases for each value were determined according to the cut-off values. As a result of ROC analysis, the parameters were given as AUC (Area), %sensitivity (%sns), %specificity (%sps) and cut-off value. Significance levels were accepted as $p<0.05$. Parameters were expressed as mean±standard deviation (mean±SD), median, minimum-maximum (min-max). SPSS 27.0 for Windows® package program (version 27.0 for Windows, SPSS Inc, Chicago) was used to perform the statistical analysis.

RESULTS

In the study, serum concentrations of ASP ($p<0.05$), INS ($p<0.05$), HOMA-β ($p<0.05$) and IGR ($p<0.05$) were significantly higher in both overweight and obese dogs than ideal weight dogs. Additionally, FRU ($p<0.01$) and HOMA-IR ($p<0.01$) values of obese dogs were found to be higher than those of ideal weight group, however, these parameters of obese dogs were not statistically different those of overweight dogs (Table 1).

In the study, cut-off values were calculated for each parameter in the ROC analysis (Table 2), and the number and percentages of dogs showing an increase for a parameter were calculated (Table 3). In the obese group, increases in ASP, GLU, INS, FRU, HOMA-IR, HOMA-β and IGR values were detected in 8(80%), 9(90%), 9(90%), 10(100%), 9(90%), 8(80%) and 7(70%) dogs, respectively (Table 3). However, an increase in these parameters was detected in fewer dogs in the overweight group than in obese dogs (Table 3).

Table 2. Cut-off values of the parameters.

	AUC (Area)	Cut-off (95 confidence intervals) (lower-upper bound%)	p value	sensitivity%-specificity%
ASP (ng/mL)	0.125	1.62 (0-0.273)	0.002	31.8-75
GLU (mg/dL)	0.338	76.5 (0.124-0.553)	0.181	40.9-75
INS (mU/L)	0.227	15.89 (0.063-0.392)	0.024	36.4-62.5
FRU (µmol/L)	0.151	295.5 (0.013-0.288)	0.004	27.3-75
HOMA-IR	0.216	2.4 (0.056-0.376)	0.019	27.3-75
HOMA-β (%)	0.239	60.23 (0.07-0.407)	0.031	31.8-62.5
IGR (µU/mL)	0.253	0.175 (0.082-0.423)	0.041	31.8-62.5

ASP: asprosin. GLU: glucose. INS: insulin. FRU: fructosamine. HOMA-IR: homeostasis model assessment of insulin resistance. HOMA-β: homeostasis model assessment of beta-cell function. IGR: Insulin/glucose ratio.

Table 3. Number and percentages of dogs showing increases in parameters.

Parameters	Cut-off	Overweight (n=10)	Obese (n=10)
ASP (ng/mL)	1.62	7(70%)	8(80%)
GLU (mg/dL)	76.5	6(60%)	9(90%)
INS (mU/L)	15.89	7(70%)	9(90%)
FRU (µmol/L)	295.5	4(40%)	10(100%)
HOMA-IR	2.4	6(60%)	9(90%)
HOMA-β (%)	60.23	6(60%)	8(80%)
IGR (µU/mL)	0.175	6(60%)	7(70%)

AASP: Asprosin. GLU: glucose. INS: insulin. FRU: fructosamine. HOMA-IR: homeostasis model assessment of insulin resistance. HOMA-β: homeostasis model assessment of beta-cell function. IGR: Insulin/glucose ratio.

Pearson correlation test was applied to determine correlations between parameters obtained from overweight and obese dogs. As a result of the analyses, very strong positive correlations were detected between INS and HOMA-IR, HOMA-β and IGR, between HOMA-IR and HOMA-β and IGR, and also between HOMA-β and IGR ($p<0.01$).

Asprosin is produced from adipose tissue in cases of hunger and anorexia and stimulates both glucose production from the liver and appetite by crossing the brain barrier (Duerrschmid et al., 2017; Li et al., 2021). Blood asprosin levels are found to be high in type 2 DM cases with insulin resistance (Li et al., 2021; Naiemian et al., 2020; Wang et al., 2018). However,

Table 4. Correlation coefficient (r) values between parameters of overweight and obese dogs.

Groups		ASP	INS	GLU	FRU	HOMA-IR	HOMA-β	IGR
Overweight	**ASP**	1	0.279	-0.059	0.578	0.294	0.249	0.257
	INS		1	-0.330	-0.150	0.947**	0.962**	0.961**
	GLU			1	0.069	-0.029	-0.558	-0.560
	FRU				1	-0.106	-0.189	-0.182
	HOMA-IR					1	0.823**	0.823**
	HOMA-β						1	1.00**
	IGR							1
Obese	**ASP**	1	-0.269	0.552	0.411	-0.038	-0.463	-0.462
	İNS		1	0.196	-0.254	0.953**	0.939**	0.940**
	GLU			1	0.472	0.453	-0.109	-0.108
	FRU				1	-0.131	-0.373	-0.377
	HOMA-IR					1	0.794**	0.796**
	HOMA-β						1	1.00**
	IGR							1

ASP: Asprosin. GLU: glucose. INS: insulin. FRU: fructosamine. HOMA-IR: homeostasis model assessment of insulin resistance. HOMA-β: homeostasis model assessment of beta-cell function. IGR: Insulin/glucose ratio. Pearson's correlation test: *: $p<0.05$. **:$p<0.01$.

DISCUSSION

Body weight gain is defined as overweight or obesity and characterized by excess fat tissue increase. It is a increasing common nutritional disease in cats and dogs. An increase of 10-20% in ideal body weight is considered overweight, and increases above 20% are considered obesity (Preet et al., 2021). The causes of obesity are diverse and often result from an imbalance between energy intake and use. In other words, the dog takes in more calories than it consumes, and the excess energy consumed is stored as fat in the body. Nowadays, obesity emerges as a chronic problem, especially in animals that are housed in a home environment, neutered, and fed with a high-energy diet (Preet et al., 2021; Ronja and Kölle, 2021). It is a growing problem and 40-60% of dogs are reported to be overweight or obese (Munoz-Pierto et al., 2018; Preet et al., 2021). Studies have revealed that there is a relationship between obesity and the incidence of diseases such as osteoarthritis, diabetes mellitus, hypothyroidism, hypertension, cardiovascular diseases, respiratory distress, hyperthermia and cancer (Munoz-Pierto et al., 2018, Preet et al., 2021; Ronja and Kölle, 2021). Diabetes mellitus, hypothyroidism and hyperadrenocorticism have been reported to occur in 9%, 6% and 13% of dogs, respectively. It has also been shown that 40% of dogs with at least one of these diseases are obese (Oh, 2011; Preet et al., 2021).

it has also been shown that ASP contributes to the development of insulin resistance by impairing β cells secretion (Jung et al., 2019). Studies conducted in obese children and adults indicate that the level of asprosin in the circulation increases depending on the degree of obesity, and that there is a relationship between asprosin and obesity and insulin resistance (Li et al., 2021; Naiemian et al., 2020; Silistra and Hatipoglu, 202). In present study, ASP values of both overweight and obese dogs were found to be significantly higher than the ideal weight group ($p<0.05$). However, no statistically significant difference was found between these parameters in obese and overweight dogs. On the other hand, ASP values were found to be high in 7(70%) overweight and 8(80%) obese dogs compared to the ASP cut-off value. The reason for the high blood asprosin value determined in this study is probably due to stimulation of asprosin production from adipose tissue to balance the diet-induced energy consumption, which has been shown to decreases in obesity (Watanabe et al., 2006; Velasquez-Mieyer et al., 2003). It should not be forgotten that high blood asprosin level determined in obese dogs in this study may also play a role in the development of insulin resistance by affecting pancreatic functions as described by Jung et al (2019).

Insulin is a hormone produced by pancreatic β cells, and its production is stimulated when blood glucose rises above 110 mg/dl. It ensures that circulating glucose is taken up by cells and used for energy production. In cases where

blood glucose increases excessively, insulin induce that excess glucose is stored as glycogen in the liver and muscles (Li et al., 2021; Mehran and Johnson, 2012; Wondmkun, 2020). Maintenance of blood sugar homeostasis depends on the insulin sensitivity of tissues such as muscle, liver, and fat (Fazakerley et al., 2019; Petersen and Shulman, 2018). Insulin resistance is the phenomenon of liver, muscle and fat tissue cells not responding adequately to insulin. If this situation continues, insulin resistance develops and this situation ends with type 2 DM. In this case, pancreas begins to produce more insulin to keep blood sugar balanced. Depending on the degree of insulin resistance, blood insulin level increases while glucose level is normal/high. Over time, animals with insulin resistance develop complications such as obesity, high blood pressure, high cholesterol and triglycerides, and low HDLP (Munoz- Prieto et al., 2018; Ramos and Castillo, 2020; Wondmkun, 2020). Type-1 DM may develop in obese dogs when the pancreas cannot synthesize sufficient amounts of insulin, and insulin resistance may develop as a result of the pancreas producing excessive insulin (Petersen and Shulman, 2018). In Type 2 DM cases, glucose is constantly released from the liver and the pancreas has to constantly secrete insulin to reduce glucose (Sung et al. 2010; Villar and Bravo 2022). As a result, hyperglycemia, insulin resistance and pancreatic β cell dysfunction develop (Li et al., 2021; Titchenell et al., 2017). A link between insulin resistance and obesity has been indicated in studies. Diet-related energy expenditure decreases in obesity, and this decrease has been shown to be related to the degree of insulin resistance (Mehran and Johnson, 2012; Petersen and Shulman, 2018; Watanabe et al., 2006). Insulin resistance accompanied by hyperinsulinemia reduces diet-induced energy consumption despite increased appetite and decreased fat oxidation (Kasuga, 2006; Watanabe et al., 2006; Velasquez-Mieyer et al., 2003). In the current study, hyperinsulinaemia was observed in both obese and overweight dogs. However, no statistical difference was detected between glucose values of all the groups. According to the cut-off values, INS and GLU levels increased in 9 (90%) of the obese dogs, while INS and GLU levels increased in 7 (70%) and 6 (60%) of the overweight dogs, respectively. It has been reported that plasma insulin levels increase and glucose levels are normal or high due to the development of insulin resistance. (Sung et al., 2010; Villar and Bravo, 2022). Therefore, in this study, more insulin is probably produced by the pancreas to keep plasma glucose values at normal levels. Despite insulin resistance, glucose was kept at normal levels in some dogs, while in others this was not achieved (Sung et al., 2010; Villar and Bravo, 2022).

Fructosamine and HbA1C are used to monitor changes in blood glucose levels over the previous days. (Oikonomidis et al., 2023; Zeugswetter, 2021). According to the updated values of fructosamine levels in dogs (Idexx), the reference range for healthy dogs is given as 177-314µmol/L. In the present study, a similar cut-off value was calculated for dogs as 295.5µmol/L. In this study, FRU levels were found to be significantly higher in obese dogs than in both overweight and ideal weight dogs ($p<0.05$). According to cut-off values, FRU values were found to be high in 4 (40%) overweight and 10 (100%) obese dogs. It is thought that the number of dogs with increased FRU values observed in the study is related to the degree of obesity and insulin resistance.

Energy metabolism has been reported to be affected in obese dogs, and in addition to increases in insulin and fructosamine levels, HOMA-IR level has also been reported to increase (Ramos and Castillo, 2020; Sung et al., 2020; Villar and Bravo,2022; Zeugswetter, 2021). HOMA-IR, HOMA-β, and IGR are suggested to be useful biomarkers in diagnosing insulin resistance and type 2 DM in humans (Imamura et al., 2013; Sung et al., 2020; Villar and Bravo, 2022). However, there is no standard cut-off value for HOMA-IR and HOMA-β in both humans and animals, and different values have been obtained in studies. It is stated that the cut-off value for HOMA-IR varies between 2.54 and 2.80, and the cut-off value for HOMA-β (%) ranged between 72% and 87%. Therefore, values above 2.5 for HOMA-IR were considered insulin resistance in humans (Chissini et al., 2020; Harbuwono et al., 2023). Furthermore, HOMA-β, below 72-87% is considered a loss of pancreatic β-cell function, and above this value is considered an increase in pancreatic β-cell function (Endukuru et al., 2020; Ghasemi et al., 2015). In the present study, the cut-off values for HOMA-IR and HOMA-β (%) were found to be 2.4 and 60.23%, respectively. HOMA-β and IGR values of overweight and obese dogs were determined to be significantly higher than the ideal weight group ($p<0.05$). Additionally, HOMA-IR values of obese dogs were higher than ideal weight dogs ($p<0.01$). However, these parameters of obese dogs were not significantly different from those of overweight dogs. According to the cut-off values, increases in HOMA-IR, HOMA-B and IGR values were observed in 9 (90%), 8 (80%) and 7 (70%) dogs in the obese group, respectively. On the other hand, increases in these parameters were detected in a smaller number of overweight dogs. Increases in HOMA-IR, HOMA-β and IGR levels indicate that more insulin is produced from pancreatic β cells in obese dogs than in the ideal weight group, but the sensitivity of the cells to insulin decreases. Most likely, the severity and duration of insulin resistance affects blood insulin and glucose levels in obese and overweight dogs.

In the present study, very strong correlations were observed between INS and HOMA-IR, between HOMA-β and IGR, between HOMA-IR and HOMA-β and IGR, and between HOMA-β and IGR in both groups. Similar correlations between obesity and asprosin, insulin resistance, HOMA-β and HOMA-IR have also been reported in obese individuals (Li et al., 2021; Silistre and Hatipoğlu, 2020; Xu et al., 2021). The existence of strong positive correlations between HOMA-IR, HOMA-β and IGR reveals that insulin resistance develops in obese dogs and these parameters can be used in the diagnosis of insulin resistance in obese dogs.

Increases in INS, ASP, FRU, HOMA-β, HOMA-IR and IGR values reveal that energy metabolism is also affected in obese dogs and insulin resistance has developed in some of obese and overweight dogs. Results of the study indicated that insulin resistance in obese dogs is more severe than in overweight dogs. The possible reason for this is that the severity and period of obesity affect the development of insulin resistance, as reported in previous studies (Mehran and Johnson, 2012; Petersen and Shulman, 2018; Watanabe et al., 2006).

CONCLUSION

In the present study, ASP, INS, FRU, HOMA-IR, HOMA-β and IGR values were high in both obese and overweight dogs, and insulin resistance developed in 60% of overweight and 90% of obese dogs. The existence of strong correlations between insulin resistance indices such as HOMA-IR, HOMA-β and IGR, and an increase in INS, FRU and ASP indicated that these parameters can be used to evaluate insulin resistance in obese dogs.

DECLARATIONS

Ethics Approval

This study was approved by the Animal Ethics Committee (AEC), Burdur Mehmet Akif University, Türkiye (No:929/2022).

Conflict of Interest

Authors do not have any conflict of interest fort his study.

Consent for Publication

Consent on publication was confirmed with approval from the Republic of Türkiye Ministry of Agriculture and Forestry, Directorate of Burdur Provincial (No: E-69877819-325.04.02-5917267).

Competing Interest

The authors declare that they have no competing interests

Author contribution

Idea, concept and design: HİG, EES

Data collection and analysis: HİG, EES

Drafting of the manuscript: HİG, EES

Critical review: HİG, EES

Data Availability

Not applicable.

Acknowledgements

This research study was supported by Burdur Mehmet Akif Ersoy University, Scientific Research Projects Coordinator ship with project number 0854-YL 22.

REFERENCES

Buishand, F.O., & Kirpensteijn, J. (2023). Canine and feline insulinoma. In: E. Monnet (Ed.). Small Animal Soft Tissue Surgery, (2nd ed., pp.785-797). Balckwell Publishing.

Chissini R.B.C., Kuschnir, M.C., Oliveira, C.L., Giannini, D.T. & Santos, B. (2020). Cut-off values for HOMA-IR associated with metabolic syndrome in the Study of Cardiovascular Risk in Adolescents (ERICA Study). Nutrition, 71, 1-5. https://doi.org/10.1016/j.nut.2019.110608

Chun, J.L., Bang, H.T., Ji , S.Y., Jeong, J.Y., Kim, M., Kim, B., Lee, S.D., Lee, Y.K., Reddy, K.E., & Kim, K.Y. (2019). A simple method to evaluate body condition score to maintain the optimal body weight in dogs. Journal of Animal Science and Technology., 61(6), 366-37. https://doi.org/10.5187/jast.2019.61.6.366

Duerrschmid, C., He, Y., Wang, C., Li, C., Bournat, J.C., Romere, C., Saha, P.K, Lee, M.E., Phillips, K.J, Jain, M., Jia, P., Zhao, Z., Farias, M., Wu, Q., Milewicz, D.M., Sutton, V.R., Moore, D.D., Butte, N.F., Krashes, M.J., Xu, Y., & Chopra, A.R. (2017). Asprosin is a centrally acting orexigenic hormone. Nature Medicine, 23(12), 1444-1456. https://doi.org/10.1038/nm.4432.

Endukuru, C.K., Gaur, G.S., Yerrabelli, D., Sahoo, J. & Vairappan, B. (2020). Cut-off Values and Clinical Utility of Surrogate Markers for Insulin Resistance and Beta-Cell Function to Identify Metabolic Syndrome and Its Components among Southern Indian Adults. J Obes Metab Syndr, 29(4), 281-291. https://doi.org/ 10.7570/jomes20071

Fazakerley, D.J., Krycer, J.R., Kearney, A.L., Hocking, S.L. & James, D.E. (2019). Muscle and Adipose Tissue Insulin Resistance: Malady without Mechanism? Journal of Lipid Research, 60(10), 1720–1732. https://doi.org/10.1194/jlr.R087510

Ghasemi, A., Tohidi, M., Derakhshan, A., Hasheminia, M., Azizi, F. & Hadaegh, F. (2015). Cut-off points of homeostasis model assessment of insulin resistance, betacell function, and fasting serum insulin to identify future type 2 diabetes: Tehran Lipid and Glucose Study. Acta Diabetologica, 52, 905–915. https://doi.org/ 10.1007/s00592-015-0730-3.

Harbuwono, D.S., Nenfiati, T.D.L., Setiati, S., Yunihastuti, E. & Tarigan, T.J.E. (2023). Defining the optimum HOMA-IR cut-off value for insulin resistance among ARV-treated HIV patients in Indonesia, Diabetes & Metabolic Syndrome: Clinical Research and Reviews, 17(2), 1-10. https://doi.org/10.1016/j.dsx.2023.102719.

Imamura, F., Mukamal, K.J., Meigs, J.B., Luchsinger, J.A., Ix, J.H., Siscovick, D.S. & Mozaffarian, D. (2013). Risk Factors for Type 2 Diabetes Mellitus Preceded by β-Cell Dysfunction, Insulin Resistance, or Both in Older Adults The Cardiovascular Health Study. American Journal of Epidemiology, 177(12), 1418–1429. https://doi.org/ 10.1093/aje/kws440.

Jung, T.W., Kim, H.C., Kim, H.U., Park, T., Park, J., Kim, U., Kim, M.K., & Jeong, J.H. (2019). Asprosin attenuates insulin signaling pathway through PKCδ-activated ER stress and inflammation in skeletal muscle. Journal of Cell Physiolgy, 234(11), 20888-20899. https:/doi.org/ 10.1002/jcp.28694

Kasuga, M. (2006). Insulin resistance and pancreatic β cell failure. Journal of Clinical Investigations, 116, 1756–1760. https://doi.org/10.1172/JCI29189

Li, Q., Hagberg, C.E., Cascales, H.S., Lang, S., Hyvönen, M.T., Salehzadeh, F., Chen, P., Alexandersson, I., Terezaki, E., Harms, M.J., Kutschke, M., Arifen, N., Krämer, N., Aouadi, M., Knibbe, C., Boucher, J., Thorell, A. & Spalding, K.L. (2021). Obesity and hyperinsulinemia drive adipocytes to activate a cell cycle program and senesce, Nature Medicine, 27, 1941-1953. https://doi.org/10.1038/s41591-021-01501-8.

Marchi, P.H., Vendramini, T.H.A., Perini, M.P., Zafalon, R.V.A., Amaral, A.R., Ochamotto, V.A., Da Silveira, J.C., Dagli, M.L.Z. & Brunetto, M.A. (2022). Obesity, inflammation, and

cancer in dogs: Review and perspectives. Frontiers, 3, 1-16. https://doi.org/ 10.3389/fvets.2022.1004122.

Mehran, A.E. & Johnson, J.D. (2012). Hyperinsulinemia Drives Diet-Induced Obesity Independently of Brain Insulin Production. Cell Metabolism, 6(5), 723-737. https://doi.org/10.1016/j.cmet.2012.10.019

Muñoz-Prieto, A., Nielsen, L.R., Dąbrowski, R., Bjørnvad, C.R., Söder, J., Lamy, E., Monkeviciene, I., jubić, B.B., Vasiu, L., Savic, S., Busato, F.,Yilmaz, Z., Bravo-Cantero, A.F., Öhlund, M., Lucena, S., Zelvyte, S., Aladrović, J., Lopez-Jornet, P., Caldin, M., Lavrador, C., Karveliene, B., Mrljak, V., Mazeikiene, J., & Tvarijonaviciute, A. (2018). European dog owner perceptions of obesity and factors associated with human and canine obesity. Scientific reports, 8, 1-10. https:/doi.org/10.1038/s41598-018-31532-0

Naiemian, S., Naeemipour, M., Zarei, M., Najaf, M.L., Gohari, A., Behroozikhah, M.R., Heydari, H. & Miri, M. (2020). Serum concentration of asprosin in new-onset type 2 diabetes. Diabetology and Metabolic Syndrome, 12(65), 1-8. https://doi.org/10.1186/s13098-020-00564-w.

Oh, W. (2011). Prevalence and risk factors for obesity in dogs and cats. In 36th World Small Animal Veterinary Congress, Jeju/Korea. pp: 244-246.

Oikonomidis, I.L., Tsouloufi, T.K., Tzenetidou, Z., Ceron, J.J., Tvarijonaviciute, A., Konstantinidis, A.O. & Soubasis, N. (2023). Diagnostic performance of glycated haemoglobin (HbA1c) for diabetes mellitus in dogs. The Veterinary Journal, 294, 1-6. https://doi.org/10.1016/j.tvjl.2023.105958

Petersen, M.C. & Shulman, G.I. (2018). Mechanisms of insülin action and insulin resistance. Physiological Reviewes, (98), 2133-2223. https://doi.org/10.1152/physrev.00063.2017

Preet, G.S., Turkar, S., Gupta, S., & Kumar, S. (2021). Dog obesity: Epidemiology, risk factors, diagnosis and management: A review paper. The Pharma Innovation Journal, 10(5), 698-705.

Ramos, J.R., & Castillo, V. (2020). Evaluation of insulin resistance in overweight and obese dogs. Internal Journal of Veterinary Sciences Research, 6(1), 58-63. https:/doi.org/10.17352/ijvsr.000055

Romere, C., Duerrschmid, C., Bournat, J., Constable, P., Jain, M., Xia, F., Saha, P.K., Del Solar, M., Zhu, B., York, B., Sarkar, P., Rendon, D.A., Gaber, M.W., LeMaire, S.A., Coselli, J.S., Milewicz, D.M., Sutton, V.R., Butte, N.F., Moore, D.D. & Chopra, A.R. (2016). Asprosin, a Fasting-Induced Glucogenic Protein Hormone. Cell, 165, 566–579. https://doi.org/10.1016/j.cell.2016.02.063.

Ronja, N., & Kölle, P. (2021). Obesity in dogs-A review of underlying reasons. Tierarztl Prax Ausg K Kleintiere Heimtiere, 49(4), 284-293. https:/doi.org/ 10.1055/a-1548-2293

Silistre, E.S. & Hatipoğlu, H.U. (2020). Increased serum circulating asprosin levels in children with obesity. Pediatrics International, 62, 467–476. https://doi.org/10.1111/ped.14176

Sung, K.C., Reaven, G.M. & Kim, S.H. (2010). Utility of Homeostasis Model Assessment of β-Cell Function in Predicting Diabetes in 12,924 Healthy Koreans. Diabetes Care, 33(1), 200–202. https://doi.org/10.2337/dc09-1070

Taguchi, A.L., Wartschow, M. & White, M.F. (2007). Brain IRS2 signaling coordinates life span and nutrient homeostasis. Science, 317, 369–372. https://doi.org/10.1126/science.1142179

Titchenell, P.M., Lazar, M.A. & Birnbaum, M.J. (2017). Unrevealing the regulation of hepatic metabolism by insulin. Trends in Endocrinology & Metabolism, (28), 497-505. https://doi.org/10.1016/j.tem.2017.03.003

Velasquez-Mieyer, P.A., Cowan, P.A., Arheart, K.L., Buffington, C.K., Spencer, K.A., Connelly, B.E., Cowan, G.W. & Lustig, R.H. (2003). Suppression of insulin secretion is associated with weight loss and altered macronutrient intake and preference in a subset of obese adults. International Journal of Obesity and Related Metabolic Disorders, 27, 219–226. https://doi.org/10.1038/sj.ijo.802227

Villar, G.F. & Francisco Pérez-Bravo, F. (2022). Analysis of insulin resistance using the non-linear homeostatic model assessment index in overweight canines. Veterinary World, 15(6), 1408–1412. https://doi.org/10.14202/vetworld.2022.1408-1412

Wang, Y., Qu, H., Xiong, X., Qiu, Y., Liao, Y. & Chen, Y. (2018). Plasma Asprosin Concentrations Are Increased in Individuals with Glucose Dysregulation and Correlated with Insulin Resistance and First-phase Insulin Secretion. Mediators of. Inflammation, 18, 1–7. https://doi.org/10.1155/2018/9471583

Watanabe, T., M. Nomura, K. Nakayasu, T. Kawano, S. & Ito Y. Nakaya. (2006). Relationships between thermic effect of food, insulin resistance and autonomic nervous activity. Journal of Medical Investigation, 53, 153–158. https://doi.org/10.2152/jmi.53.153

Williams, K., & Buzhardt, L. (2022). Body condition scores. Vca Animal hospital. https://vcahospitals.com/know-your-pet/body-condition-scores

Wondmkun, T.Y. (2020). Obesity, Insulin Resistance, and Type 2 Diabetes: Associations and Therapeutic Implications. Journal of Diabetes, Metabolic Syndrome and Obesity: Targets and Therapy, 13, 3611–3616. https://doi.org/10.2147/DMSO.S275898

Xu, C., Zhou, G., Zhao, M., Zhang, X., Fang, L., Guan, Q., Zhang, H., Gao, L., Zhang, T. & Zhao, J. (2021). Bidirectional temporal relationship between obesity and hyperinsulinemia: longitudinal observation from a Chinese cohort. BMJ Open Diabetes Research & Care, 9, 1-7. https://doi.org/10.1136/bmjdrc-2020-002059

Zeugswetter, F.K., Beer, R. & Schwendenwein, I. (2021). Evaluation of fructosamine concentration as an index marker for glycaemic control in diabetic dogs, Veterinary Record, 190(2), 1-9. https://doi.org/10.1002/vetr.244

Medit Vet J, 9(3): 371-376, 2024
DOI: 10.24880/meditvetj. 1611166

Research Article

The effect of diet composition on the digestibility and fecal excretion of trace minerals in horses

Gülşah Karasu Kaya[1], Hıdır Gümüş[2]

[1]Van Hall Larenstein University of Applied Sciences, Netherlands
[2]Department of Animal Nutrition and Nutritional Diseases, Faculty of Veterinary Medicine, Burdur Mehmet Akif Ersoy University, Burdur, Türkiye

Key Words:
digestion
excretion
equine
nutrition
trace mineral

Received : 23 May 2024
Revised : 17 October 2024
Accepted : 27 November 2024
Published : 31 December 2024
Article Code : 1611166

Correspondence:
G. KARASU KAYA
(Gulsah.kayakarasu@hvhl.nl)

ORCID
G. KARASU KAYA : 0009-0000-4741-2545
H. GÜMÜŞ : 0000-0001-7077-1036

ABSTRACT

This study investigates the correlation between dietary intake of these trace minerals and their fecal excretion rates, aiming to enhance our understanding of equine mineral metabolism and improve dietary recommendations. The criteria for selection included healthy horses aged 4 to 14, weighing 400 to 600 kg, with a good body condition score (BCS, 3/5) across 14 yards in the Netherlands. Data on yard type, size, and location, as well as horse demographics (age, sex, breed, weight), were collected. Each horse's diet was analyzed concerning daily nutritional intake and requirements according to National Research Council (NRC). Fecal samples were randomly collected from stables (n=14) for dietary analysis and stored in three labeled jars. Samples, approximately 200 g each, were frozen at -20°C and later analyzed for cobalt (Co), copper (Cu), manganese (Mn), and zinc (Zn) using inductively coupled plasma mass spectroscopy (ICP-MS). Among the 14 horses, all were geldings, with one being a cold blood and another a Welsh pony, while the rest were warmbloods. Their median age was 10 years, mean body weight (BW) 506 ± 82.3 kg. Most horses grazed, averaging 8.6 ± 8.5 h/day. All received commercial concentrate feed, with nine also receiving supplements. Energy intakes varied, with ten horses consuming more than required. Trace mineral intake was classified by the NRC; two horses had high Cu intake. Manganese intake exceeded NRC recommendations significantly (618.6 ± 125.1 mg vs. 1403.8 ± 312.7 mg), while Co intake was 2.3 ± 1.6 mg against a requirement of 0.8 ± 0.2 mg. Manganese excretion in feces was highest (459.1 ± 386.4 mg/day), followed by Zn (58.3 ± 46.0 mg), Cu (2.7 ± 3.2 mg), and Co (1.5 ± 0.4 mg). This study emphasizes the need for tailored diets to prevent excess mineral intake in horses, which mainly originates from concentrate feed and supplements. Further research with a larger sample size is necessary for a deeper understanding.

INTRODUCTION

Maintaining optimal levels of trace minerals is paramount for the health and performance of horses (Jackson, 1997). Trace minerals, including Co, Zn, Co, and Mn play indispensable roles in various physiological processes essential for equine well-being. These encompasses Cu; including proper coat and hoof health Zn; skin health, wound healing, and immune function Co; the synthesis of vitamin B12 crucial for energy metabolism and nerve function Mn; contributes to bone formation, cartilage development, and enzyme function (NRC, 2007). Despite their significance, achieving and maintaining the delicate balance of trace minerals in equine diets is challenging. Horses acquire minerals primarily through their diet, with excess amounts often excreted through feces (Coenen, 2013). This excretion pattern underscores the intricate relationship between dietary intake and fecal excretion rates, which can be influenced by factors such as mineral form, interactions among supplemented minerals, and individual variations in mineral metabolism. Deficiencies in trace minerals can have profound implications for equine health. Cu deficiency, for instance, may manifest as poor coat quality, joint issues, and anemia, while Zn deficiency can lead to skin problems, impaired wound healing, and compromised immunity (Baltaci et al., 2019). Co and Mn deficiencies similarly contribute to anemia, decreased energy levels, and skeletal abnormalities. Therefore, ensuring adequate intake of these trace minerals is imperative for safeguarding equine health and preventing associated health complications. There exists a positive linear relationship between dietary mineral intake and fecal excretion (Coenen, 2013). Supplementation of trace minerals in horse diets is common practice, yet it often exceeds dietary requirements, resulting in elevated fecal excretion rates (Harper et al., 2009). Studies have shown that higher plasma concentrations of certain minerals, such as Zn, may not always correlate with the highest dietary intakes, highlighting the complex dynamics of mineral metabolism in horses (Cymbaluk and Christensen, 1986). Moreover, the environmental impact of excessive mineral excretion in horse manure cannot be overlooked. Minerals excreted in feces due to oversupply from supplements can disrupt the agricultural cycle, affecting soil health and potentially contaminating water sources (Hsu et al., 2000). Understanding the mobility of trace minerals in horse manure and their subsequent impact on the environment is crucial for sustainable equine management practices. Consideration of mineral forms in horse ration formulation is essential, as interactions between dietary compounds and mineral availability can influence overall mineral absorption (Kaya Karasu et al., 2018). While organic trace mineral compounds are often presumed to offer superior bioavailability compared to inorganic salts,

To cite this article:
Karasu Kaya G, Gümüş H. The effect of diet composition on the digestibility and fecal excretion of trace minerals in horses. Medit Vet J. 2024; 9(3): 371-376.

this assumption remains uncertain in horses. Assessing true mineral digestibility provides a more accurate estimation of bioavailability, aiding in the formulation of balanced equine diets. Despite advancements in understanding mineral nutrition in other species, research specific to horses is limited, particularly regarding the effect of mineral form on availability. Studies investigating plasma responses to different mineral forms have shown varying degrees of availability, emphasizing the need for further research in this area (Wichert et al., 2002).

This study aims to bridge existing knowledge gaps by assessing the correlation between dietary intake of trace minerals (Co, Cu, Mn, and Zn) in horses and the subsequent excretion rates observed in feces. By elucidating the relationship between dietary mineral intake and fecal excretion, this research seeks to enhance our understanding of equine mineral metabolism, inform more precise dietary recommendations.

MATERIALS and METHODS

The selection criteria included a healthy horse aged 4 to 14, a gelding weighing 400 to 600 kg, in good health, and in good body condition score (BCS, 3/5) in the 14 yards in the Netherlands. Data were gathered regarding geographical location, yard size (number of horses), yard type, and demographic details of the horses (body weight (BW), breed, age, and sex). Each horse's daily level of activity was recorded, as well as information about their dietary intake (grazing duration, forage intake, concentrate intake, supplements with types, brands, and quantities). Feces samples were collected from the same yards, and the ration was calculated for horses.

Ration calculation

The nutritional requirements and total diet of each horse were assessed based on their daily intake of nutrients. The nutrient intake for crude protein (CP), crude fiber (CF), starch, energy, and micro minerals such as Zn, Co, Mn, and Co were calculated, an estimate of workload was also calculated and these data were utilized to compare the estimated intake with the estimated horse requirements based on National Research Council recommendation (NRC, 2007). The estimated nutritional content of the pasture and forage given were predicted using published NRC recommendations (NRC, 2007), while the data for feed and supplements was based on publicly available product data. A 500 kg horse was estimated to consume pasture dry matter (DM) of 1.2 g DM/kg$^{0.75}$ (NRC, 2007). The pasture DM intake was estimated for the initial 4h at pasture as 1.5 g DM/kg BW/h and for every hour after the initial 4 hours as 0.9 g DM/kg BW/h based on published estimated intakes (Dowler, 2009).

The metabolizable energy (ME) requirement for horses between 200 and 800 kg was determined based on the calculation by Kienzle and Zeyner. (Kienzle and Zeyner, 2010). The energy requirement calculation included an adjustment for activity level as classifications "light," "moderate," "heavy," and "very heavy"(NRC, 2007). The provision of nutrients for energy, starch, sugar, crude fat, crude protein, energy, crude protein, and trace minerals for Co, Cu, Mn, and Zn were classified as low (<90%), normal (90%–110%), and high (>110) of the requirement compared to the NRC recommendations (NRC, 2007). The mineral intake for trace minerals Co, Cu, Mn, and Zn by diet minus the requirement, which is defined as "potential mineral excretion".

Feces samples collection and analysis

Feces samples were collected as randomly from horse stables in the Netherlands (n=14) to gather data for dietary plans and samples for feces as part of their assignments. The fresh feces samples after horses are defecated immediately collected without bedding contamination to a minimum. Then composited into 3 disposable sample jars that were kept closed to prevent moisture loss. Mix the feces with the plastic spoon. Fill wet feces samples in such a way that all 3 disposable sample jars numbered as A, B and C. Each jars feces capacity is approximately 200 g. Placed the samples at −20 ◦C in the freezer within a maximum of 3 hours. The selected horses' feces analyzed trace minerals Co, Cu, Mn, and Zn which were identified as "actual mineral excretion". The fecal samples were homogenized to achieve consistency, and 1 gram of the sample was weighed to ensure appropriateness for analysis. The samples were analyzed for minerals for Co, Cu, Mn, and Zn using inductively coupled plasma mass spectroscopy (ICP-MS). Total fecal excretion was calculated as a 500 kg horse will generally produce about 25 kg of manure (feces and urine) per day which means approximately %5 BW (Westendorf, 2004).

Data Analysis

Plots and descriptive statistics were examined in the initial analysis of the data. Kolmogorov Smirnov and Levene's tests assessed the data's normal distribution and homogeneity, respectively. Data with a normal distribution were shown as mean ± standard deviation (SD), while data with a skew were shown as median and range. Descriptive statistics were performed on the quantitative data describing percentage responses with 95% confidence intervals. To determine whether the relationship between variables was statistically significant, the chi-squared test and the k-independent test (Kruskal-Wallis) were used. Data were analyzed using SPSS 16.0 (IBM, 2021), with a value of $P < 0.05$ assumed to be statistically significant for all analyses.

RESULTS

Demographics

The horses (n=14) were all geldings. One horse was a cold blood, one was a Welsh pony, and the remaining horses were warmbloods. The median age of the population was 10, ranging from 4 to 22 years. Horses' average BW was 506 ± 82.3 kg. The median BW of the horses was 496.5 kg. The horses were all in BCS 5/9. The majority of the horses (n=9) were sport horses, with the remainder being livery yard horses (n=5).

Forage, Concentrate and Supplement intake

Only two horses did not have access to pasture; the rest were grazing, with an average grazing time of 8.6 ± 8.5 h/day (range, 2-24). Nine horses were grazed with continuous grazing method while four horses were grazed rotational grazing

method. Hay (n=11) or haylage (n=4) was fed to all horses. Hay intake averaged was 9 ± 1.9 haylage was 6.7 ± 4.7 kg/d. All horses received at least one commercial concentrate feed, with one horse receiving two different commercial concentrate feeds and four horses receiving three different commercial concentrate feeds. The average intake of concentrate feed was 2.5 ± 1.8 kg/d. Nine horses were fed supplements, two of which received only one supplement, three of which received two supplements, and three of which received three supplements. All trace minerals in supplements (Zn, Co, Cu, and Mn) were not chelated. Vitamin-mineral mixtures were the most commonly used supplement (n=8).

Nutrient Analysis

Horse owners/trainers fed their horses an average of 141.52 ± 25.85 MJ ME/d. The energy intakes varied in comparison to requirements, 10 horses had higher intakes than required with a further 1 horse fed under the recommended energy levels, the rest had optimum intake. The crude protein intake was higher in 13 of the horses compared to NRC recommendations (NRC, 2007), one horse CP intake was lower than the requirement. The CP intake was 3.39 ± 0.71 g/kg BW. The mean CP requirement of these horses was 1.79 ± 0.17 g/kg BW on the base of NRC recommendations (NRC, 2007). The estimated lysine intake was within the normal range for 11 horses, with the remaining horses receiving less than recommended (NRC, 2007). Mean CF intake was 5.7 ± 1.3 g/kg BW, and crude fat intake was 0.7 ± 0.1 g/kg BW, both being within NRC recommendations (NRC, 2007). Mean starch intake was 1.1 ± 0.8 g/kg BW, which is within the NRC recommendation although sugar intake was 2.3 ± 0.4 g/kg BW, both of which were high compared to the NRC recommendations (NRC, 2007).

Potential and measured excretion of trace minerals in feces

The NRC has classified the trace mineral intake as low, normal, and high groups. Based on these categorizations, five horses maintained a normal Cu intake, while seven horses had a low intake, and two horses had a high intake. All horses used in the research were classified in the high-intake Mn group. Eight horses were placed in the high-intake Zn group, while the same number of horses were classified in both the low-intake and the normal-intake Zn groups also. The low-intake Co group had no horses, whereas the normal-intake Co group had one horse, and the high-intake Co group had thirteen horses (Table 1).

The mean weight of the horse was determined to be 508 kg. The mean daily weight of the fresh and dry feces was measured to be 16.3 kg and 4.3 kg, respectively (Table 2). The Cu intake was lower (146.9 ± 83.3 mg) compared to the mean requirements of the NRC recommendations (154.6 ± 31.3 mg). The

Table 1. Trace minerals intakes (number of horses) of horses and mean values compared to NRC recommendations (n=14)

Minerals	Low intake	Normal intake	High intake
Cu, mg	7	5	2
Mn, mg	-	-	14
Zn, mg	3	3	8
Co, mg	-	1	13

Low intake <90%; Normal intake 90-110%; High intake >110 of the requirement compared to NRC recommendations

Table 2. Average horse manure and feces generated per day (n=14)

Weight of horse (kg) (mean ± SD)	*Manure excretion (kg/day) (mean ± SD)	**Fresh feces (kg/day) (mean ± SD)	Feces (DM) (kg/ day) (mean ± SD)
508.9 ± 83.0	25.3 ± 4.1	16.3 ± 4.1	4.3 ± 1.6

*%5 BW is used for manure excretion; ** %26 DM is used for feces (mean ± DM 26.5 ± 7.5)

Table 3. Average minerals requirements, intake and calculated minerals excretion per day per horse according to laboratory results (n=14)

Minerals	*Mean requirement (mean ± SD)	Mean intake (mean ± SD)	Mean excretion by horse per kg wet feces (with lab results) (mean ± SD)	Mean excretion by horse feces per day (with lab results) (mean ± SD)
Cu, mg	154.6 ± 31.3	146.9 ± 83.3	0.1 ± 0.1	2.7 ± 3.2
Mn, mg	618.6 ± 125.1	1403.8 ± 312.7	29.5 ± 23.9	459.1 ± 386.4
Zn, mg	618.6 ± 125.1	755.7 ± 316.1	3.5 ± 2.5	58.3 ± 46.0
Co, mg	0.8 ± 0.2	2.3 ± 1.6	0.09 ± 0.01	1.5 ± 0.4

*requirement calculated on the base of NRC

Mn intake was notably higher (618.6 ± 125.1 mg) compared to the mean requirements of the NRC recommendations (1403.8 ± 312.7 mg). The intake of Co was found to be 2.3 ± 1.6 mg, whereas Co requirements for horses were 0.8 ± 0.2 mg. Mn excretion (459.1 ± 386.4 mg) by horse feces per day was the highest of the mineral excretions, followed by Zn (58.3 ± 46.0 mg), Cu (2.7 ± 3.2 mg), and Co (1.5 ± 0.4 mg) excretion (Table 3).

DISCUSSION

In the present study, nutritional factors that could affect the trace minerals status of horses fecal excretion were evaluated. There are dietary factors include consumption level (relative to requirements), intake of other minerals, and intake of substances that may improve or prevent the mineral's absorption. Furthermore, some factors are associated with the mineral compound used, including its water solubility and chelating properties. (Kirchgessner, 2004). An oversupply of minerals from supplements in horse diets, with possible interactions and interferences (Kaya Karasu et al., 2018), are excreted in manure (Fowler, 2020) and can have a potentially negative impact on the agricultural cycle. According to National Institute for Public Health and the Environment (Rijksinstituut voor Volksgezondheid en Milieu, RIVM) report (Vos and Janssen, 2008), reducing the amount of Cu and Zn leaching from agricultural soils is particularly challenging in the Netherlands, although there are no restrictions under Regulation (EU) 2018/848 on the organic production of agricultural goods regarding the Cu and Zn content in horse manure (Regulation, 2018). Small changes in daily horse feeding management practices can have positive impacts on the environment, circular agriculture, and horses. Improper management of compost heaps can result in nutrient leaching, raising environmental concerns such as eutrophication. Moreover, high concentrations of trace minerals like Co, Cu, Mn, and Zn can be toxic to plants, microorganisms, and aquatic organisms (Nagpal, 2004; Harford, 2015).

Bioavailability

The bioavailability of a mineral in an animal is a rather elusive entity which may be changing relatively quickly. Factors which affect bioavailability of minerals relating to the animal are species, life stage, health and nutritional status. A mineral's bioavailability may be impacted by nutritional status. The animal's ability to absorb a mineral may enhance during this mineral deficiency whereas it may diminish during excessive intake of this mineral (Kirchgessner, 2004). The bioavailability of minerals can also be impacted by an excess or deficiency of other nutrients. Several interactions between minerals such as Several interactions between minerals such as zinc and copper are commonly assumed to occur in both experimental and domestic animals. (Mertz, 1986; Meyer and Coenen 2002; Kirchgessner, 2004). However, few of these interactions have been confirmed in the target species of horses; they may not occur at all or may differ slightly. For copper it is likely that bioavailability plays a highly important role in the horse. There is no clear consensus on the amounts of copper requirements. (Meyer et al. 1994; Hintz 1996). Variation of bioavailability of copper is an obvious reason for differing evidence on copper requirements. Zn is an effective Cu antagonist. In the horse, however, 500 mg of Zn/kg of diet did not have obvious effects on Cu metabolism (Hoyt et al., 1995). Ascorbic acid, cadmium, iron, and calcium are other potential antagonists of Cu (Meyer et al., 1994). Dietary factors may influence the bioavailability of Zn. Various compounds, including Ca, Fe, and phytate, have been documented as blocking Zn absorption in other species (Mertz, 1986). There is, however, only one study on experimental Zn deficiency in the horse and naturally occurring clinical zinc deficiency has not been unequivocally described so far in the horse. Excess intake of Fe decreased plasma and liver zinc content in ponies (Lawrence et al., 1987).

Mineral source

A 500 kg horse produces around 25 kilogram of manure daily, reaching around 9 tons per year. The manure usually comprises around 5 kg nitrogen (N), 0.9 kg phosphorus (P), and 3.6 kg potassium (K) per ton (Annete, 2013). Supplementing horses with an excessive amount of trace minerals that is higher than their requirements which may results in an increase in fecal output (Harper et al., 2009). However, the accumulation of trace minerals may lead to environmental concerns despite being excreted in smaller amounts (Brugger and Windisch, 2015). Supplementing trace minerals such as Cu, Mn, Zn, and Co with the diet resulted in an increased loss of Cu via feces compared to the control diet, which may lead to raise concerns about water quality (Fowler et al., 2019). In the current study, five horses remained in the normal-intake Cu group, seven in the low-intake Cu group, and two in the high-intake Cu group. The mean intake and mean daily excretion of Cu were found to be 146.9 and 2.7 mg, respectively. The endogenous Cu losses from feces may be established at a rate of 35 µg per kilogram of body weight per day (Coenen, 2013). Zn toxicosis is uncommon in horses because large animals generally have a high tolerance for this dietary mineral (Aragona et al., 2024). Zn use as a feed additive for horses is subject to legal restrictions in the European Union. The maximum amount of Zn allowed for equines' total diet (with 88% DM) is 120 mg/kg (PaBlack et al., 2022). Mineral additives are commonly used in animal feed in excess of the physiological requirements in order to prevent deficiencies and improve animal health. Therefore, this excessive supplementation may lead to more excretion of trace minerals, resulting in soil and surface water contamination (Xiong et al., 2023). Fowler et al (2019) showed that supplementing the diet with organic Zn resulted in higher levels of Zn in the fecal bacteria. Dietary strategies that improve gut bacteria's Zn absorption may help mitigate the effects of Zn leaching into water systems. The current study showed that the mean intake of Zn was higher than the mean requirement of Zn. The mean daily excretion of Zn in horse feces was 58.3 mg. Considering the excretion of 5 kg fecal DM per day, Zn losses via feces in horses fed without additives would be 80 mg/d, but horses fed with organic trace mineral supplements would lose 210 mg/d of Zn or horses fed with inorganic trace minerals would lose 134 mg/d of Zn (Fowler et al., 2019). A minimum daily Mn intake of 0.3 mg/kg BW is recommended. The amount of feces excreted is directly related to the Mn intake (Coenen et al., 2013). A study by Fowler et al. (2019a) indicated that the Mn content

of horse fecal compost was 481.23 mg/kg. The current study showed that the mean Mn intake was 1403.8 mg, whereas the mean Mn loss via feces was 459.1 mg. The NRC established the minimal threshold for horses at 0.05 mg of Co kg/d DM, which was lower than the 0.1 mg Co/kg DM recommended in the 1989 NRC guidelines (NRC, 2007). Excessive intake of Co may disrupt normal organ function and result in thyroid dysfunction, cardiotoxicity, as well as heart failure (Mørkeberg, 2013). A study conducted by Semenza (2003) showed that the possibility of tumor growth due to excessive being overexposed of Co intake. Adequate amounts of Co are necessary for the microflora in the large intestine's colon and cecum to synthesize vitamin B12, or cobalamin. Therefore, a decrease in vitamin B12 concentrations in the tissues is most likely the cause of clinical Co deficiency (Mitchell et al., 2007).

CONCLUSION

This study underscores that the examined minerals Zn, Cu, Co, and Mn were consumed by the horses in quantities surpassing their requirements and subsequently excreted in feces. Given that all horses received concentrate feed and additional supplements, these excessive mineral sources likely originated from these dietary components. Thus, individualized diet calculations are crucial to ensure a balanced nutritional intake for the welfare and health of horses, while also mitigating potential environmental impacts. To gain a clearer understanding, further studies with a larger sample size are warranted.

DECLARATIONS

Ethics Approval

Not applicable.

Conflict of Interest

The authors declare that there is no conflict of interest

Consent for publication

Not applicable.

Author Contributions

Idea, concept and design: G.K.K

Data collection and analysis: G.K.K

Drafting of the manuscript: G.K.K and H.G

Critical review: G.K.K and H.G

Data availability

The data used to prepare this manuscript are available from the corresponding author when requested.

Acknowledgements

This research is co-financed by the SIA Agency part of the Netherlands Organization for Scientific Research (NWO), Taskforce for Applied Research.

REFERENCES

Aragona, F., Cicero, N., Nava, V., Piccione, G., Giannetto, C., & Fazio, F. (2024). Blood and hoof biodistribution of some trace element (Lithium, Copper, Zinc, Strontium and, Lead) in horse from two different areas of Sicily. Journal of Trace Elements in Medicine and Biology, 82, 127378.

Baltaci, A.K., Mogulkoc, R., & Baltaci S.B. (2019). The role of zinc in the endocrine system. Pakistan Journal Pharmaceutical Science, 32, 231-239.

Brugger, D., & Windisch, W. M. (2015). Environmental responsibilities of livestock feeding using trace mineral supplements. Animal Nutrition, 1, 113–118.

Coenen, M. (2013). Macro and Trace elements in equine nutrition. In: R.J. Geor, P. A. Harris, & M. Coenen (Eds.), Equine Applied and Clinical Nutrition (pp. 190–228). Saunders: Philadelphia, PA, USA

Cymbaluk, N. F., & Smart, M. E. (1993). A review of possible metabolic relationships of copper to equine bone disease, Equine Veterinary Journal. Supplement, 16, 19-26

Dowler, L. E., Siciliano, P. D. (2009). Prediction of hourly pasture dry matter intake in horses. Journal of Equine Veterinary Science, 29, 354-355.

Fowler, A. L., Brummer-Holder M., &Dawson, K. A. (2020). Trace mineral leaching from equine compost. Sustainability, 12(17), 7157.

Fowler, A. L., Brummer-Holder, M., & and Dawson K. A. (2019a). Trace Mineral Leaching from Equine Compost. Sustainability, 12, 7157.

Fowler, A. L., Brümmer-Holder, M., & Dawson, K. A. (2019). Dietary trace mineral level and source affect fecal bacterial mineral incorporation and mineral leaching potential of equine feces. Sustainability, 11, 7107.

Harford, A. J., Mooney, T. J., Trenfield, M. A. & Van Dam, R. A. (2015). Manganese toxicity to tropical freshwater species in low hardness water. Environmental Toxicology and Chemistry, 3412, 2856-2863.

Harper, M., Swinker, A., Staniar, W., & Welker, A. (2009). Ration evaluation of Chesapeake Bay watershed horse farms from a nutrient management perspective. Journal of Equine Veterinary Science, 529, 401-402.

Hintz, H. F. (1996). Mineral requirements of growing horses. Pferdeheilkunde, 12(3), 303-306.

Hoyt, J. K., Potter, G. D., Greenead, L. W., & Anderson., J. G. (1995). Copper balance in miniature horses fed varying amounts of zinc. Journal of Equine Veterinary Science, 15, 357-359.

Hsu, J. H., & Lo, S. L. (2000). Characterization and extractability of copper, manganese, and zinc in swine manure composts. Journal of Environmental Quality, 292, 447-453.

IBM Corp. Released 2021. IBM SPPS Statistics for Windows. Version 28.0. Armonk, NY: IBM Corp.

Jackson, S.G. (1197). Trace minerals for the performance horse: known biochemical roles and estimates of requirements. Irish Veterinary Journal, 50, 668-674.

Kaya Karasu, G., Huntington, P., Iben, C., & Murray, J. A. (2018). Feeding and management practices for racehorses in Turkey. Journal of Equine Veterinary Science 61, 108-113.

Kienzle, E., Zeyner, A. (2010). The development of a metabolizable energy system for horses. Journal of Animal Physiology Animal Nutrition, 94:, 231-240.

Kirchgeßner, M. (2004): Tierernährung, 11. Auflage, DLG-Verlag

Lawrence, L. A., Ott, E. A., Asquith, R. L., & Miller, G. J. (1987). Influence of dietary iron on growth, tissue mineral composition, apparent phosphorus absorption, and chemical properties of bone. Proceedings of the Nutrition Society, 10, 563-568.

Mertz, W. (1986). Trace Elements in Human and animal nutrition, 5th edition. Beltsville, Maryland Academic press.

Meyer, H. (1994). Kupferstoffwechsel und Kupferbedarf beim Pferd. Übersichten zur. Tierernährung, 22, 363-394.

Meyer, H., Coenen, M. (2002) Pferdefütterung. Parey Verlag, Berlin

Mitchell, L. M., Robinson, J. J., Watt, R. G., McEvoy, T. G., Ashworth, C. J., Rooke, J. A., & Dwyer, C.M. (2007). Effects of cobalt/vitamin B12 status in ewes on ovum development and lamb viability at birth. Reproduction Fertility and Development, 19, 553-562.

Mørkeberg, J. (2013). Blood manipulation: current challenges from an anti-doping perspective. Hamatology, 1, 627-631.

Nagpal, N. (2004). Water Quality Guidelines for Cobalt: Water Protection Section, Water, Air and Climate Change Branch; Technical Report; Ministry of Water, Land, and Air Protection: Victoria, BC, Canada.

Nijs, A. C. M., Driesprong, A., Hollander, H. A., Poorter, L. R. M., Verweij, W. H. J., Vonk, J. A., & Zwart D (2008). Risico's van toxische stoffen in de Nederlandse oppervlaktewateren. RIVM (National Institute for Public and Environment) report 607340001.

NRC (2007). National research council. The Nutrient Requirement of Horses. 6th revised edition Washington, USA. National academic press.

Paßlack, N., Bömmel-Wegmanna, S., Vahjena, W., & Zenteka, J. (2022). Impact of dietary zinc chloride hydroxide and zinc methionine on the faecal microbiota of healthy adult horses and ponies. Journal of Equine Veterinary Science, 110, 103804.

Regulation (EU) 2018/848 of the European Parliament and of the council of 30 May 2018 on organic production and labelling of organic products and repealing Council Regulation (EC) No 834/2007

Semenza, G. (2003). Targeting HIF-1 for cancer therapy. Nature Reviews Cancer, 3, 721-732.

Annete, C. J. (2013). Pastures and pastures management. In: R. J. Geor, P. A. Harris, & M. Coenen (Eds.), Equine Applied and Clinical Nutrition (pp. 332-349). Philadelphia, PA, USA, Saunders press.

Vos, J. H., & Janssen M. P. M. (2008). EU-wide control measures to reduce pollution from WFD relevant substances: Copper and zinc in the Netherlands. RIVM (National Institute for Public and Environment) report 607633002

Westendorf, W. (2004). Horses and manure. Rutgers Equine Science Center Publications: Factsheet 036, Rutgers, New Brunswick

Wichert, B., Kreyenberg, K., & Kienzle, E. (2002). Serum response after oral supplementation of different zinc compounds in horses. Journal of Nutrition, 132(6), 1769-70.

Xiong, Y., Cui, B., He, Z., Liu, S., Wu, Q., Yi, H., Zhao, F., Jiang, Z., Hu, S., & Wang L. (2023). Dietary replacement of inorganic trace minerals with lower levels of organic trace minerals leads to enhanced antioxidant capacity, nutrient digestibility, and reduced fecal mineral excretion in growing-finishing pigs. Frontiers Veterinary Science 10, 1142054.

Medit Vet J, 9(3): 377-384, 2024
DOI: 10.24880/meditvetj.1528408

Research Article

Histopathology of gill parasites ın cultured seabream *(Sparus Aurata)* and seabass *(Dicentrarchus Labrax)*

Melike Dereli[1], Şule Yurdagül Özsoy[1]

[1]Department of Pathology, Faculty of Veterinary Medicine, Aydın Adnan Menderes University, Aydın, Türkiye

Key Words:
gill
histopathology
parasite
seabass
seabream

Received : 5 August 2024
Revised : 5 November 2024
Accepted : 13 November 2024
Published : 31 December 2024
Article Code : 1528408

Correspondence:
SY. ÖZSOY
(suleozsoy@gmail.com)

ORCID
M. DERELI : 0000-0001-9952-2279
SY. ÖZSOY : 0000-0002-0743-2063

ABSTRACT

This study was carried out to define the gill parasitic diseases and histopathological findings of sea bream and sea bass cultured in Turkey. Dead fish suspected of disease that came to the Kanyon Akua Veterinary Clinic Disease Diagnosis Laboratory between January 2021 and January 2022 were included in the study. A total of 5,250 fish, including 3,150 sea bass *(Dicentrarchus labrax) (D. labrax)* and 2,100 sea breams *(Sparus aurata) (S. aurata)*, weighing between 2-350 g, were used in the study. After the measurement of total length and weight, samples were divided into groups for pathological and parasitological examinations. Eight different parasites were detected that caused intense infestation in sea bream and sea bass. Among these, *Diplectanum spp.*, *Cryptocaryon spp.*, *Amyloodinium spp.*, *Trichodina spp.*, *Cryptobia spp.*, and *Costia spp.* were seen in sea bass. Parasites seen in sea bream were *Microcotyle spp.*, *Furnestinia spp.*, *Trichodina spp.*, and *Costia spp.*, *Trichodina spp.* and *Costia spp.* were seen in both sea bass and sea bream. The most common histopathological findings were epithelial lifting, necrosis, hemorrhage, telangiectasia, lamellar fusion, spills, infiltration of macrophage, lymphocyte and eosinophilic granulated cells. The most common parasitic agent in the field sea bass was *Diplectanum spp.* and the most common parasitic agent in sea bream was *Microcotyle spp.* The highest mortality (10%) and the severe histopathological lesions were detected in *Amyloodinium spp.* The incidence of multiple agents (multi-parasitism) in the cases was higher than the incidence of single agents.

INTRODUCTION

In recent years, the increasing population and therefore the need for protein has led to an increase in the demand for aquatic products. The fact that aquaculture resources are not infinite and efficient use has become a necessity that has led to the development of sustainable production (Arıkan and Aral, 2019; Demir, 2011; FAO, 2018; TAGEM, 2019).

The intensification of aquaculture and the globalization of seafood trade have led to a remarkable development in the aquaculture industry. However, the aquaculture industry is also grappling with disease problems caused by viral, bacterial, fungal, and parasitic pathogens. The most important parasites for farmed sea bass and/or sea bream are *Microcotyle spp., Diplectanum spp., Furnestinia spp., Cryptocaryon spp., Amyloodinium spp., Trichodina spp., Chilodonella spp., Scuticociliate spp., Epistylis spp., Cryptobia spp.,* and *Costia spp* (Çoban et al., 2020).

Disease outbreaks in aquaculture are becoming more frequent and cause significant mortality rates and economic losses. Therefore, diseases are undoubtedly one of the biggest constraints to the profitability and sustainability of aquaculture. Increasing growth is directly related to the effort to reduce the gap between supply and demand for fish products. However, parasitic infections and other related diseases have emerged in aquaculture systems in many parts of Europe, causing significant economic losses. Marine wild fish are believed to be the primary reservoirs of parasite infection for cage-raised fish. However, environmental conditions in aquaculture systems can facilitate disease transmission thereby threatening the productivity. (Antonelli et al., 2010, Çoban et al., 2020).

The negative effects of gill pathologies caused by gill parasites in aquaculture farms are not taken into consideration sufficiently. Fish diseases, which have become increasingly more complicated in recent years, have created a need for veterinarians to be employed who specialize in fish diseases. Although there are many studies on gill parasites in our country, the limited number of studies on their histopathological findings increases the value of our study. The purpose of our study was to diagnose and reveal the histopathology of gill parasites seen in sea bream (*Sparus aurata*) and sea bass (*Dicentrarchus labrax*) cultured in Turkey.

MATERIALS and METHODS

Study site

Dead fish samples with suspicion of disease were used in the study which were brought to the disease diagnosis laboratory of Kanyon Akua Veterinary Clinic between January 2021 and January 2022. In the study, a total of 5,250 fish weighing between 2-350 g were used, 3,150 of these were sea bass (*D. labrax*) and 2,100 were sea bream (*S. aurata*). After the total length and weight of the samples were measured, they were divided into groups for pathological and parasitological examinations.

To cite this article:
Dereli M, Özsoy ŞY. Histopathology of gill parasites ın cultured seabream *(Sparus Aurata)* and seabass *(Dicentrarchus Labrax)*. Medit Vet J. 2024; 9(3): 377-384.

Pathological Examination

Approximately 2-3 transverse sections were made on fish weighing between 2-5 g. Gills were fixed in 10% buffered formalin solution. All gill arches of fish larger than 5 g were removed and fixed in 10% buffered formalin solution and routinely processed for histological examination (graduated alcohol series and xylene) and by embedding in paraffin wax to use for histopathologic evaluations. A five **µm thick section w**as taken from the tissues, which were routinely monitored on an automatic tissue tracking device (Leica TP 1020) and deparaffinized in xylene, treated in graduated alcohol series respectively. All sections were stained with hematoxylin-eosin (HxE) and examined under a light microscope (Olympus BX 51) (Culling et al., 1985; Roberts, 2012).

Parasitological Examination

Preparations were prepared by taking scrapings from the right gill arches of fish that had just died and were sent to the laboratory. The left gill arches were removed separately and placed in petri dishes containing sterile sea water. It was quickly examined under stereo and light microscopes. Identification of parasites seen in gills was made based on morphological criteria. Only protozoan parasites were photographed by applying Giemsa stain (Lom, 1958; Roberts, 2012; Stoskopf, 1993).

RESULTS

The most common parasitic agent in the sea bass in the field was *Diplectanum spp.* and the most common parasitic agent in seabream was *Microcotyle spp*. Severe histopathological lesions with the highest mortality (10%) were detected in the *Amyloodinium spp* species. The most observed histopathological findings were desquamation, hyperplasia, epithelial lifting and hyperemia in the lamellar epithelium. The incidence of multiple factors (multiparasitism) was higher than the incidence of single agents in the cases. Since the sample was sent as soon as the disease was detected, no severe pathological conditions were encountered.

Microcotyle spp. was detected extensively in seabream weighing between 20-350 g in June-July-August. Mortality remained at 6% with epitheliocyst cases. Among 2,100 sea breams, 650 breams had the *Microcotyle spp*. As a clinical finding, severe anemia with the color of the gills changing to white was observed. In the native examination of gills, adult individuals were seen in the lower part of the body, penetrating the gill epithelium with their opisthaptors, having eggs in their ovaries (Figure 1A), and releasing their eggs into the environment. In microscopic examination, parasite sections with epitheliocysts were seen in the gill filaments. In the lamellae containing the parasites, pressure, epithelial lifting, hyperplasia, lamellar fusion, and epithelial desquamation were observed (Figures 2A and 2B).

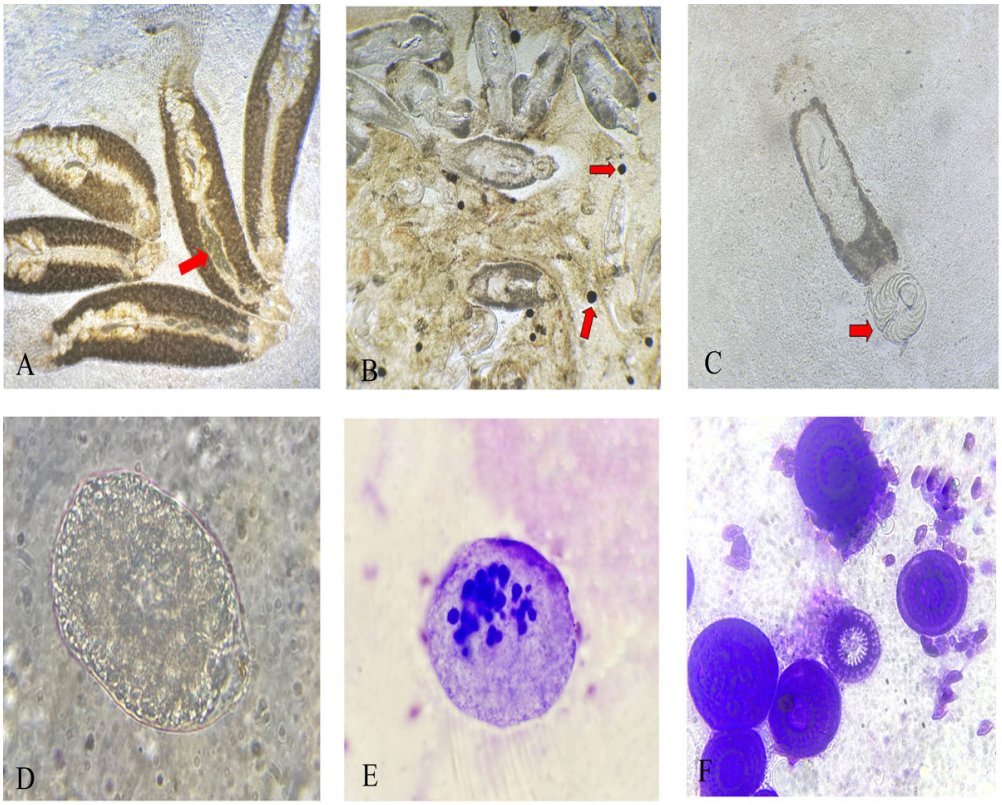

Figure 1. A) Adult, egg-bearing (arrow) Microcotyle spp. in native examination. Seabream. B) Amyloodinium spp. parasites (arrow) and the co-occurring Diplectanum spp. infestation. Seabass. C) Specific haptor (arrow) and 4 eyespots on the back of the Furnestinia spp. parasite. sea bream D) Pear-shaped Amyloodinium spp. agent in the trophont stage. Seabass. E) Amyloodinium spp. agent in the trophont stage. Seabass. Giemsa. Bar=40 µm. F) Distinctive appearance of hooked teeth of Trichodina spp. with Giemsa stain. Seabass. Giemsa. Bar=100 µm.

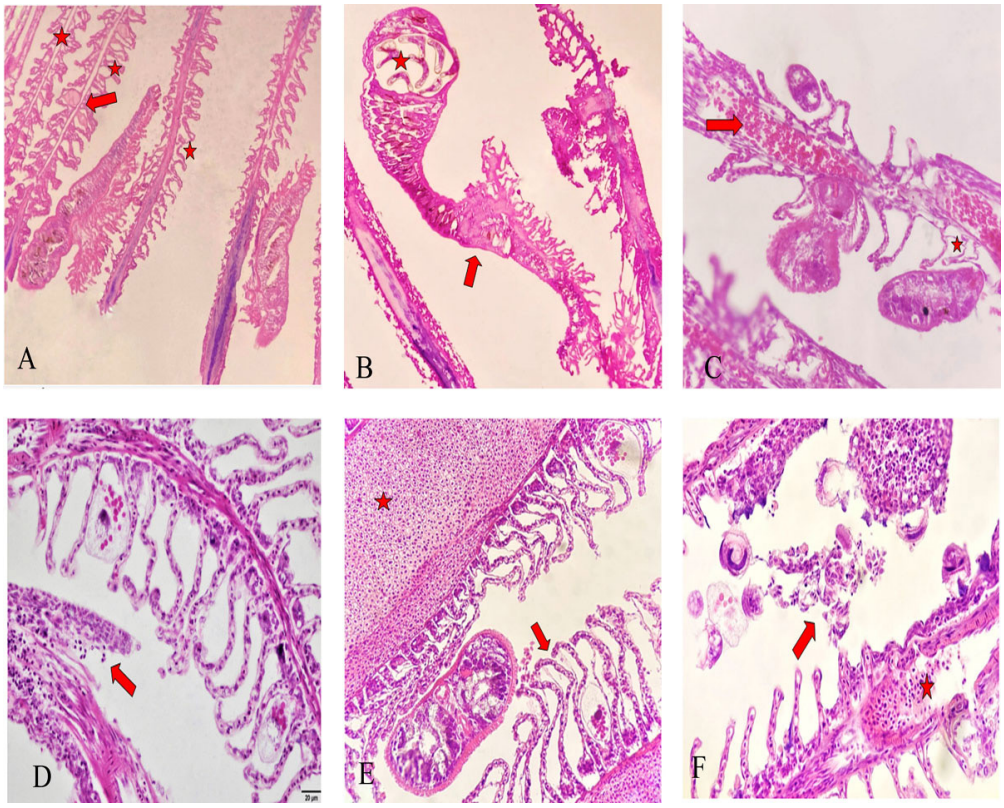

Figure 2. A) Epithelial lifting in gill filaments (star), Epitheliocyst spp. factors (arrow) and Microcotyle spp. attached to the filaments with their opisthaptors. Seabream HxE. Bar=10 µm. B) Microcotyle spp. (arrow) and eggs (star) attached to the gill filaments by their opisthaptors and carrying eggs. seabream HxE. Bar=10 µm. C) Intense hyperemia (arrow) and epithelial lifting (asterisk) caused by Diplectanum spp. in the penetration area. HxE. Bar=100 µm. D) Amyloodinium spp. trophonts penetrated between the secondary lamellae, Desquamative epithelial cells (arrow). Seabass. HxE. Bar=20 µm. E) Amyloodinium spp. and Diplectanum spp. parasites causing intense hyperemia (asterisk) in the primary lamella and epithelial lifting (arrow) in the secondary lamellae. Seabass. HxE. Bar=40 µm. F) Amyloodinium spp. and Trichodina spp. parasites causing desquamation (arrow) and hyperemia (asterisk) in secondary lamellar epithelium. Seabass HxE. Bar=40 µm.

Diplectanum spp. parasite was detected especially in seabass between 10-100 grams in July-August. Mortality remained at 3%, except for cases associated with *Amyloodinium spp*. Among 3,150 sea basses, 550 sea basses had the *Diplectanum spp*.. As a clinical finding, increased mucus secretion and petechial bleeding were observed in the gills. Native examination revealed individuals with 4 eye spots (Figure 1B). In microscopic examination, hyperplasia, hyperemia, hemorrhages, telangiectasia, epithelial lifting (Figure 2C and 2E), fusion, and necrosis were observed in the gill epithelium.

Furnestinia spp. was detected in seabream weighing between 2-100 g in October-November. Mortality remained at 0.5% except for cases with epitheliocyst. Among 2,100 seabreams, 400 breams had the *Furnestinia spp*. As a clinical finding, no changes were seen in the gills. In the native examination of gills, around-cup-shaped haptor and 4 eyespots were seen on the back of its body, which are unique to the parasite (Figure 1 C). Histopathologically, cysts in the secondary lamellae, epithelial shedding, hyperplasia, fusion were observed in cases accompanied by epitheliocyst, and macrophage, lymphocyte and eosinophilic granulated cell infiltrates were observed in cases presenting alone.

Cryptocaryon spp. was detected in August, especially in seabass between 5-200 grams. Mortality remained at 2%. Among 3,150 sea basses, 350 sea basses had the *Cryptocaryon spp.* parasite. As a clinical finding, pale white color, mild anemia and mucus in the gills were observed. Native examination of the gills revealed single or paired parasites with a 4-part macronucleus and peripheral cilia covering the entire body. Histopathologically, single or double factors embedded in the filament bottoms, epithelial lifting in gill epithelium, shedding in epithelial cells, increase in mucus cell size and number, necrosis, hyperemia, hemorrhage, and hyperplasia was seen.

Amyloodinium spp. parasite was detected especially in seabass between 20-250 gin April-May-June-July-August. Mortality remained at 10%. Among 3,150 sea basses, 500 sea basses had the *Amyloodinium* spp. As a clinical finding, bleeding and small blisters were observed in the gills. In the native examination of gills, pear-shaped trophont (Figures 1D and 1E), cystic tomont and motile dinospore forms of the parasite were observed. Histopathological examination revealed shedding of the gill epithelium, gill hyperplasia, epithelial lifting, macrophage, lymphocyte and eosinophilic granule cell infiltrates, intense hyperemia, and hemorrhage (Figures 2D and 2F).

Trichodina spp. was detected in June-July, especially in sea bass weighing 2-100 g and sea bream weighing 5-50 g. Mortality was around 3% in sea bass and 2% in sea bream. Among 3,150 sea basses, 550 sea basses and among 2,100 sea breams, 500 sea breams had the *Trichodina spp* parasite. As a clinical finding, epithelial lifting and regional bleeding were observed in the gills. In the native examination of gills, circle-saucer shaped parasites with a horseshoe-shaped macronucleus, hooked teeth and ciliary spiral were seen (Figure 1F). Histopathological examination revealed shedding, hyperemia, epithelial lifting, hyperplasia, and fusion in the secondary lamellar epithelium (2F).

Cryptobia spp. was detected in all months of the year, especially in sea bass between 2-200 g. Mortality was around 1% in sea bass weighing 2-10 grams. Among 3,150 sea basses, 400 sea basses had the *Cryptobia spp*. parasite. As a clinical finding, an increase in mucus was observed in the gills. In the native examination of gills, *Trypanoplasma* parasites with a triangle-like shape, a wavy membrane, and two flagella facing the opposite direction were seen. Histopathological examination revealed shedding, hemorrhage, mild epithelial lifting, and hyperplasia in the gill epithelium.

Costia spp. was detected especially in sea bass between 10-350 g and sea bream between 25-200 g in April-May-June. Mortality was around 2% in sea bass. Since it was seen together with *Flexibacter spp*. in sea bream, this rate remained at 5.5%. *Costia spp*. parasite was observed in 300 of 3,150 sea basses and 150 of 2,100 sea breams. Any clinical changes were observed in the gills of the sea bass. Necrotic white areas caused by *Flexibacter spp*. were observed in sea bream. In the native examination of gills, oval-comma-shaped parasites with two flagella of different sizes in the same direction were observed. Histopathologically, loss of gill filaments, epithelial lifting, and hyperemia were observed in the seabass. As for seabream, in addition, necrosis and *Flexibacter spp*. bacteria were seen.

DISCUSSION

Microcotyle spp.

According to Alvarez-Pellitero (2004), Vagianou et al. (2006), it is a monogenean gill parasite specific to *Sparus aurata* fish and has caused deaths when contacted with a high prevalence (61.5%) in fish cages. Researchers reported that it was isolated from both wild sea bream (Faisal and Imam, 1990; Rajdukovic and Euzet, 1989) and cultured sea bream (Mladineo and Marsic-Lucic, 2007). In our study, 6% mortality was recorded by isolating only from bream fish. From all fish *Microcotyle spp*. and *Epitheliocyst spp*. was also both isolated. The mortality rate, determined as 6%, included two factors together. The cause of death in fish infested with *Microcotyle* species was determined to be anemia (Sitja-Bobadilla and Alvarez-Pellitero, 2009). Throughout the study, *Microcotyle spp*. intense anemia and a pure white color prevailed in the gills of sea bream. While investigating the histopathology of infestation, attention has been drawn to the shortening of lamellae and the proliferation of epithelial tissue resulting in fusion of secondary lamellae and an increase in chloride cells (Sitja-Bobadilla and Alvarez-Pellitero, 2009). *Microcotyle spp*. caused severe pathogenicity, including systemic anemia, fusion of lamellae, and shedding of gill epithelium, even at densities of 8 parasites per gill arch (Mahmoud et al., 2014). In our study, pressure was observed in the gill epithelium in the lamellae where the parasite opisthaptors were attached, epithelial lifting in the lamellae where the parasites were present, necrosis in the epithelium, lamellar fusion, and shedding of the epithelium. *Microcotyle spp*. secondary infections caused by other parasites and bacteria are common in sea bream infested with sea bream (Cruz Silva et al., 1997).

Diplectanum spp.

In heavy infestations of *Diplectanum* seen in the spring months of each year, it causes a loss of 5-10% of the annual fry stock (Wagener (1857). In this study, it was seen in July-August and caused a loss of 3%. Llewellyn (1957) reported that; parasites are commonly found in the middle and apical parts of the lamellae. The attachment of the parasites to the gill epithelium of the host is provided by the dorsal and ventral spines of the squamodiscs and the hamuli penetrating deep into the epithelial cells, and they have 4 eyespots. In the present study, it was determined that *Diplectanum spp*. was seen singly or in clusters. The 4 eyespots were one of the most important features used in diagnosis. Oliver (1968) reported that the most common pathological findings in *D. aequans* infestations were hyperplasia and hemorrhages. Gonzalez-Lanza et al. (1991) also reported that leukocyte infiltrates were observed. In gills infested with *Diplectanum spp*., excessive mucus hypersecretion, hemorrhage and swelling, especially in the apical parts of the secondary gill lamellae were observed. Compared to non-infested fish, higher numbers of mucus cells (MC) and rodlet cells (RC) were observed in infested gills. (Oliver 1968, Yardimci and Pekmezci 2012). However, in our study, a high number of mucus and rodlet cells could not be observed.

Furnestinia spp.

It has been reported that the most common example in sea bream is *Furnestinia echeneis* from the Diplectanid family (Desdevises, 2001). In the present study, the factor was found only in sea bream. Oliver (1982) reported that, the highest density was recorded in autumn and the lowest values were recorded in spring. During periods when the water temperature dropped to 13°C, a weakening of the fish's immune system was observed. It has been stated that this situation causes a rapid increase in the parasite population (Oliver, 1982). In our study, parasites were found in October and November. High mortality rates due to this Monogenean parasite have been recorded in countries such as Spain, Italy, and Greece (Reversat et al., 1992; Silan et al., 1985). In our study, a high mortality rate was not observed, the rate was determined as 0.5%. It was reported that all fish examined did not show any macroscopic symptoms and were in good general health (Antonelli et al., 2010). flammatory reactions, cell infiltration and epithelial hyperplasia were observed in the lamellae of the connecting parts of the haptor of the parasite (Roubal, 1989). In our study, in cases with epitheliocyst, cysts and fusion in the secondary lamellae whereas, in cases where the *Furnestinia spp*. disease progressed alone, only macrophage, lymphocyte and eosinophilic granulated cell infiltrates were observed.

Cryptocaryon spp.

Lom (1984) has been reported that *Cryptocaryon* irritants, which causes white patches on the skin, are slightly smaller than Ich and therefore appear as slightly smaller nodules. Studies have found that infested skin looks like salt has been sprinkled on it. It has been stated that skin lesions appear more like multifocal white spots and sometimes as discrete white spots. In our study, no macroscopic findings were found in the sea bass that came to our laboratory. In histopathological sections, it was observed that it had a granular macronucleus with abundant cytoplasm, consisting of four interconnected bead-like sections. Multigranular macronuclei were seen in native examinations. Studies have stated that native gill examination or skin scraping is performed to detect the trophont stage of Ich (Yanong, 2009). In the present study, a horseshoe-shaped macronucleus was seen in both native examinations and histopathological sections. It has been observed that both types of Ich show a slow rotational movement originating from peripheral cilia (Yanong, 2009). In our study, it was observed that *Cryptocaryon spp.* were not yet dead and were slowly rotating around themselves with their cilia in the smears prepared from the gills of dead fish. With this finding, it was thought to be a late-dying ciliate. In studies, ich parasites caused damage to the host by initiating a hyperplastic host response in the gills and skin they invaded. During the trophont stage, ruptures in the gill and skin epithelium, loss of skin integrity, and respiratory distress in the gills due to osmotic stress were observed. Any deterioration in skin integrity and any change found macroscopically in the gills However, the shedding seen in the gill epithelium in histopathological sections was considered as the initial stage of these findings. Embedded parasite trophonts accompanied by granulomatous inflammation were observed at the tips of the gills of seabass and seabream infested with Cryptocaryon irritans. The presence of trophozoites has also been reported between the skin and muscle bundles of infested fish (Khalil et al., 2018). In our study, this parasite was not found in seabream. In seabass, trophozoites were seen in all parts of the gills, not just the tips.

Amyloodinium spp.

Amyloodinium spp., which is widespread all over the world. Infestation has been reported to be one of the most important diseases of warm water marine fish (Noga and Levy, 2006). In our study, this parasite was seen especially in sea bass reared in earthen ponds. The optimum temperature for most isolates is between 23-27°C. In the studies conducted, *Amyloodinium spp.* the factors caused infestation in salinities varying between 3-45 ppt. It has been stated that Red Sea isolates do not divide below 12 ppt salinity, outbreaks in the Gulf of Mexico are generally seen at 3 ppt salinity, and Australian outbreaks are seen at 5 ppt salinity. Salinity tolerance decreased at low temperatures (Paperna, 1984). In our study, the fact that this parasite was more common in soil ponds producing at low salinity levels supported the researchers' data. Guerra Santos et al. (2012) has reported that hemorrhage and inflammation occur in the gill filaments. Acute pathological changes include increased mucus secretion and decreased respiratory surface, resulting in difficulty breathing. In histopathological examinations, it was determined that the parasites attached to the filaments between the lamellae caused varying degrees of epithelial hyperplasia, hypertrophy in the primary and secondary lamellae, vacuolization in the lamellar epithelium, and fusion in the secondary lamellae. In addition, vacuolar degeneration, loss of epithelial tissue integrity, hyperplasia of secondary lamellae, fusion of secondary lamellae and necrosis were observed. Clinical symptoms have been reported to include anorexia, irregular and dizzy swimming at the surface, emaciation, and hyperventilation (Abreu et al., 2005; Francis and Floyd, 2011). In our study, acute deaths were observed at a rate of 10%. Any examination of the skin was performed, but macroscopically, bleeding was observed in the gills. Histopathological sections showed different forms of parasites, hyperplasia, epithelial shedding, epithelial lifting, bleeding, macrophage, lymphocyte, and eosinophilic granule cell infiltration.

Trichodina spp.

Trichodina spp. has been reported to be a parasite that infests many marine or freshwater fish. It has been observed that many species cause infestation of both skin and gills (Basson and Van, 2006). In the presented study, it was seen in both sea bream and sea bass. It has been stated that trichodinids are motile ciliates characterized by a body covered with a thin membrane surrounded by an adoral ciliary spiral, a horseshoe-shaped macronucleus, and the presence of an adhesive disc equipped with a ring of denticles (Basson and Van, 2006). It has been emphasized that the parasite appears as a saucer from above and as a circle, dome or hat when viewed from the side, that the cilia surround the entire body, that when viewed from above the parasite has a hooked part called a toothed ring, and that it characteristically rotates quickly around itself and exhibits a scooping movement (Noga, 2010; Zhao). and Thong, 2011). In our study, specific for *Trichodina spp.* in smears and histopathological sections; macronucleus, dendritic ring, rotational movement, and dome shape were observed. *Trichodina* infestation has been observed to be a relatively milder disease than other parasitic infestations, resulting in chronic morbidity or mortality (Hoffmann, 1999). However, in some cases it has caused significant losses, especially in young fish. No obvious macroscopic findings were observed in infected fish and mortality was reported to be low. It has been determined that the parasites damage the epithelial tissue in the areas they irritate with their adhesive discs and cause hyperplasia in the gill tissue. Excessive mucus production has also been observed in infested skin. According to Basson and Van As (2006), a *Trichodina spp.* is tightly attached to the surface of epithelial cells. Connection and rotation movements caused serious damage and destruction to the epithelial or epidermal cells of the fish. In acute infestations, ulcers, subepithelial epithelial lifting, hyperplasia of secondary lamellae and mononuclear cell infiltrates were observed. In chronic infestations, an increase in the mucus cells of the gill epithelium and filaments, partial or complete fusion of secondary lamellae, hyperplasia, inflammatory infiltration, and gill necrosis have been observed (Valladö et al., 2013). In this study, histopathologically; shedding and damage, hyperplasia, epithelial lifting, and fusion were observed in secondary lamellar epithelial cells.

Cryptobia spp.

Cryptobia spp. were identified by examining native preparations from skin and gills under a microscope (Kozloff, 2004). Due to the similarity between *Cryptobia spp.* and *Costia spp.*; flagella, length of the parasite, body width, nucleus diameter, and cell shape are important for differential diagnosis. It has been determined that the observation of a ripple-like tendency and contraction movement in the flagella differs from the circular movements of *Costia spp.* Kuperman et al. (2002) suggested that the parasite does not invade host cells during the attachment process and does not cause pathological changes. However, in highly infested juvenile fish, causes such as increased mucus production, epithelial lifting and necrosis in gill filaments were directly related to the decrease in respiration. In our study, any parasites were found in seabass weighing between 2-200 g. Mortality occurred at a rate of 1%, only in juvenile seabass weighing between 2-10 g. Histopathologically, shedding, epithelial lifting, slight bleeding and hyperplasia were observed in the gill filament epithelium.

Costia spp.

It has been stated that *Ichthyobodo necator* (*Costia necatrix*) is one of the smallest ectoparasites that infect fish, being the size of an erythrocyte. Noga (2010) reported that *Ichthyobodo* agents have been shown to be especially dangerous for young fish, attacking healthy fry and eggs, and being a stress factor in larger fish. It has been reported that *Ichthyobodo necator* causes disease in a wide temperature range (2-30°C), causing intense mortality in warm water fish by causing infestations mostly at temperatures below 25°C or above 30°C. It has been reported to be found in the skin and gills of infested fish. In our study, parasites were observed in seabass between 10-350 g and seabream between 25-200 g. No species specificity was observed. *Costia spp.* Infested samples were obtained in April-May-June.

Ichthyobodo spp

It has been reported that *Ichthyobodo spp.* can sometimes cause death with very few pathological findings, and tissue irritation also causes epithelial hyperplasia and increased mucus production (Isaksen, 2013; Lom and Dykova, 1992; Todal et al., 2004). In our study, a mortality rate of 2% was found in sea bass and 5.5% in sea bream. It was thought that the reason for the higher mortality rate in sea bream than in sea bass might be *Flexibacter spp.* infection. Fish that were with intense infestation, vacuolar degeneration, intense hyperplasia of goblet cells and a spongiosis appearance were observed to predominate. It has been reported that epidermis cells lose their cell membranes and begin to shed, and although there is infection in the gill filaments, there is no obvious pathological change (Yardımcı et al., 2016). Urawa et al. (1998) showed that; mild inflammatory symptoms on the ventral body surface in fish weighing between 226-463 grams. Erosion and bleeding caused by unidentifiable secondary bacterial infection also attracted attention. In the presented study, only epithelial lifting and epidermal erosion were observed in seabass in histopathological preparations, while in addition. necrotic changes were observed in the area due to rod-shaped bacteria *Flexibacter spp.* infection.

CONCLUSION

For early diagnosis of parasitic diseases, a sufficient number of samples should be taken from suspicious fish and examined as soon as possible. Duration is also a critical factor for the proliferation of parasites. However, classical methods are used as a diagnostic method and there is no different diagnostic method. There are various methods used for the treatment of parasites in the field. Applications may vary depending on the parasite type, size and family. For example, garlic extract feed additive products work for Monogeneans. For smaller ciliate and flagellate parasites, bath applications such as formaldehyde and oxygen peroxide are effective instead of oral treatment. Copper sulfate bath or copper plate is used specifically for the *Amyloodinium spp.* parasite. In the study, native examination, native examination after Giemsa staining and examination of histopathological sections were performed using light microscopy. It was deemed sufficient for species determination and description of histopathological findings. However, electron microscopy can be used for further research and studies. Our work, consists of data obtained by examining the parasitic diseases seen in sea bream and sea bass fish farmed in the Milas region for a period of one year. It is important as it is the first comprehensive study to use the histopathology method for sea bream and sea bass parasites in our country. Although there are many studies on gill parasites in our country, the limited number of studies on their histopathological findings increases the value of our study. For future studies, different geographic regions, different fish species, longer sample collection time and larger numbers of fish, and electron microscopy may be used.

DECLARATIONS

Ethics Approval

Since paraffin sections of the gills of fish that had died naturally were examined in the study, an ethics committee certificate was not required.

Conflicts Of Interest

The authors declare that there is no known financial or personal conflict that may affect the research (article).

Consent for Publication

Not applicable.

Author contribution

Idea, concept, and design: MD

Data collection and analysis: MD,SYO

Drafting of the manuscript: MD, SYO

Critical review: MD

Data Availability

The data used to prepare this manuscript are available from the corresponding author when requested.

Acknowledgements

This study is summarized from the doctoral thesis of the same

name and was supported by Research Fund the Aydın Adnan Menderes University. Project number: VTF-19032.

REFERENCES

Abreu, P.C., Robaldo, R.B., Sampaio, L.A., Bianchini, A., & Odebrecht, C. (2005). Recurrent Amyloodiniosison broodstock of the Brazilian flounder Paralichthys orbignyanus: dinospore monitoring and prophylactic measures. The Journal of the World Aquaculture Society, 36(1), 42-50.

Alvarez-Pellitero, P. (2004). Report about fish parasitic diseases. In: P. Alvarez-Pellitero JL, Barja B, Basurco F, Berthe A.E, Toranzo, editors. Mediterranean Aquaculture Diagnostic Laboratories. CIHEAM/FAO. Etudes et Recherches. Zaragoza, p.103-129.

Antonelli, L., Quilichini, Y., & Marchand, B. (2010). Biological study of Furnestinia echeneis Euzet and Audouin 1959 (Monogenea: Monopisthocotylea: Diplectanidae), parasite of cultured Gilthead sea bream Sparus aurata (Linnaeus 1758) (Pisces: Teleostei) from Corsica. Aquaculture, 307, 179-186.

Arıkan, M.S., & Aral, Y. (2019). Economic analysis of aquaculture enterprises and determination of factors affecting sustainability of the sector in Turkey. Ankara Üniversitesi Veteriner Fakültesi Dergisi, 66, 59-66.

Basson, L., & Van As J. (2006). Trichodinidae and other ciliophorans (Phylum Ciliophora). Fish Diseases and Disorders; Vol. 1. Protozoan and Metazoan Infections. 2nd. ed. CABI, Oxford, p. 154-182

Cruz Silva, M.P., Freitas, M.S., & Orge, M.L. (1997). Co-infection by monogenetic trematodes of the genus Microcotyle, (Beneden&Hesse 1863), Lamellodiscus ignoratus (Palombi 1943), the protozoan Trichodina sp. (Ehrenberg 1838) and the presence of epitheliocystis, Vibrio alginolyticus and V. vulnificus in cultured sea bream (Sparus aurata) in Portugal. European Association of Fish Pathologists, 17, 40-2.

Culling, A.F., Allison, T.R., & Barr, T.W. (1985). Cellular Pathology Technique. 4th. ed. London: Butterworth&Co, p.269-270.

Çoban, D., Demircan, M.D., & Tosun, D.D. (2020). Disease problems of marine cultured fish in Turkey: Agents, detection and treatments. Demircan MD, Midilli, S, Dereli M, Otgucuoğlu Ö, editors. Marine Aquaculture in Turkey: Advancements and Management İstanbul: Turkish Marine Research Foundation (TUDAV), p.165-199.

Demir, O. (2011). Türkiye Su Ürünleri Yetiştiriciliği ve Yem Sektörüne Genel Bakış-II, ISUBÜ. Suleyman Demirel University, Egirdir Fisheries Faculty, 7(1), 39-49.

Desdevises, Y. (2001). The phylogenetic position of Furnestinia echeneis (Monogenea, Diplectanidae) based on molecular data: a case of morphological adaptation. International Journal for Parasitology, 31, 205-8.

Faisal, M., & Imam, E.A. (1990). Microcotyl echrysophrii (Monogenea: Polyopisthocotylea), a pathogen of cultured and wild gilthead sea bream, Sparus aurata. Perkins FO, Cheng TC, editors. Pathology in Marine Science. San Diego: Academic Press, p.283-290.

Francis, R.F., &Floyd, M.R. (2011). Amyloodinium ocellatum, an Important Parasite of Cultured Marine Fish. Southern Regional Aquaculture Center, 4705, 1-11.

Gıda ve Tarım Örgütü [FAO]. Dünyada Balıkçılık ve Su Ürünleri Yetiştiriciliğinin Durumu. 2018;http://www.fao.org/3/CA0191TR/ca0191tr.pdf.

González-Lanza, C., Alvarez-Pellitero, P., & Sitja-Bobadilla, A. (1991). Diplectanidae (Monogenea) infestations of sea bass, Dicentrarchus labrax (L.), from the Spanish Mediterraneanarea. Parasitology Research, 77, 307-314.

Guerra Santos, B., Albinati, R.C., Moreira, E.L.T., Lima, F.W., Azevedo, T.M., & Costa, D.S.P. (2012). Parametros hematologicos e alteraçoes histopatologicas em bijupira (Rachycentron canadum; Linnaeus, 1766) com amyloodiniose. Pesquisa Veterinaria Brasileira, 32(11), 1184-1190.

Hoffman, G.L. (1999). Parasites of North American Freshwater Fish, 2nd ed. Ithaca: Cornell University.

Isaksen, T.E. (2013). Ichthyobodo infections on farmed and wild fish Methods for detection and identification of Ichthyobodo spp., PhD, Norway:University of Bergen.

Khalil, R.H., Medhat, S.S., Hanan, A.G., Khallaf, M., Sherif, E.S., Amira, A.E.D.O. (2018). Seasonal Parasitic Infestations and their Close Relationship to Immune Suppression in Cultured Sea Bass (Dicentrarchus labrax) and Sea Bream (Sparus auratus). Biomed J Sci&Tech R Biomedical Journal of Scientific & Technical Research, 6(4), 1-9.

Kozloff, E.N. (2004). Redescription of Cryptobiahelicis (Leidy, 1846) (Kinetoplasta: Bodonea: Cryptobiidae), disposition of flagellates mistakenly assigned to this species and description of a new species from a North American Pulmonate Snail. Acta Protozoologica, 43, 123-132.

Kuperman, B.I., Matey, V.E., & Barlow, S.B. (2002). Flagellate Cryptobia branchialis (Bodonida: Kinetoplastida), ectoparasite of tilapia from the Salton Sea. Hydrobiological, 473(1/3), 93-102.

Llewellyn, J. (1957). The larvae of some monogenetic trematode parasites of Plymouth Fishes. Journal of the Marine Biological Association UK, 36, 243-259.

Lom, J. (1958). A contribution to the systematic and morphology of end oparasitictrichodinids from amphibians with proposal of uniform specific characteristics. The Journal of protozoology, 5, 251-263.

Lom, J. (1984). Diseases caused by Protista. Diseases of Marine Animals. Hamburg: FRG, p.114-168.

Lom, J., & Dykova, I. (1992). Protozoan parasites of fish developments in Aquaculture and Fisheries Science. New York: Elsevier.

Mahmoud, N.E., Mahmoud, A.M., & Fahmy, M.M. (2004).

Parasitological and comparative pathological studies on Monogenean infestation of cultured sea bream (Sparus aurata) in Egypt. Oceanographic, 2, 4.

Mladineo, I., & Marsic-Lucic, J. (2007). Host switch of Lamellodiscus elegans (Monogenea: Monopisthocotylea) and Sparicotyle chrysophrii (Monogenea: Polyopisthocotylea) between cage-reared sparids. Veterinary Research Communications 31(2), 153-160.

Noga, E.J. (2010). Fish Disease Diagnosis and Treatment, II. Iowa: Wiley.

Noga, E.J., & Levy, M.G. (2006). Phylum Dinoflagellata. Fish Diseases and Disorders, Protozoan and Metazoan Infections. Oxford: CABI, p. 16-45.

Oliver, G. (1968). Recherches sur les Diplectanidae (Monogenea) parasites de téléostéens du Golfedu Lion. I. Diplectaninae Monticelli, 1903. Vie et Milieu, 19, 95-138.

Oliver, G. (1982). Microcotyle chrysophrii Van Beneden et Hesse, 1863 (Monogenea, Polyopisthocotylea, Microcotylidae) parasite de Sparus aurata Linneaus, 1758 (Teleostei, Sparidae) dans lesétangslittorauxdu Languedoc-Roussillon (France). Parasitology, 20, 113-8.

Paperna, I. (1984). Reproduction cycle and tolerance to temperature and salinity of Amyloodinium ocellatum (Dinoflagellida). Annales de Parasitologie Humaine et Comparée, 5, 7-30.

Rajdukovic, B.M., & Euzet, L. (1989). Parasites of Marine Fishes of Montenegro: Monogeneans. Acta Adriatica, 30(1-2), 51-135.

Reversat, J., Silan, P., & Maillard, C. (1992). Structure of monogenean populations, ectoparasites of the gilthead sea bream Sparus aurata. Marine Biology, 112, 43-7.

Roberts, RJ. (2012). Fish Pathology, 4th. ed. United Kingdom: Blackwell.

Roubal, F.R. (1989). Comparative pathology of some monogenean and copepod ectoparasites on the gills of Acanthopagrus australis (family Sparidae). Journal of Fish Biology, 34, 503-514.

Silan, P., Cabral, P., & Maillard, C. (1985). Enlargement of the host rang of Polylabris Tubicirrus (Monogenea, Polyopisthocotylea) under fish-farming conditions. Aquaculture, 45, 267-270.

Sitja-Bobadilla, A., & Alvarez-Pellitero, P. (2009). Experimental transmission of Sparicotyle chrysophrii (Monogenea: Polyopisthocotylea) to gilthead sea bream (Sparus aurata) and histopathology of the infection. Folia Parasitologica, 56(2), 143-151.

Stoskopf, M.K. (1993). Fish Medicine. London: W.B. Saunders. Philadelphia.

Tarımsal Araştırmalar ve Politikalar Genel Müdürlüğü [TAGEM]. (2019). Su Ürünleri Sektör Politika Belgesi, Tarım ve Orman Bakanlığı Tarımsal Araştırmalar ve Politikalar Genel Müdürlüğü .https://www.tarimorman.gov.tr/TAGEM.

Todal, J.A., KarlsbakkIsaksen, T.E., Plarre, H., Urawa, S., Mouton, A., Hoel, E., & Nylund, A. (2004). Ichthyobodo necator (Kinetoplastida)- a complex of sibling species. Diseases of Aquatic Organisms, 58, 9-16.

Urawa, S., Ueki, N., & Karlsbakk, E. (1998). A review of Ichthyobodo infection in marine fishes. Fish Pathology, 33(4), 311-320.

Vagianou, S., Athanassopoulou, F., Ragıas, V., DiCave, D., Leontides, L., & Golomazou, E. (2006). Prevalence and pathology of ectoparasites of Mediterranean Sea bream and sea bass reared under different environmental and aquaculture conditions. Israelı Journal of Aquaculture-Bamıdgeh, 58, 78-88.

Valladö, G.M.R., Gallanı, S.U., Padua, S.B., Martins, M.L., & Pilarski, F. (2013). Trichodina heterodentata (Ciliophora) infestation on Prochilodus lineatus larvae: a host–parasite relationship study. Parasitology, 141(05), 662-9.

Wagener, G.R. (1857). Heminthologische Bemcrkungenauseinem Sendschreibcs an. Zeitschrift für wissenschaftliche Zoologie, 9, 73-90.

Yanong, R.P.E. (2009). Cryptocaryon irritans infections (Marine White Spot Disease) in Fish. IFAS Extension University of Florida. FA, p.1-9.

Yardımcı, B., & Pekmezci, G.Z. (2012). Gill histopathology in cultured sea bass (Dicentrarchus labrax L.) co-infected by Diplectanum aequans (Wagener, 1857) and Lernanthropus kroyeri (vanBeneden, 1851). Ankara Üniversitesi Veteriner Fakültesi Dergisi, 59, 61-4.

Yardımcı, B., Pekmezci, G.Z., Didinen, B.I., & Metin, S. (2016). Ichthyobodo spp. infection in Meagr(Argyrosomus regius) from Turkey: Parasitological and Pathological Findings. Turkish Journal of Parasitology, 40, 48-50.

Zhao, Y.J., & Thong, F.H. (2011). Study of trichodinids (Protozoa, Ciliophora) parasitic on gills of freshwater fishes from Chongqing, China, and identification of a new species, Trichodina cyprinocola sp. nov. African Journal of Microbiology Research, 5(26), 5523-7.

Medit Vet J, 9(3): 385-394, 2024
DOI: 10.24880/meditvetj.1528441

Research Article

Quantitative evaluation of limb conformation in various age cohorts of thoroughbreds

İsmail Gökçe Yıldırım[1], Hasan Erden[1]

[2]Department of Anatomy, Faculty of Veterinary Medicine, Aydın Adnan Menderes University, Aydın, Türkiye

Key Words:
conformation
horse
limb
thoroughbred

Received : 9 August 2024
Revised : xx xxxxxx 2024
Accepted : 9 November 2024
Published : 31 December 2024
Article Code : 1528441

Correspondence:
İG. YILDIRIM
(gyildirim@adu.edu.tr)

ORCID
İG. YILDIRIM : 0000-0003-3458-0827
H. ERDEN : 0000-0002-6470-0220

Aydın Adnan Menderes University Research Foundation (VTF-11010) funded this research, which was a component of the first author's unpublished PhD thesis.

ABSTRACT

An ideal horse should possess a limb conformation that enhances athletic capabilities and adjusts to varying loads. The structure of the limbs greatly influences a horse's performance and overall success. The study aimed to identify the limb conformations of Thoroughbreds across various age groups through quantitative assessments. Limb conformation data were captured from the horse's front, left side, and rear using simultaneous photographs. Simultaneous photography ensured that snapshots of the horse were consistent, with no variations between photographs caused by movement. The limb conformation of 137 Thoroughbred horses was assessed recording measurements of limb length, and angles at ages 6, 12, 18, 24, 36, and 48 months. From 6 to 36 months, the heights of withers and croups increased consistently, with the most significant growth occurring within the first 24 months. Forelimb length saw notable increases from 6 to 24 months in both genders, but the growth between 24 and 48 months was not significant. The angle of the front fetlock was straightest in the 6-month-old group, decreasing to mature levels after 12 months. The findings indicate that the croups of horses were higher than their withers across all assessed ages, potentially altering the horse's center of gravity and placing more stress on the forelimbs. The ratio of distal extremity lengths to total leg length increased with age.

INTRODUCTION

The concept of conformation in horses, referring to their overall body shape and structure, has been a subject of interest dating back to the earliest documented analysis by the Greek historian and philosopher Xenophon (430–354 BC). The evolution of this interest has led to extensive research exploring the correlation between a horse's physical attributes and its performance capabilities. Conformation is often interpreted as the interplay between form and function, suggesting a link between a horse's physical appearance and its potential for athletic performance (Hedge and Wagoner, 2004). This relationship extends to the selection process in breeding, where both conformation and behavioral traits are considered significant factors (Van Weeren and Denoix, 2006). In the context of racehorse breeding, specific body structure traits are pivotal for selection, emphasizing the need for breeding programs to prioritize structural characteristics conducive to high athletic performance (Jakubec et al., 2009; Belloy and Bathe, 1996). The establishment of evaluation criteria for a horse's body structure is vital, aiming at identifying the ideal traits that enhance athletic abilities (Belloy and Bathe, 1996). Moreover, recognizing age-related morphological changes is fundamental to understanding the potential for disabilities in horses. The goal of conformation assessments is to meticulously analyze the body's measurements, such as lengths and angular values, to delineate the synergistic relationships among various body parts (Hedge and Wagoner, 2004; Yıldırım, 2014). Such assessments are essential for elucidating the connection between conformation and performance in sport horses, which remains a critical area of research (Moore, 2010). Furthermore, a lack of understanding regarding the impact of conformation on health and performance can lead to suboptimal decisions in horse selection (Sanchez et al., 2013).

Clinical experiences have shown a link between abnormalities in the limbs and specific diseases of the locomotor system in sport horses (Dolvik and Klemetsdal, 1999; Smith et al., 2006; Van Weeren and Denoix, 2006). Assessing conformation is crucial for evaluating the musculoskeletal health, balance, and athletic capabilities of thoroughbreds (Harris, 1993; Bakhtiari and Heshmat, 2009). Objective assessment of conformation requires the collection of quantitative data, eg limb measurements.

Measurements can be directly taken on the animal, yet fully preventing movement during this process is challenging. The horse's movement during or between measurements can lead to varied results. Therefore, despite reliance on direct observation in conformation research, photograph-based measurements are often preferred. Photographic methods enable various individuals to conduct measurements at different times,

To cite this article:
Gökçe Yıldırım İ, Erden H. Quantitative evaluation of limb conformation in various age cohorts of thoroughbreds. Medit Vet J. 2024; 9(3): 385-394.

ensuring consistency. This approach has been widely utilized and supported by numerous studies in the field (Fedorski and Pikula, 1988; Delahunty et al., 1991; Stover, 2003; Kavazis and Ott, 2003; Anderson and McIlwraith, 2004; Mawdsley et al., 1996; Yıldırım and Erden, 2023).

The conformation of a racehorse's body and limbs significantly impacts its health and performance (Anderson et al., 2004). Investigating the limb structures of horses across different age groups can enhance our understanding of these correlations. This study is designed to analyze the limb conformation of Thoroughbred horses in various age groups using morphometric measurements. The findings are anticipated to deepen our knowledge of how limb structures in horses evolve with age and gender, and how conformation in horses changes with age and gender, and how these changes may influence the risk of injury.

MATERIALS and METHODS

Study Population

All horses involved in this study were thoroughbreds born in Türkiye, specifically bred for flat racing and listed in the racing pedigree. Rigorous screening was conducted to exclude any horses with visible injuries or abnormalities in their musculoskeletal systems. Additionally, a thorough visual inspection ensured the absence of conformational defects in the horses' bodies and limbs. From an initial pool of 300, 137 horses were deemed suitable for the study. The younger horses, aged 6–18 months, were sourced from stud farms located in İzmir. The older group, aged 24-48 months, consisted of horses that had participated in flat races held by the Turkish Jockey Club at the Izmir Şirinyer Hippodrome. Rather than continuously monitoring the developmental progress of the same horses throughout the study, we opted for a population comprising various horses. This decision was made to address time limitations. However, it remained essential that all horses within the same age group were reared on the same farm, adhering to identical care conditions.

The structure of a horse's hooves significantly impacts limb conformation. Standardizing this variable was crucial. In Türkiye, Turkish Jockey Club grants licenses to farriers responsible for hoof care. As a result, consistent monthly hoof care practices were established, effectively eliminating variations arising from differences in nail structure.

The descriptive age and gender characteristics of the horses included in the study are presented in Table 1.

Photographs Characteristic

For the photo session, the horses were positioned on a level surface and maintained in the correct posture by the support staff. Proper posture is defined as the horse standing with all four feet evenly on the ground, limbs positioned naturally, and the head oriented forward. Each horse was photographed on a stable, flat surface. Once the horses were properly positioned, three photos were taken simultaneously from the left, front, and rear using Canon EOS 350D digital cameras, set to a resolution of 4752x3168 dpi. This approach follows the methods used in previous studies (Anderson and McIlwraith, 2004; Sadek et al., 2006), ensuring consistency in the photographic documentation of the horses' conformation. The cameras were set up on tripods positioned three meters from the horse and at a height of 0.9 meters, as shown in Figure 1.

In the context of photographing horses, specific guidelines were followed to ensure consistent and accurate measurements. These guidelines were crucial for maintaining uniformity across all images. The left side of the horse was aligned perpendicular to the camera. The horse itself stood squarely relative to the camera. Both the left forelimb and hind limb were positioned as vertically as possible concerning the ground. The horse was centered within the frame. Photographers maintained perfect parallel alignment with the horse's horizontal axis. The camera was positioned just behind the horse's center of gravity (specifically, the 9th to 11th costal part) along the lateral thoracic wall. Importantly, the camera was neither higher, lower, nor offset forward or backward from this position. The photographer ensured that the camera was exactly at the midpoint between the two forelimbs or hind limbs. All photographs adhered to the same distance, height, and focus settings. This consistency allowed for standardized images of both upper and lower extremities. As long as this measurement technique remains consistent, the resulting values will be repeatable.

A radio-frequency remote control facilitated the synchronized operation of the three cameras. To ensure the photographs accurately reflected the horse's true size, the lengths of Mc3 (the third metacarpal bone) and Mt3 (the third metatarsal bone) on the left front and hind legs, respectively, were measured and noted. Once the images were uploaded to a computer, calibration was performed using the Mc3 measurements for the forelimbs and the Mt3 measurements for the hind limbs. This calibration process, along with all measurements, was conducted using the Vet Eickemeyer® Medizintechnik für Tierärzte (EIVIS) software, with the first author (IGY) responsible for all measurements.

Table 1. The descriptive age and gender properties of the horses in the study.

Sex	6 months	12 months	18 months	24 months	36 months	48 months	Total
♂	12	12	12	11	10	10	67
♀	12	16	11	10	10	11	70
Total	24	28	23	21	20	21	137

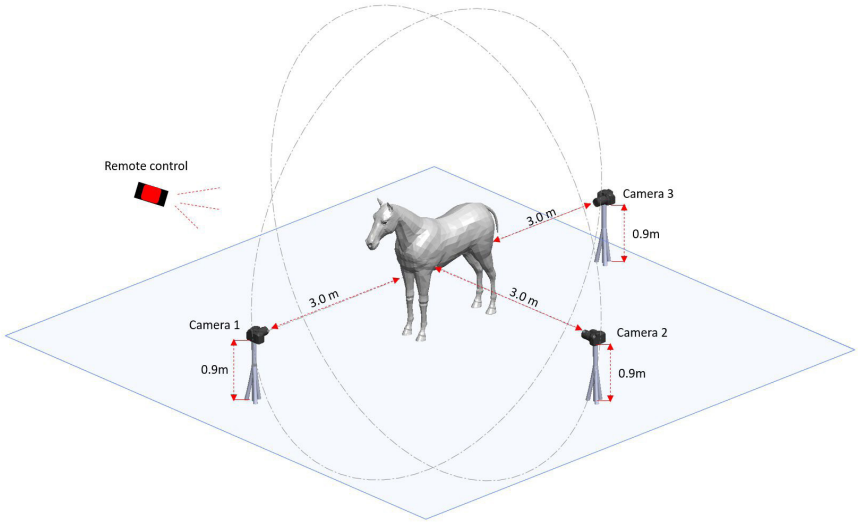

Figure 1. Simultaneous photo image technique. Three cameras are synchronized to capture photographs simultaneously, operated by a radiofrequency remote control.

Table 2. The descriptive of the variables studied.

Trait	Side	Description
Upper Leg Length	front	Shoulder joint (1) to carpal joint (2)
Mc3 Length	front	Carpal joint to metacarpophalangeal joint (3)
Pastern Length	front	Metacarpophalangeal joint to mid-coronary band (4)
Carpal Angle	front	Shoulder joint to carpal joint to metacarpophalangeal joint
Fetlock Angle	front	Carpal joint to metacarpophalangeal joint to mid-coronary band
Coronary Angle	front	Metacarpophalangeal joint to mid-coronary band to hoof tip (5)
Coronary Width	front	Medial to lateral width of the coronary band
Hoof Width	front	Medial to lateral width of hoof at ground touch region (6-6')
Wither Height	left	Heighest point of withers (7) to ground
Elbow Angle	left	Shoulder joint (8) to elbow joint (9) to mid-carpus (10)
Carpal Angle	left	Elbow joint to carpal joint to metacarpophalangeal joint (11)
Forelimb Length	left	Elbow joint to mid-carpal joint
Fetlock Angle	left	Carpal joint to metacarpophalangeal joint to mid-coronary band (12)
Lateral Hoof Angle	left	Between the dorsal and palmar edges of the hoof (orange lines)
Front Pastern Angle	left	Metacarpophalangeal joint to mid-coronary band to hoof axis
Croup Height	left	Heighest point of croup (13) to ground
Stifle Angle	left	Hip joint (14) to stifle joint (15) to tarsal joint (16)
Hock Angle	left	Stifle joint to tarsal joint to metatarsophalangeal joint (17)
Rear Fetlock Angle	left	Tarsal joint to metatarsophalangeal joint to hoof axis
Rear Pastern Angle	left	Metatarsophalangeal joint to mid-coronary band (18) to hoof axis
Rear Hoof Angle	left	Between the dorsal and plantar edges of the hoof
Caudal Genu Angle	rear	Ischiatic tuberosity (19) to mid-popliteal regio (20) to calcaneal tuberosity (21)
Caudal Tarsal Angle	rear	Mid-popliteal regio to calcaneal tuberosity to metatarsophalangeal joint
Mt3 Length	rear	Base of 3rd metatarsal (22) to metatarsophalangeal joint (23)
Rear Fetlock Angle	rear	Calcaneal tuberosity to metatarsophalangeal joint to mid-hoof at central sulcus (24)
Rear Pastern Length	rear	Metatarsophalangeal joint to mid-hoof at central sulcus

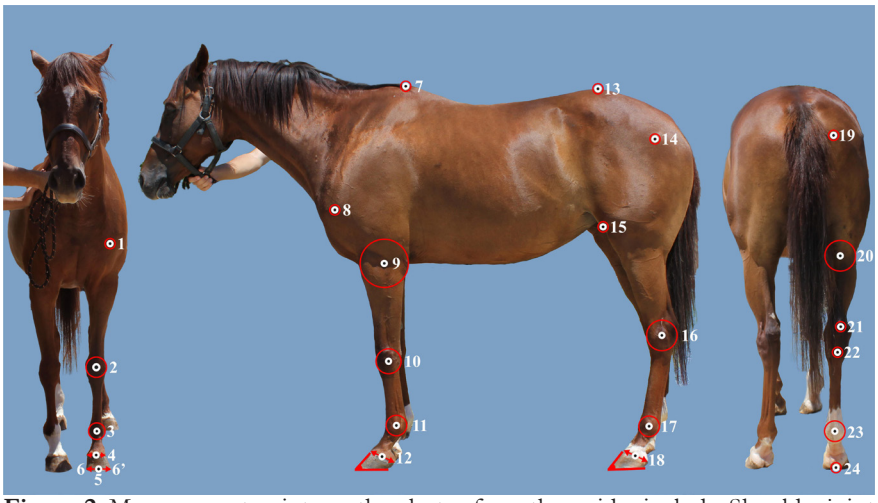

Figure 2. Measurement points on the photos from three sides include: Shoulder joint (1), Carpal joint (2), Metacarpophalangeal joint (3), Mid-coronary band on the forelimb (4), Hoof tip (5), Ground contact region of the hoof (6-6'), Highest point of the withers (7), Shoulder joint (8), Elbow joint (9), Mid-carpus (10), Metacarpophalangeal joint (11), Mid-coronary band on the forelimb (12), Highest point of the croup (13), Hip joint (14), Stifle joint (15), Tarsal (hock) joint (16), Metatarsophalangeal joint (17), Mid-coronary band on the hind limb (18), Ischiatic tuberosity (19), Mid-popliteal region (20), Calcaneal tuberosity (21), Basis base of 3rd metatarsal (22), Metatarsophalangeal joint (23), and Central sulcus on the mid-hoof (24).

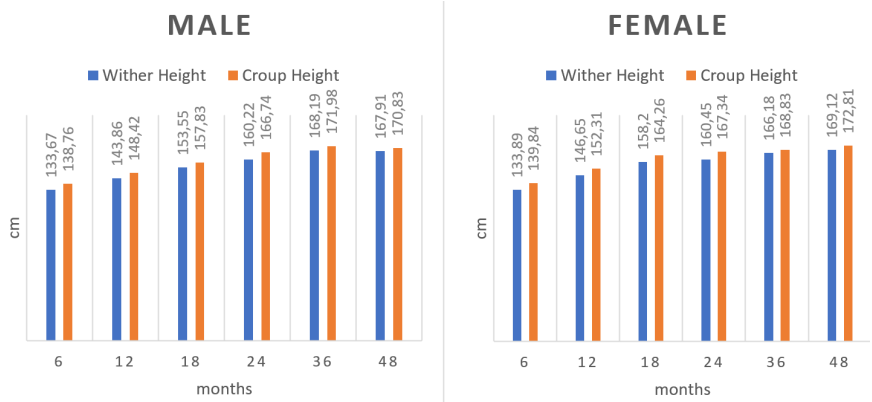

Figure 3. Changes in mean withers and croup heights in male and female horses aged 6 to 48 months (Height in cm).

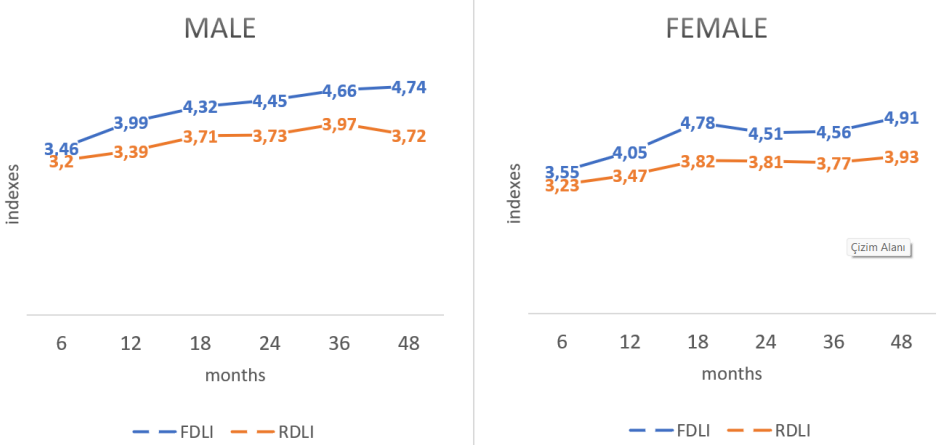

Figure 4. Changes in front (FDLI) and rear (RDLI) distal extremity indexes for males and females from 6 to 48 months.

Table 3. The measurements on the male horses (cm and degree). The data is presented as mean and standard error (MV± SEM).

Traits	Side	6 month	12 month	18 month	24 month	36 month	48 month	P
Upper Leg Length	front	57.40±1.05^{d}	59.93±1.25^{cd}	65.65±0.96^{a}	62.09±1.32^{bc}	66.44±0.65^{a}	64.78±0.53^{ab}	0.000
Mc3 Length	front	25.11±0.34^{a}	24.07±0.27^{ab}	23.56±0.35^{b}	24.40±0.54^{ab}	23.74±0.11^{b}	23.71±0.29^{b}	0.022
Pastern Length	front	13.49±0.26^{a}	11.91±0.34^{b}	11.96±0.32^{b}	11.60±0.20^{b}	12.35±0.27^{b}	11.68±0.22^{b}	0.000
Carpal Angle	front	175.66±0.47^{ab}	176.54±0.62^{a}	175.90±0.64^{ab}	175.57±1.08^{ab}	174.16±0.41^{b}	177.17±0.38^{a}	0.65
Fetlock Angle	front	176.03±0.74^{abc}	174.19±0.82^{c}	177.06±0.62^{ab}	176.21±0.57^{abc}	175.36±0.61^{bc}	177.83±0.40^{a}	0.006
Coronary Angle	front	178.28±0.35^{a}	178.40±0.42^{a}	178.85±0.30^{a}	178.64±0.28^{a}	178.33±0.31^{a}	178.04±0.29^{a}	0.625
Coronary Width	front	8.56±0.13^{c}	8.95±0.19^{c}	10.33±0.17^{a}	9.63±0.14^{b}	9.50±0.13^{b}	9.48±0.11^{b}	0.000
Hoof Width	front	9.84±0.23^{d}	11.00±0.12^{c}	12.74±0.26^{a}	11.83±0.27^{b}	12.30±0.15^{ab}	12.62±0.15^{a}	0.000
Wither Height	left	133.67±1.72^{e}	143.86±1.39^{d}	153.55±2.56^{c}	160.22±1.95^{b}	168.19±0.78^{a}	167.91±0.97^{a}	0.000
Elbow Angle	left	145.02±1.46^{ab}	141.04±1.37^{bc}	141.62±1.26^{bc}	139.38±1.27^{c}	149.82±2.87^{a}	145.00±1.13^{ab}	0.001
Carpal Angle	left	177.97±0.32^{a}	177.99±0.12^{a}	178.57±0.25^{a}	178.50±0.35^{a}	178.59±0.20^{a}	178.45±0.21^{a}	0.331
Forelimb Length	left	35.29±0.92^{d}	39.03±1.01^{c}	41.82±0.79^{b}	43.30±0.61^{ab}	45.33±0.17^{a}	45.23±0.37^{a}	0.000
Fetlock Angle	left	151.95±0.97^{a}	148.16±0.62^{b}	145.46±1.32^{b}	146.90±1.44^{b}	145.92±0.64^{b}	145.70±0.96^{b}	0.000
Lateral Hoof Angle	left	55.76±1.29^{cd}	61.21±0.64^{a}	58.39±0.78^{b}	58.01±0.86^{bc}	54.47±0.27^{d}	54.06±0.82^{d}	0.000
Front Pastern Angle	left	165.61±1.57^{c}	173.81±1.09^{b}	176.65±0.80^{a}	176.99±0.63^{a}	177.73±0.49^{a}	178.13±0.26^{a}	0.000
Croup Height	left	138.76±1.31^{e}	148.42±1.77^{d}	157.83±2.60^{c}	166.74±2.69^{b}	171.98±1.13^{a}	170.83±1.39^{a}	0.000
Stifle Angle	left	114.34±1.02^{b}	115.40±1.13^{b}	115.37±1.44^{b}	116.76±1.02^{b}	115.52±0.58^{b}	120.57±0.56^{a}	0.003
Hock Angle	left	146.54±0.93$^{a.b}$	145.49±0.57^{b}	146.71±0.75^{ab}	148.30±1.10^{a}	146.25±0.56^{ab}	144.30±0.67^{b}	0.032
Rear Fetlock Angle	left	159.61±1.23^{a}	154.24±1.44^{b}	153.18±1.57^{b}	152.34±1.80^{b}	154.76±0.52^{b}	159.20±0.45^{a}	0.000
Rear Pastern Angle	left	170.72±1.69^{b}	175.16±0.67^{a}	176.09±0.84^{a}	176.60±1.12^{a}	178.00±0.21^{a}	174.94±0.63^{a}	0.000
Rear Hoof Angle	left	58.91±1.25^{ab}	61.02±0.88^{a}	60.66±1.05^{a}	57.41±1.26^{bc}	54.80±0.41^{c}	57.47±0.93^{bc}	0.001
Caudal Genu Angle	rear	177.21±0.56^{a}	174.57±0.60^{b}	176.70±0.87^{ab}	175.67±0.77^{ab}	174.90±0.92^{ab}	176.11±0.80^{ab}	0.113
Caudal Tarsal Angle	rear	176.74±0.74^{a}	177.45±0.75^{a}	173.62±1.52^{b}	176.50±0.60^{a}	176.72±0.86^{a}	177.38±0.38^{a}	0.041
Mt3 Length	rear	29.69±0.58^{c}	30.12±0.45^{bc}	29.58±0.68^{c}	31.25±0.50^{ab}	30.69±0.21^{abc}	31.85±0.27^{a}	0.014
Rear Fetlock Angle	rear	177.76±0.46^{a}	177.24±0.86^{a}	176.90±0.43^{a}	176.70±0.40^{a}	177.69±0.38^{a}	177.87±0.42^{a}	0.56
Rear Pastern Length	rear	13.56±0.42^{ab}	13.64±0.31^{ab}	12.94±0.28^{cb}	13.39±0.36^{abc}	12.53±0.06^{c}	14.06±0.20^{a}	0.024

a,b,c,d: Different letters in the same line are statistically significant (P<0.05).

Table 4. The measurements on the female horses (cm and degree). The data is presented as mean and standard error (MV± SEM).

Traits	Side	6 month	12 month	18 month	24 month	36 month	48 month	P
Upper Leg Length	front	57.61±0.93^{b}	58.19±1.03^{b}	60.08±0.96^{b}	63.94±0.87^{a}	64.74±0.97^{a}	64.59±0.74^{a}	0.000
Mc3 Length	front	24.75±0.24^{a}	23.76±0.41^{ab}	21.98±0.45^{b}	24.04±0.34^{ab}	25.04±0.35^{a}	23.06±1.98^{ab}	0.154
Pastern Length	front	12.96±0.16^{a}	12.43±0.29^{a}	11.08±0.28^{b}	11.49±0.17^{b}	11.35±0.18^{b}	11.40±0.28^{b}	0.000
Carpal Angle	front	175.53±0.56^{abc}	175.04±0.46^{bc}	177.30±0.36^{a}	174.24±1.01^{bc}	173.91±0.44^{c}	176.03±0.71^{ab}	0.005
Fetlock Angle	front	177.22±0.56^{a}	173.93±0.71^{b}	177.70±0.54^{a}	176.42±0.66^{a}	176.90±0.46^{a}	176.76±0.60^{a}	0.000
Coronary Angle	front	178.27±0.33^{a}	178.11±0.37^{a}	178.35±0.38^{a}	178.81±0.24^{a}	178.35±0.31^{a}	178.39±0.12^{a}	0.789
Coronary Width	front	8.58±0.10^{b}	9.04±0.18^{ab}	9.10±0.19^{ab}	9.55±0.28^{a}	9.18±0.11^{a}	9.31±0.14^{a}	0.014
Hoof Width	front	9.98±0.18^{b}	11.83±0.30^{a}	12.24±0.30^{a}	11.89±0.15^{a}	11.58±0.10^{a}	12.23±0.25^{a}	0.000
Wither Height	left	133.89±1.71^{d}	146.65±1.47^{c}	158.20±2.58^{b}	160.45±1.90^{b}	166.18±0.49^{a}	169.12±0.87^{a}	0.000
Elbow Angle	left	144.82±0.87^{a}	138.06±1.43^{b}	144.95±1.84^{a}	139.54±0.94^{b}	145.36±0.34^{a}	145.69±0.47^{a}	0.000
Carpal Angle	left	177.89±0.39^{b}	177.61±0.17^{b}	178.15±0.34^{ab}	178.75±0.23a	178.89±0.19^{a}	178.40±0.22^{ab}	0.012
Forelimb Length	left	38.23±0.58^{c}	39.56±0.56^{bc}	41.04±0.80^{b}	43.67±0.87^{a}	44.10±0.18^{a}	45.34±0.68^{a}	0.000
Fetlock Angle	left	150.85±0.67^{a}	145.24±0.77^{bc}	146.57±1.22^{bc}	146.69±1.00^{b}	143.90±0.79^{c}	146.19±0.69^{bc}	0.000
Lateral Hoof Angle	left	58.38±1.40^{a}	57.97±0.60^{ab}	57.30±0.95^{ab}	57.45±0.71^{ab}	55.22±1.24^{bc}	53.32±0.65^{c}	0.003
Front Pastern Angle	left	171.09±2.01^{b}	174.18±0.93^{ab}	175.90±0.91^{a}	175.30±0.72^{a}	176.08±0.35^{a}	176.44±0.41^{a}	0.011
Croup Height	left	139.84±2.30^{d}	152.31±1.65^{c}	164.26±2.56^{b}	167.34±1.98^{ab}	168.83±1.14^{ab}	172.81±0.98^{a}	0.000
Stifle Angle	left	114.45±1.22^{c}	114.76±0.35^{c}	115.51±1.77^{c}	116.75±0.77^{bc}	119.07±0.55^{ab}	121.03±1.06^{a}	0.000
Hock Angle	left	148.53±1.16^{ab}	146.47±0.60^{bc}	145.86±0.79^{c}	145.10±0.84^{c}	150.53±0.75^{a}	144.72±0.90^{c}	0.000
Rear Fetlock Angle	left	159.20±1.70^{a}	156.56±0.95^{ab}	152.74±0.55^{cd}	155.06±1.87^{bc}	150.71±0.90^{d}	157.34±0.93^{ab}	0.000
Rear Pastern Angle	left	172.43±1.43^{b}	172.87±0.85^{b}	177.51±0.74^{a}	177.25±0.52^{a}	176.65±0.32^{a}	175.90±0.33^{a}	0.000
Rear Hoof Angle	left	60.29±1.17^{a}	61.35±0.77^{a}	57.42±1.00^{bc}	59.18±0.98^{ab}	55.99±0.36^{c}	55.34±0.26^{c}	0.000
Caudal Genu Angle	rear	176.88±0.34^{ab}	174.89±0.86^{bc}	177.57±0.42^{a}	174.39±0.75^{c}	176.33±0.85^{abc}	176.09±0.60^{abc}	0.022
Caudal Tarsal Angle	rear	175.98±0.70^{ab}	174.50±0.92^{b}	175.54±0.90^{ab}	176.15±0.79^{ab}	176.02±0.76^{ab}	177.49±0.38^{a}	0.170
Mt3 Length	rear	29.38±0.45^{b}	30.20±0.31^{ab}	30.18±0.33^{ab}	30.59±0.22^{a}	30.88±0.51^{a}	31.17±0.36^{a}	0.026
Rear Fetlock Angle	rear	176.72±0.64^{cb}	176.05±0.64^{c}	176.60±0.49^{cb}	177.69±0.61^{abc}	178.69±0.12^{a}	177.98±0.36^{ab}	0.011
Rear Pastern Length	rear	13.80±0.44^{a}	13.68±0.25^{ab}	12.79±0.42^{b}	13.30±0.23^{ab}	13.88±0.27^{a}	12.72±0.15^{b}	0.039

a,b,c,d: Different letters in the same line are statistically significant (P<0.05).

Measuring Points

Reference points for the measurements were established based on previous studies (McIlwraith et al., 2003; Anderson and McIlwraith, 2004; Sadek et al., 2006; Weller et al., 2006). Easily identifiable bone protrusions in the photographs were chosen as reference points. Additionally, the midpoint of the circles drawn around the elbow, carpal, fetlock, and hock joints served as reference points for measurements. These measurements and their corresponding reference points are detailed in Table 2 and illustrated in Figure 2.

The term "distal extremity" was used to describe the forelimbs below the carpal joints and the hindlimbs below the tarsal joints. To determine the lengths of the distal extremities for both the front and hind limbs, the lengths of Mc3 and Mt3, along with the pastern lengths for the respective limbs, were added together. Additionally, front (FDLI) and rear (RDLI) distal limb indexes were calculated by dividing the total distal extremity lengths by the wither height for the forelimbs and the croup height for the hindlimbs. These calculations helped assess the proportional changes in the lengths of the distal extremities relative to the horse's age, as measured at the withers for the forelimbs and at the croup for the hindlimbs.

Data Analysis

All measurements were conducted by the same researcher (IGY) to avoid any interobserver variability issues. The data was analyzed using SPSS 15.0 for Windows. To test the reliability and validity of the measurements, one horse was randomly selected and measured five times at different intervals. Additionally, measurements from photographs of five different horses were taken at various intervals. The coefficient of variation (%CV) was then calculated based on these measurements, as outlined by Özdamar (2004). The Student's t-test was applied to compare the front and hindlimb parameters across genders for each age group. To examine the differences in mean values of conformation parameters across age groups, a One-Way Analysis of Variance (ANOVA) was conducted. For any significant differences found, Duncan's multiple comparison test was used to further analyze the data.

RESULTS

The coefficient of variation (CV) for all measurements was below 5%, indicating high repeatability and reliability in measurements obtained from photographs. The heights of the withers and croups showed a consistent and significant increase from 6 to 36 months, with the most substantial growth occurring in the first 24 months. After 24 months, the growth rate stabilized, and there was no statistically significant difference in the increase between 36 and 48 months. According to the data, croup heights exceeded wither heights across all age groups examined in this study (Figure 3).

The FDLI and FDLI, which show the ratio of the lengths of the limbs' distal parts to the height of the body, tended to rise with age (Figure 4). However, this trend was not consistently stable.

The measurement values for male and female horses across various age groups are detailed in Table 3 and 4. A significant increase in forelimb length was noted in both genders from 6 to 24 months, with no marked changes observed from 24 to 48 months. The values for the front carpal angle and Mc3 length in males and females did not show significant differences across the age groups. The front fetlock angle was higher in the 6-month age group, indicating the steepest structure at this early age. As the horses aged, the fetlock angle gradually aligned with the mature anatomical norms, reducing the differences observed between age groups. Front pastern angle, 6-month-old males exhibited values of 165°, while females showed 171°. These angles were observed to adjust to 178° for males and 176° for females over time.

DISCUSSION

Photographic methods are widely used in horse conformation research, as evidenced by several studies that have utilized images taken from the front, side, and rear of horses (McIlwraith et al., 2003; Andersson and McIlwraith, 2004; Senna et al., 2015; Mostafa and Elemmawy, 2020). A common challenge in such research is that horses cannot remain completely still for each photo, potentially leading to variations in the images due to movement. In our study, measures were taken to minimize the differences between images caused by the horse's movement. Specifically, photos were captured simultaneously from three different angles using cameras positioned around the horse. This method aimed to reduce discrepancies in the images, especially in angular measurements involving the length of joints and bones, by ensuring consistency across all photographs.

In studies examining the conformation of the horse, it can be quite challenging to achieve perfect posture in photographs taken from the front and back. It may not always be possible to maintain perfect posture. However, this methodology appears to have been used in previous studies (McIlwraith et al., 2003; Andersson and McIlwraith, 2004; Senna et al., 2015; Mostafa and Elemmawy, 2020). Therefore, to avoid possible misrepresentation, a real, unaltered photo was deliberately chosen to include in the article. To avoid these mistakes, researchers need to be more meticulous, patient, and perfectionist, especially when taking photos from the front and back.

The risk of injury in horses is significantly influenced by age, which is a key factor in assessing the distribution and origin of injuries (Stover, 2003). Up to 13% of postnatal foal conformation defects, which usually corrected by the age of three (McIlwraith et al., 2003). By three years old, horses typically achieve normal body conformation. The development of thoracic and pelvic limb bones occurs at different times, from 3-4 months to 24-36 months (Butler et al., 2005). Musculoskeletal issues are more common in two-year-old horses due to intense training and racing, while older horses more often face tendon and ligament injuries (Perkins et al., 2005; Cogger et al., 2008). In our study, significant changes in limb length and angle were noted in Thoroughbred horses, especially in the first two years, continuing until three years of age. As tissues adapt to changes in limb morphology in the two to three-year age range, the stress of training and racing can predispose them to injuries.

Withers and croup heights are key indicators of a horse's morphological structure. Mawdsley et al. (1996) found the wither height to be 157.20 cm in two-year-old female horses and 158.34 cm in males, with three-year-old thoroughbreds measuring 160.30 cm and 161.91 cm, respectively. Bakhtiari and Heshmat (2009) reported wither heights in thoroughbreds to be 163.4 cm for males and 161.8 cm for females. In our study, the wither height was observed to be 168.19 cm in three-year-old (36 months) males and 166.18 cm in females, with no significant differences between three- and four-year-old horses. The variations between these studies could be attributed to differences in measurement and calibration techniques.

Andersson and McIlwraith (2004) documented wither and croup heights in thoroughbreds as 122.28 cm and 125.32 cm in weanlings, 142.80 cm and 143.79 cm in 1-year-olds, 154.66 cm and 153.64 cm in 2-year-olds, and 154.61 cm and 153.09 cm in 3-year-olds, respectively. In our research, the wither and croup heights for male horses were measured at 133.67 cm and 138.76 cm in 6-month-old foals, 143.86 cm and 148.42 cm in 1-year-olds, 160.22 cm and 166.74 cm in 2-year-olds, and 168.19 cm and 171.98 cm in 3-year-old horses, respectively. For females, these values were 133.89 cm and 139.84 cm in 6-month-olds, 146.45 cm and 152.31 cm in 1-year-olds, 160.45 cm and 167.34 cm in 2-year-olds, and 166.18 cm and 168.63 cm in 3-year-olds. Minor differences in measurements between our study and that of Andersson and McIlwraith were anticipated. However, a notable distinction was that in their study, wither height exceeded croup height from the yearling stage onwards, whereas in our study, croup height was greater than wither height across all age groups. This higher croup structure in our study's horses, despite no current or past musculoskeletal issues, suggests a deviation from the ideal conformation where the croup and withers are level, facilitating optimal agility, balance, and gait. A croup higher than the withers, indicating disproportionately long hindlimbs, can affect stride and lead to forging issues (Thomas, 2005; Ross and McIlwraith, 2011). Gruyaert et al. (2022) found that 29% of horses with lameness or performance issues had higher tuber sacrale compared to the withers. This underscores the need for further exploration into the implications of wither and croup height discrepancies on performance and injury risks.

The pastern length value represents the distance between the metacarpophalangeal joint and the mid-coronary band. However, photographic measurements do not fully capture changes in the length of the phalanges. Specifically, the fetlock angle decreases from 151.99 to 145.70 degrees in males and from 150.85 to 146.19 degrees in females during the 6–48-month period. Concurrently, the fetlock angle in male horses decreased from 151.95° to 145.70°, and in females from 150.85° to 146.19°. These findings suggest that this joint gradually transitions toward a more slopped wrist structure over time. Consequently, there is a reduction in the pastern length value in 2D images taken from the front. These changes in the front pastern length and fetlock angle were found to be consistent, indicating a harmonious adjustment in the metacarpophalangeal joints. However, this type of consistent relationship was not observed between the rear pastern lengths and angles.

The study also tracked changes in limb length relative to the overall body height using the front distal limb index (FDLI) and rear distal limb index (RDLI). According to these indices, the distal sections of both the front and hind limbs tended to grow proportionally larger with age. Notably, the increase in FDLI was more pronounced than that in RDLI for both males and females, suggesting a greater relative growth in the distal parts of the front limbs compared to the hind limbs.

The axis of the limb should be straight when viewed from in front of the limb (Thomas 2005). Deviations from this ideal angle can indicate disruptions in the limb's axial alignment, as described by Hedge and Wagoner (2004). In the study, the front pastern angle in males increased from 165.61° to 178.13° and in females from 171.09° to 176.44°. The rear fetlock angle in males rose from 170.72° to 174.94° and in females from 172.43° to 175.90°. These increases suggest that, while younger horses showed more pronounced breaks due to their angles deviating further from 180°, older horses' measurements tended to align more closely with the ideal. One factor that might influence these observations is the hoof care practices, specifically whether hooves are trimmed in a way that complements the individual conformation characteristics of each horse. The coronary angle, a measurement taken from the front, consistently reached the standard value of 178° across both genders and all age groups in this study, suggesting a generally well-maintained mediolateral balance of the hoof (Colles et al., 2022).

In a study focused on limb conformation in Thoroughbreds used for jumping, Senna et al. (2015) reported front limb length measurements as follows: forelimb at 46.02 cm, Mc3 at 28.67 cm, and Mt3 at 37.44 cm. In contrast, the measurements in our study for both males and females ranged from 35–45 cm for the forelimb, 23–25 cm for Mc3, and 29–31 cm for Mt3. The discrepancy in measurements could be attributed to Senna et al. taking their measurements from the front, whereas ours were taken from the left side of the horse. Regarding angular measurements, Senna et al. reported the elbow angle at 138.30°, carpal angle at 177.70°, front pastern angle at 142.70°, stifle angle at 114.9°, and rear pastern angle at 149.8°. In our study, these angles were found to be within 139-145° for the elbow angle, 177-178° for the carpal angle, 145-151° for the front pastern angle, 114-120° for the stifle angle, and 152-159° for the rear pastern angle. The angular measurements between the two studies showed similarities, suggesting a consistency in angular measurements. However, the variation observed in the front and rear pastern angles could potentially be linked to differences in hoof trimming practices, influenced by the distinct functional requirements of the horses in each study. This highlights the potential need for further research into how conformation aligns with function in horses of the same breed but used for different purposes.

In their research on the conformation characteristics of Thoroughbreds, both healthy and with musculoskeletal disabilities, Mostafa and Elemmawy (2020) found the rear pastern angle to average 152.8° in healthy horses and 144.7° in those with musculoskeletal issues. In our study, the rear pastern angles ranged from 152.34° to 159.61° in males and 150.71° to

159.20° in females. These findings suggest that the horses in our study, which did not include any with a history of injury, exhibited rear pastern angles within a range indicative of a low risk for musculoskeletal disorders. Thus, the outcomes of our research align with those of Mostafa and Elemmawy, further supporting the correlation between rear pastern angles and musculoskeletal health in Thoroughbreds.

Hoobs et al. (2022) highlighted that hoof shape and functionality in Thoroughbred racehorses evolve with growth and the physical demands placed upon them. In our investigation, the narrowest front hoof width measurements were recorded at the 6-month mark for both sexes. Beyond the age of 1, no significant changes in hoof width were observed in females, whereas in males, an increase in hoof width continued until the age of two. Furthermore, a reduction in the angles of both front and rear hooves was noted in females from 6 months to 4 years. In contrast, males exhibited varying differences across different age groups. This suggests that hoof development follows a more consistent pattern in females compared to males.

The study's findings provide insights into the changes in limb anatomy across different genders and age groups. While these data allow for comparisons with results from other studies, the emergence of unexplained findings highlights areas for future research and raises questions that warrant further investigation.

Limitations: The study utilized distinct horses across various age groups, contributing significant data to an under-researched area. Future research should ideally monitor the same horses over extended periods and include a broader sample size for more comprehensive insights. The process of standard photographic measurements presents challenges, necessitating careful consideration of environmental factors, stress conditions, and the perspectives of breeders and owners during the planning stages. Due to concerns from breeders and horse owners about potential speculation on their horses' conformation traits, private records were kept confidential. Consequently, this study does not include data on the horses' eventual performance outcomes.

CONCLUSIONS

The findings from this study provide valuable insights into the conformational changes in different limb regions, influenced by age and gender. Notably, the distal limbs experienced significant changes and development, demonstrated by an increase in distal extremity indices with age. In all age groups studied, the croup was consistently higher than the withers, potentially shifting the horse's center of gravity forward and placing additional strain on the forelimbs. Despite these observations, there were no reported injuries across the different age groups. Future research could be directed toward understanding the implications of these conformational characteristics and their potential impact on horse health and performance.

DECLARATIONS

Ethics Approval

This study was carried out with the permission of Aydın Adnan Menderes University, Animal Experiments Local Ethics Committee, numbered B.30.2.ADÜ.0.06.00.00/124-HEK/2009/64.

Conflict of Interest

The authors declare that they have no competing interests.

Consent for publication

Not applicable.

Author Contributions

Idea, concept, and design: İGY, HE

Data collection and analysis: İGY

Drafting of the manuscript: İGY, HE

Critical review: HE

Data availability

The data that support the findings of this study are available from the corresponding author upon reasonable request.

Acknowledgements

Thanks to the Turkish Jockey Club. Biologist Naci Özat and Veterinarian Melis Erdölek assisted us with the required horses for the study.

REFERENCES

Anderson, T. M., & McIlwraith, C. W. (2004). Longitudinal development of equine conformation from weanling to age 3 years in the Thoroughbred. Equine Veterinary Journal, 36(7), 563–570. https://doi.org/10.2746/0425164044864507

Anderson, T. M., McILWRAITH, C. W., & Douay, P. (2004). The role of conformation in musculoskeletal problems in the racing Thoroughbred. Equine Veterinary Journal, 36(7), 571–575. https://doi.org/10.2746/0425164044864462

Bakhtiari, J., & Heshmat, G. (2009). Estimation of genetic parameters of conformation traits in Iranian Thoroughbred horses. Livestock Science, 123(2–3), 116–120. https://doi.org/10.1016/j.livsci.2008.10.014

Belloy, E., & Bathe, A. P. (1996). The importance of standardising the evaluation of conformation in the horse. Equine Veterinary Journal, 28(6), 429–430. https://doi.org/10.1111/j.2042-3306.1996.tb01613.x

Butler, J.A., Colles, C.M., Dyson, S.J., Kold, S.E., & Poulos, W.E. (2005). Fusion times of physes and suture lines. In: Clinical Radiology of the Horse (pp. 585-588). Blackwell Science.

Cogger, N., Evans, D. L., Hodgson, D. R., Reid, S. W., & Perkins, N. (2008). Incidence rate of musculoskeletal injuries and determinants of time to recovery in young Australian Thoroughbred racehorses. Australian Veterinary Journal, 86(12), 473–480. https://doi.org/10.1111/j.1751-0813.2008.00359.x

Delahunty, D., Webb, S., Kelly, E., & Smith, F. (1991). Intermandibular width and and cannon bone length in "winners" versus "others." Journal of Equine Veterinary Science, 11(5), 258–259. https://doi.org/10.1016/s0737-0806(06)81310-9

Dolvik, N. I., & Klemetsdal, G. (1999). Conformational

Traits of Norwegian Cold-blooded Trotters: Heritability and the Relationship with Performance. Acta Agriculturae Scandinavica Section a – Animal Science, 49(3), 156–162. https://doi.org/10.1080/090647099424060

Fedorski, J., & Pikula, R. (1988). Heritability of some body conformation traits in the Thoroughbred horse. Animal Science Papers and Reports, 3, 53–57.

Gruyaert, M., Pollard, D., & Dyson, S. (2022). Relative heights of the withers and the tubera sacrale and angulation of the lumbar and pelvic regions in horses with hindlimb proximal suspensory desmopathy, sacroiliac joint region pain and other orthopaedic injuries. Equine Veterinary Education, 35(5). https://doi.org/10.1111/eve.13724

Harris, S.E. (1993). Horse gaits, balance, and movement. Wiley Publishing.

Hedge, J., & Wagoner, D. (2004). Horse Conformation. Structure, soundness and performance. The Lyons Press.

Hobbs, S. J., Curtis, S., Martin, J., Sinclair, J., & Clayton, H. M. (2022). Hoof Matters: Developing an Athletic Thoroughbred Hoof. Animals, 12(22), 3119. https://doi.org/10.3390/ani12223119

Jakubec, V., Vostrý, L., Schlote, W., Majzlík, I., & Mach, K. (2009). Selection in the genetic resource: genetic variation of the linear described type traits in the Old Kladrub horse. Archives Animal Breeding/Archiv Für Tierzucht, 52(4), 343–355. https://doi.org/10.5194/aab-52-343-2009

Kavazis, A., & Ott, E. (2003). Growth Rates in Thoroughbred Horses Raised in Florida. Journal of Equine Veterinary Science, 23(8), 353–357. https://doi.org/10.1016/s0737-0806(03)01024-4

Mawdsley, A., Kelly, E. P., Smith, F. H., & Brophy, P. O. (1996). Linear assessment of the Thoroughbred horse: an approach to conformation evaluation. Equine Veterinary Journal, 28(6), 461–467. https://doi.org/10.1111/j.2042-3306.1996.tb01618.x

McIlwraith, C. W., Anderson, T. M., & Sanschi, E. M. (2003). Conformation and musculoskeletal problems in the racehorse. Clinical Techniques in Equine Practice, 2(4), 339–347. https://doi.org/10.1053/j.ctep.2004.04.006

Moore, J. (2010). General Biomechanics: The Horse As a Biological Machine. Journal of Equine Veterinary Science, 30(7), 379–383. https://doi.org/10.1016/j.jevs.2010.06.002

Mostafa, M. B., & Elemmawy, Y. M. (2020). Relationships between morphometric measurements and musculoskeletal disorders in jumping Thoroughbred horses. Journal of Equine Science, 31(2), 23–27. https://doi.org/10.1294/jes.31.23

Özdamar, K. (2004). Statistical data analysis with package programs. Kaan Kitabevi.

Perkins, N., Reid, S., & Morris, R. (2005). Risk factors for musculoskeletal injuries of the lower limbs in Thoroughbred racehorses in New Zealand. New Zealand Veterinary Journal, 53(3), 171–183. https://doi.org/10.1080/00480169.2005.36502

Ross, M.., & McIlwraith, C.W. (2011). Conformation and lameness (2nd ed.). In: Diagnosis and Management of Lameness in the Horse (pp. 16–32.). Elsevier Saunders

Sadek, M., Al-Aboud, A., & Ashmawy, A. (2006). Factor analysis of body measurements in Arabian horses. Journal of Animal Breeding and Genetics, 123(6), 369–377. https://doi.org/10.1111/j.1439-0388.2006.00618.x

Sánchez, M. J., Gómez, M. D., Peña, F., Monterde, J. G., Morales, J. L., Molina, A., & Valera, M. (2013). Relationship between conformation traits and gait characteristics in Pura Raza Español horses. Archives Animal Breeding/Archiv Für Tierzucht, 56(1), 137–148. https://doi.org/10.7482/0003-9438-56-013

Senna, N. A., Mostafa, M. B., Abu-Seida, A. M., & Elemmawy, Y. M. (2015). Evaluation of Limb Conformation in Jumping Thoroughbred Horses. Asian Journal of Animal Sciences, 9(5), 208–216. https://doi.org/10.3923/ajas.2015.208.216

Smith, A. M., Staniar, W. B., & Splan, R. K. (2006). Associations between yearling body measurements and career racing performance in Thoroughbred racehorses. Journal of Equine Veterinary Science, 26(5), 212–214. https://doi.org/10.1016/j.jevs.2006.03.002

Stover, S. M. (2003). The epidemiology of Thoroughbred racehorse injuries. Clinical Techniques in Equine Practice, 2(4), 312–322. https://doi.org/10.1053/j.ctep.2004.04.003

Thomas, H.S. (2005). The Horse Conformation Handbook. Storey Publishing

Weeren, P. R., & Crevier-Denoix, N. (2006). Equine conformation: clues to performance and soundness? Equine Veterinary Journal, 38(7), 591–596. https://doi.org/10.2746/042516406x159007

Weller, R., Pfau, T., Verheyen, K., May, S. A., & Wilson, A. M. (2006). The effect of conformation on orthopaedic health and performance in a cohort of National Hunt racehorses: preliminary results. Equine Veterinary Journal, 38(7), 622–627. https://doi.org/10.2746/042516406x159034

Yıldırım, I. G. (2014). Atlarda Vücut Yapısının Değerlendirilmesi. Neden bazı atlar daha başarılıdır? Nobel Tıp Kitabevleri

Yildirim, S. G., & Erden, H. (2023). Conformational characteristics in Arabian and Thoroughbred horses. Animal Health Production and Hygiene. https://doi.org/10.53913/aduveterinary.1330533

Medit Vet J, 9(3): 395-402, 2024
DOI: 10.24880/meditvetj.1544695

Research Article

The use of infrared thermography in the identification of surface temperatures in fast and slow-growing broiler chickens

Solmaz Karaarslan[1], Ahmet Nazlıgül[1]

[1]Department of Animal Science, Faculty of Veterinary Medicine, Aydın Adnan Menderes University, Aydın, Türkiye

Key Words:
broiler chickens
fast-growing
infrared thermography
slow-growing
surface temperature

Received : 6 September 2024
Revised : 30 October 2024
Accepted : 12 November 2024
Published : 31 December 2024
Article Code : 1544695

Correspondence:
S. KARAARSLAN
(solmazkaraarslan@adu.edu.tr)

ORCID
S. KARAARSLAN : 0000-0002-6239-2439
A. NAZLIGÜL : 0000-0003-1476-4039

ABSTRACT

This study aimed to identify through infrared thermal imaging technology the surface temperature of the eye, beak, head, trunk, leg, and body of fast- and slow-growing broiler chickens at 2, 4, and 6 weeks of age. A total of 140 1-day-old broiler chicks were used in the study. Two treatments were included: fast-growing (Ross 308) and slow-growing (Hubbard JA57), with two replicates for each treatment. Thirty-five broiler chickens were placed in each pen. Beak and leg surface temperatures were consistently higher in fast-growing broiler chickens during the 2nd, 4th, and 6th weeks. Except for the 4th week, the surface temperature differences in the eyes and other feathered areas between fast- and slow-growing broiler chickens were not statistically significant. Eye surface temperature was not influenced by age in either genotype. In both genotypes, the beak and head surface temperatures increased with age, while the body and trunk surface temperatures decreased. Additionally, leg surface temperatures increased with age in fast-growing broiler chickens. The litter surface temperature was consistently higher in pens housing the fast-growing genotypes across all measured weeks. As a result, it was determined that age and genotype affected the surface temperatures of broiler chickens and litter. It is thought that continuous monitoring of potential fluctuations in ambient and body surface temperatures using infrared thermal cameras during the rearing period can contribute to the maintenance of thermal comfort.

INTRODUCTION

Broiler chicken farming is the world's largest terrestrial animal production sector, with nearly 70 billion chickens slaughtered annually (Berg et al., 2021; Wilcox et al., 2024). Over the last century, in response to this high demand, poultry production systems have been intensified to maximize efficiency and productivity (Azarpijouh et al., 2022). Consequently, broiler chickens have been selectively bred for generations to focus on a small range of traits, such as rapid growth and more meat yield. This selective breeding has, however, resulted in broiler chickens developing a genetic predisposition to various health and welfare issues (Wilcox et al., 2024). Therefore, developing new commercial applications in the poultry sector is significant to ensure continued economic production and maintain animal health and welfare. Such advancements are also necessary to tackle the challenges posed by global climate change and the growing need for cost-effective meat sources in response to the world's expanding population (Yahav and Giloh, 2012). Infrared thermographic imaging is a recent technology used to assess housing thermal conditions and their effects on animal welfare (Ferreira et al., 2011). Additionally, it facilitates the monitoring of animal surface temperature, which is a key indicator of an animal's physiological state under various conditions, including stress, fertility, welfare, metabolism, health, and disease detection (Nääs et al., 2014; Castro et al., 2019). Computer systems process these surface temperatures generate a thermal map of the animal and perform a detailed analysis of the temperature profile (McManus et al., 2016). Infrared thermal imaging technology provides a quick, highly sensitive, non-invasive, and contactless method for measuring skin surface temperature. Consequently, it enables the efficient assessment of body surface temperatures for numerous individuals, significantly cutting down on the time and effort needed by managers, while also avoiding any stress on the animals being monitored (Kim et al., 2021). Due to these advantages, infrared thermal imaging technology has been employed in numerous studies in recent years to evaluate animal welfare standard management procedures or health status monitoring in cattle (Nikkhah et al., 2005; Stewart et al., 2008; Schaefer et al., 2012; Alsaaod et al., 2014), poultry (Cangar et al., 2008; Ferreira et al., 2011; Jacob et al., 2016; Bloch et al., 2020; Weimer et al., 2020; Kim et al., 2021), and pigs (Warriss et al., 2006; Caldara et al., 2014). When examining the applications of infrared thermography technology specifically for poultry, it is noteworthy that they are concentrated on the measurement of metabolic heat production (Cangar et al., 2008; Nääs et al., 2010; Ferreira et al., 2011; Damane et al., 2018), evaluation leg health parameters (Jacob et al., 2016; Weimer et al., 2019; 2020) and managing heat stress (Nascimento et al., 2014; Castro et al., 2019; Bloch et al., 2020; Kim et al., 2021). In poultry, the majority of the body surface is covered with feathers, and these feathers are thermal insulators that prevent most of the heat emissions (Ferreira et al., 2011). Therefore, it has been reported that the feathered areas of the body (head, neck, back, wings, chest, thighs) show lower temperatures compared to the featherless areas (eye, ear lobe, comb, legs/feet) (Shinder et al., 2007; Cangar et al., 2008; Nääs et al., 2010; Damane et

To cite this article:
Karaarslan S, Nazlıgül A. The use of infrared thermography in the identification of surface temperatures in fast- and slow-growing broiler chickens. Medit Vet J. 2024; 9(3): 395-402.

al., 2018). In addition, it has also been reported that body surface temperature varies with age (Tessier et al., 2003; Cangar et al., 2008; Damane et al., 2018). The effect of age on body surface temperature is attributed to the feathering status of the animals (Cangar et al., 2008; Damane et al., 2018). Giloh et al. (2012) reported a strong correlation between body temperature and facial surface temperature in broiler chickens. This suggests that monitoring facial surface temperature could be useful for assessing the comfort or thermal stress of chickens (Nascimento et al., 2014; Cândido et al., 2020). In addition, Weimer et al. (2020) reported that the surface temperature of the eye and especially the beak can be used as stress indicators in broiler chickens.

The broiler industry features a variety of breeds, including fast-growing genotypes that can achieve a target weight of 1.5 to 3 kg in about 30 days and slow-growing genotypes that require a longer period, around 70 to 80 days, to reach the same weight (Torrey et al., 2021). Broiler chickens with faster growth rates consume more feed and require a higher metabolic rate, which leads to increased metabolic heat production (Bloch et al., 2020). Additionally, the development of large body size and breast muscles, combined with a high metabolic rate, suggests that broiler chickens may struggle to maintain thermal balance (Tickle and Codd, 2019). Thermal balance is intrinsically linked to the environmental conditions that broiler chickens are exposed to. Therefore, understanding the metabolic heat production during the rearing period and determining the heat exchange between the animal and its environment is crucial for characterizing the animals' homeostasis (Nascimento et al., 2017). Ambient temperature is a critical climatic factor that strongly influences the maintenance of thermal balance in poultry. Therefore, monitoring the body surface temperatures of the animals can provide valuable insights into how ambient temperature affects their thermoregulatory status (Kim et al., 2021).

We had two hypotheses: first, that surface temperatures would be higher in fast-growing broiler chickens compared to slow-growing broiler chickens, and second, that surface temperatures would increase with age, particularly in fast-growing broiler chickens, due to the higher metabolic heat associated with rapid weight gain. The objective of the present study was to assess surface temperatures in fast- and slow-growing broiler chickens and to investigate how these temperatures vary with age.

MATERIALS and METHODS

Experimental procedure and husbandry

Seventy fast-growing (Ross 308) and seventy slower-growing (Hubbard JA57) 1-d-old broiler chicks were obtained from two commercial hatcheries (EGE-TAV, İzmir, Türkiye, and Orallar, Kocaeli, Türkiye) on the same day. These chicks were randomly allocated to four floor pens (2.6 kg target slaughter weight; 2.6 kg x 35 chickens/33 kg per m^2 ≈ 2.75 m^2 free floor area per pen) within an experimental room (two replicates/treatment; 35 birds/pen) at the Poultry Research Unit, Faculty of Veterinary Medicine, University of Aydın Adnan Menderes, Türkiye (latitude 37°49'37" N, longitude 27°47'29" E, and an altitude of 31 m). The experiment room had dimensions of 10 m long, 5 m wide, and a height of 6 m. Both genotypes were reared under uniform management and feeding conditions. Within each pen, the water needs of the chickens were met by one drinker line with six nipples (5.83 birds per nipple), providing continuous access to water, and feed was given *ad libitum* using two round plastic feeders with a diameter of 0.4 m (7.18 cm of feeder length per bird). Bedding material consisting of wood shavings (eight cm in depth) was utilized. All diets used in the experiment were based on corn and soybean meal. The diets were prepared in three phases during the trial as specified in the commercial hybrid catalog (Aviagen, 2019). The starter phase was used for the first 10 days (3050 kcal ME/kg, 23.5% crude protein), the grower phase from days 11 to 24 (3150 kcal ME/kg, 22% crude protein), and the finisher phase from days 25 to the slaughter day (3200 kcal ME/kg, 21% crude protein). The stocking density and lighting schedule were adjusted to the levels specified in the European Union Directive (2007/43/EC). The stocking density was 33 kg/m^2. A lighting schedule of 24 hours of light was applied for the first seven days, followed by 18 hours of light and six hours of darkness for the remaining days. In the experimental room, a temperature of 32 ± 1°C was maintained at the chicks' back level for the first three days using electric thermostatic radiant heaters. The temperature was reduced by 3°C per week until 21 days old. Temperature and humidity levels were recorded twice daily using an automatic data logger at 9:00 and 17:00. The data loggers had a humidity resolution of 1% and a temperature resolution of 0.1°C.

Data collection

Infrared thermography (IRT) images were taken of five broiler chickens from each pen at 14:00 on weeks 2, 4, and 6 of the study. The broiler chickens were handled using latex gloves to avoid the influence of heat and moisture from the hands on the temperature of the feathers. All images were taken in the same experimental room. Broiler chickens were placed at a marked point on a table in the experimental room, and images were taken as quickly as possible to minimize stress effects. IRT images were taken from the left side of broiler chickens at a distance of 1 m using an IRT camera (FLIR E6, Flir Systems®, Sweden) with high resolution (240 x 180 pixels). The camera background temperature was set to 22°C, emissivity to 0.95, and transmission to 100%. IRT images were uploaded to a computer and analyzed using FLIR Tools (v 6.4) software (Figure 1). Eye and beak surface temperatures were measured from a single point using the software's spot feature. Head and trunk surface temperatures were calculated by averaging the area within the marked regions using the ellipse feature. Leg surface temperature was determined by averaging the points along the line using the line feature. To determine a body surface temperature (approximately 3.000 data) was averaged of the head, trunk, and leg regions. In addition, the litter surface temperature of each pen was taken from three different points (the side of the wall, under the drinker line, and between the feeders). Ambient temperature and relative humidity were recorded using a data logger in the experimental room, synchronized with the infrared thermal imaging sampling time (Figure 2).

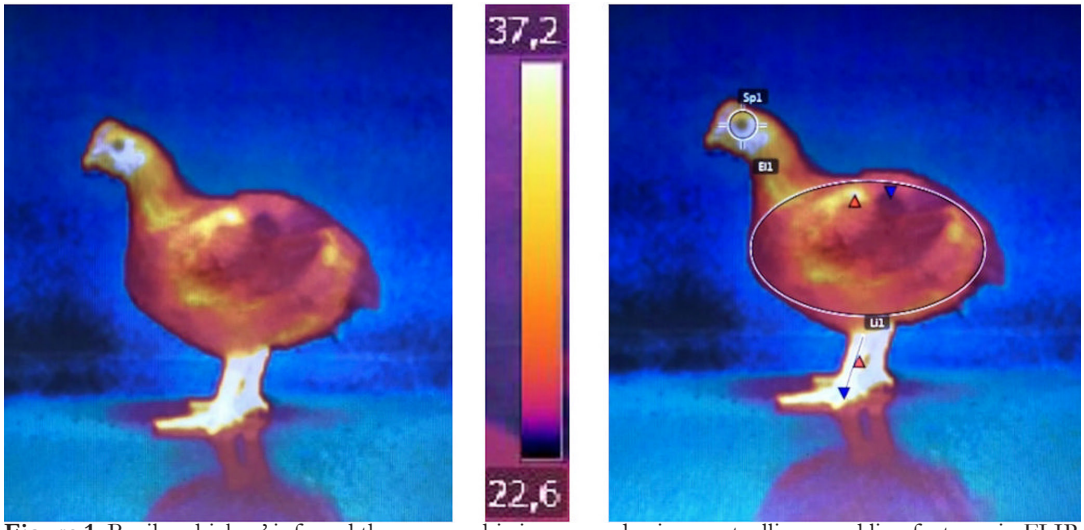

Figure 1. Broiler chicken' infrared thermographic image, and using spot, ellipse, and line features in FLIR Tools (v 6.4) software.

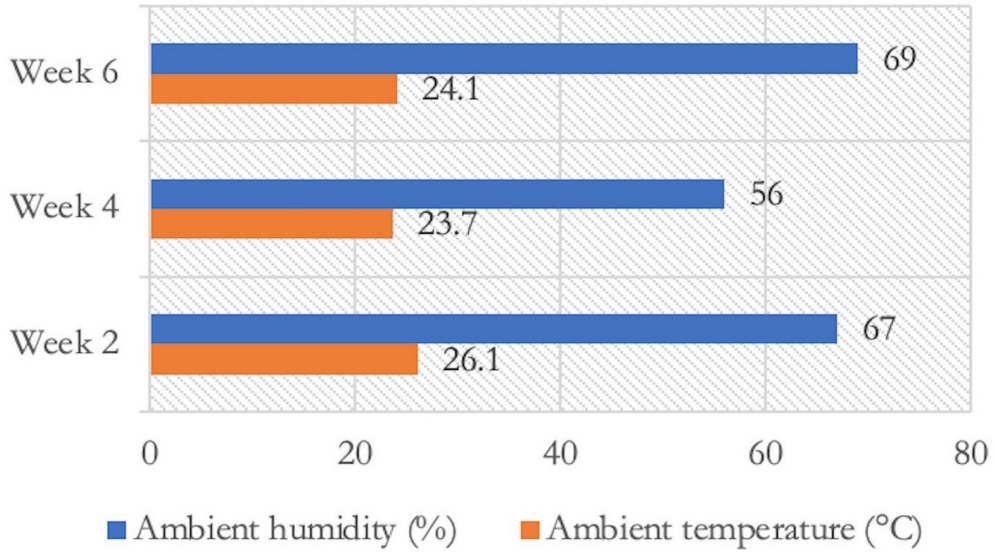

Figure 2. Ambient temperatures and humidity levels in the experiment rooms at 2, 4, and 6 weeks.

Statistical analysis

The data were analyzed statistically using the SPSS software package (version 22.0, SPSS Inc., Chicago, IL, USA). The normality of the variables was assessed using the Shapiro-Wilk test. Levene's test was used to examine the assumption of homogeneity of variances. The evaluation of IRT surface temperatures according to genotype was performed using the independent t-test, while age was conducted using the one-way ANOVA test. In the evaluation according to age for parameters that did not meet the homogeneity assumption, the Welch t-test result was considered as the significant value. For parameters that were not homogeneously distributed, the Tamhane T2 test was used as the post hoc analysis, while the Tukey HSD test was applied for homogeneously distributed data. Differences were considered significant when $P<0.05$. Descriptive statistical parameters, mean and standard error, were used to display litter surface temperatures.

RESULTS

The effects of genotype on IRT eye, beak, body, head, trunk, and leg surface temperatures in broiler chickens at 2, 4, and 6 weeks of age are presented in Table 1. Both genotypes showed similar values with eye and head surface temperatures except for week 4 ($P=0.042$, $P<0.0001$). For beak and leg surface temperatures, the fast-growing broiler chickens exhibited significantly higher temperatures compared to the slow-growing broiler chickens in weeks 2, 4, and 6 (Beak surface temperature $P<0.0001$, $P<0.0001$, $P=0.002$; Leg surface temperature $P=0.048$, $P=0.006$, $P=0.008$). No significant difference was found between genotypes for body and trunk surface temperatures in all weeks except for week 4 ($P=0.008$).

The effects of age on IRT eye, beak, body, head, trunk, and leg surface temperatures in fast- and slow-growing broiler chickens are shown in Table 2. No significant change was observed in eye surface temperature with increasing age in either genotype. In both genotypes, beak surface temperature (fast-grow-

Table 1. Effects of genotype on IRT eye, beak, body, head, trunk, and leg surface temperatures (°C) in broiler chickens at 2, 4, and 6 weeks[1,2]

IRT surface temperatures	n	Fast-growing	Slow-growing	P-value
2nd week				
Eye	10	35.86±0.09	35.69±0.21	0.482
Beak	10	30.94±0.25	28.61±0.41	<0.0001
Body	10	33.99±0.12	33.64±0.14	0.073
Head	10	34.49±0.12	34.30±0.09	0.217
Trunk	10	34.30±0.17	33.99±0.13	0.171
Leg	10	37.04±0.12	36.45±0.25	0.048
4th week				
Eye	10	35.72±0.22	35.16±0.14	0.042
Beak	10	31.79±0.35	29.16±0.25	<0.0001
Body	10	32.98±0.29	31.68±0.32	0.008
Head	10	35.91±0.18	34.92±0.11	<0.0001
Trunk	10	32.71±0.32	31.26±0.37	0.008
Leg	10	37.17±0.16	36.42±0.18	0.006
6th week				
Eye	10	35.63±0.19	35.64±0.24	0.975
Beak	10	32.53±0.45	30.27±0.47	0.002
Body	10	30.32±0.22	30.12±0.23	0.528
Head	10	36.23±0.12	35.91±0.22	0.225
Trunk	10	30.29±0.33	29.61±0.25	0.121
Leg	10	37.54±0.14	36.81±0.21	0.008

[1]Values are presented as mean ± standard error.
[2]Fast-growing: Ross 308, slow-growing: Hubbard JA57.

Table 2. The effects of age on IRT eye, beak, body, head, trunk, and leg surface temperatures (°C) in fast- and slow-growing broiler chickens[1]

IRT surface temperatures	n	2nd week	4th week	6th week	P-value
Fast-growing					
Eye	10	35.86±0.09	35.72±0.22	35.63±0.19	0.657
Beak	10	30.94±0.25^{b}	31.79±0.35^{ab}	32.53±0.45^{a}	0.014
Body[2]	10	33.98±0.12^{a}	32.98±0.29^{b}	30.32±0.22^{c}	<0.0001
Head	10	34.49±0.12^{b}	35.91±0.18^{a}	36.23±0.12^{a}	<0.0001
Trunk	10	34.30±0.17^{a}	32.71±0.32^{b}	30.29±0.33^{c}	<0.0001
Leg	10	37.04±0.12^{b}	37.17±0.16^{ab}	37.54±0.14^{a}	0.044
Slow-growing					
Eye	10	35.69±0.21	35.16±0.14	35.64±0.24	0.135
Beak[2]	10	28.61±0.41^{b}	29.16±0.25^{ab}	30.27±0.47^{a}	0.019
Body[2]	10	33.64±0.14^{a}	31.68±0.32^{b}	30.12±0.23^{c}	<0.0001
Head[2]	10	34.30±0.09^{c}	34.92±0.11^{b}	35.91±0.22^{a}	<0.0001
Trunk[2]	10	33.99±0.13^{a}	31.26±0.37^{b}	29.61±0.25^{c}	<0.0001
Leg	10	36.45±0.25	36.42±0.18	36.81±0.21	0.373

[1]Values are presented as mean ± standard error.
[2]Due to the non-homogeneity of data, the Welch test was applied.
[a,b]Means in the same row with different superscripts differ significantly (P<0.05)

ing P=0.014, slow-growing P=0.019) and head surface temperature (both genotypes P<0.0001) increased significantly with age. Conversely, a significant decrease in body and trunk surface temperatures was noted (both genotypes P<0.0001). Regarding leg surface temperatures, although similar temperatures were observed across all weeks in both genotypes, the temperature increase observed with increased age in the fast-growing genotype was found to be significant (P=0.044).

Litter surface temperatures based on genotype at 2, 4, and 6 weeks are presented in Table 3. Due to the insufficient replicate numbers, only the mean and standard error were calculated for the litter surface temperatures. It was observed that litter surface temperatures were higher in the pens where the fast-growing genotype was reared at all weeks.

Table 3. IRT litter surface temperatures (°C) in pens based on genotype[1]

IRT litter surface temperatures	2nd week	4th week	6th week
Fast-growing broiler chickens-rearing pen			
Minimum	25.93±0.40	22.32±0.33	24.85±0.44
Maximum	33.10±0.63	30.82±0.60	32.08±0.48
Average	29.23±0.42	26.57±0.40	28.10±0.56
Slow-growing broiler chickens-rearing pen			
Minimum	24.42±0.61	20.35±0.38	22.92±0.36
Maximum	29.48±0.54	26.78±1.68	27.58±0.75
Average	27.28±0.35	23.07±0.33	24.74±0.39

[1]Values are presented as mean ± standard error.

DISCUSSION

Infrared thermography offers a non-invasive method for evaluating thermal changes in a commercial poultry flock. This technique could enhance climate control systems and detect acute thermal stress, potentially leading to improvements in both flock performance and welfare (Yahav and Giloh, 2012).

In the present study, skin surface temperatures in the featherless areas were consistently higher across all weeks for both broiler genotypes. This observation aligns with previous studies that reported featherless regions, such as the eyes and legs, typically exhibit higher surface temperatures due to the absence of feather insulation (Cangar et al., 2008; Nääs et al., 2010; Damane et al., 2018; Castro et al., 2019). Furthermore, consistent with the findings of Castro et al. (2019), the highest surface temperatures were observed in the leg, eye, and head regions compared to other measurement regions across all weeks for both broiler genotypes in the current study. In comparing the surface temperatures between genotypes, it was observed that differences in the eye, body, head, and trunk surface temperatures were not statistically significant in any week except for the 4th week. Since modern broiler chickens undergo their second natural molt at around 4-5 weeks of age (Leeson and Walsh, 2004), the significant findings observed in the 4th week are likely attributable to this molt. However, the surface temperatures of the beak and legs were significantly higher in the fast-growing genotype across all weeks. The similar temperatures observed in the body, head, and trunk, which are covered with dense feathers, may be attributed to the insulating properties of the feathers. In contrast, the higher leg surface temperature in the fast-growing genotype is likely due to greater metabolic heat production. This higher temperature can be explained by the fact that broiler chickens with faster growth rates consume more feed, leading to accelerated metabolism and consequently higher metabolic heat production (Bloch et al., 2020).

When the surface temperature variation with age was examined, it was found that eye surface temperature was not related to age in either genotype. It was observed that the eye surface temperatures were at similar levels in all measurements. Damane et al. (2018) stated that the eye surface temperature of broiler chickens increased with age, though the difference between the measurements taken at 4 and 6 weeks was not statistically significant. Considering that surface temperatures obtained with a thermal camera are influenced by factors, such as ambient temperature, humidity levels, and airflow, the differences observed may be challenging to explain due to the limited number of studies with similar experimental setups. In both genotypes, the beak and head surface temperatures increased with age, while body and trunk surface temperatures decreased. Consistent with these findings, Cangar et al. (2008) reported that surface temperatures generally decrease with age in measurements taken on feathered body parts, suggesting that this decrease could be due to the increasing number and quality of feathers, which act as an insulating layer. It has been reported that rapid feather growth begins at the end of the 2nd week in broiler chickens and that the first six weeks are the period when growth is at its highest (Wecke et al., 2017). Yalcin et al. (1997) stated that all broiler chickens are fully feathered at the age of seven weeks. These observations support the decrease in surface temperatures in the feathered areas as increasing age. In all measurements, leg surface temperatures were observed above 37°C in the fast-growing genotype and above 36°C in the slow-growing genotype. The difference in surface temperatures between weeks was statistically significant in the fast-growing genotype but insignificant in the slow-growing genotype. It is thought that this significance may be due to the larger average live weight differences between

the 4th and 6th weeks in the fast-growing genotype. Supporting our observation, Nascimento et al. (2017) stated that metabolic heat production in broiler chickens increases linearly with body weight gain.

In the litter surface temperature measurements in the pens where slow- and fast-growing broiler chickens were reared, higher litter surface temperatures were consistently observed in the fast-growing genotype. Supporting this finding, Steenfeldt et al. (2019) reported that litter surface temperatures were higher in the pens where fast-growing broiler chickens were reared.

CONCLUSION

Briefly, feather development on different body parts played an important role in monitoring surface temperature by thermal imaging. Therefore, feathered and featherless parts should be considered separately to estimate the surface temperature of broiler chickens during the rearing period. The results confirmed that age and genotype are the factors affecting surface temperature. It is believed that continuous monitoring of potential fluctuations in ambient and the broiler chickens' surface temperatures using infrared thermal cameras throughout the rearing period is thought to contribute to maintaining thermal comfort and thus can improve the welfare of the broiler chickens.

DECLARATIONS

Ethics Approval

This experiment was implemented under the approval of the Animal Ethics Committee of Aydın Adnan Menderes University (64583101/2024/28).

Conflict of Interest

The authors declared that there is no conflict of interest.

Consent for Publication

Not applicable

Author contribution

Idea, concept and design: SK

Data collection and analysis: SK

Drafting of the manuscript: SK

Critical review: AN

Data Availability

The data that findings of this study are available from the corresponding author upon reasonable request.

Acknowledgements

For the infrared surface temperature measurements taken in this study, broiler chickens raised as part of a project supported by the Aydın Adnan Menderes University Scientific Research Projects Directorate (Project Code: VTF-23040) were used. The thermal camera used in this study was kindly provided by Prof. Dr. Güneş ERDOĞAN, to whom our sincere thanks are extended.

REFERENCES

Alsaaod, M., Syring, C., Dietrich, J., Doherr, M.G., Gujan, T., & Steiner, A. (2014). A field trial of infrared thermography as a non-invasive diagnostic tool for early detection of digital dermatitis in dairy cows. The Veterinary Journal, 199(2), 281-285. https://doi.org/10.1016/j.tvjl.2013.11.028

Aviagen (2019). Ross 308 Broiler: Nutrition Specifications. Huntsville, AL, USA.

Azarpajouh, S., Weimer, SL., Calderón Díaz, J.A., & Taheri H. (2022). Smart farming: a review of animal-based measuring technologies for broiler welfare assessment. CABI Reviews, 17, 033. https://doi.org/10.1079/cabireviews202217033

Berg, C., & Butterworth, A. (2021). Health and disease impacts on broiler welfare. In A. Butterworth, L. Berg, I. de Jong, J. Mench, M. Raj, & X. Manteca (Eds.). Broiler Chickens Welfare in Practice (pp. 65-86). 5m Books Ltd. Essex.

Bloch, V., Barchilon, N., Halachmi, I., & Druyan, S. (2020). Automatic broiler temperature measuring by thermal camera. Biosystems Engineering, 199, 127-134. https://doi.org/10.1016/j.biosystemseng.2019.08.011

Caldara, F.R., dos Santos, L.S., Machado, S.T., Moi, M., Nääs, I.A., Foppa, L., Garcia, R.G., & dos Santos, R.K.S. (2014). Piglets' surface temperature change at different weights at birth. Asian-Australasian Journal of Animal Sciences, 27(3), 431-438. https://doi.org/10.5713/ajas.2013.13505

Cândido, M.G.L., Tinôco, I.F.F., Albino, L.F.T., Freitas, L.C.S.R., Santos, T.C., Cecon, P.R., & Gates, R.S. (2020). Effects of heat stress on pullet cloacal and body temperature. Poultry Science, 99(5), 2469-2477. https://doi.org/10.1016/j.psj.2019.11.062

Cangar, O., Aerts, J.M., Buyse, J., & Berckmans, D. (2008). Quantification of the spatial distribution of surface temperatures of broilers. Poultry Science, 87, 2493-2499. https://doi.org/10.3382/ps.2007-00326

Castro, J.O., Yanagi Junior, T., Abreu, A.L., Ferraz, P.F.P., Moura, G.B., Cecchin, D., & Conti, L. (2019). Use of thermography for the evaluation of the surface temperature of Japanese quail submitted at different temperatures. Agronomy Research, 17(4), 1560-1567. https://doi.org/10.15159/ar.19.141

Damane, M.M., Barazandeh, A., Sattaei, M., Mokhtari, S., Esmaeilipour, O., & Badakhshan, Y. (2018). Evaluation of body surface temperature in broiler chickens during the rearing period based on age, air temperature and feather condition. Iranian Journal of Applied Animal Science, 8(3), 499-504.

EU (2007). "EU Council Directive 2007/43/EC of 28 June 2007 laying down minimum rules for the protection of chickens kept for meat production." Official Journal of the European Union, Luxembourg. http://data.europa.eu/eli/dir/2007/43/oj

Ferreira, V.M.O.S., Francisco, N.S., Belloni, M., Aguirre, G.M.Z., Caldara, F.R., Nääs, I.A., Garcia, R.G., Almeida Paz,

I.C.L., & Polycarpo, G.V. (2011). Infrared thermography applied to the evaluation of metabolic heat loss of chicks fed with different energy densities. Brazilian Journal of Poultry Science, 13(2), 113-118. https://doi.org/10.1590/S1516-635X2011000200005

Giloh, M., Shinder, D., & Yahav, S. (2012). Skin surface temperature of broiler chickens is correlated to body core temperature and is indicative of their thermoregulatory status. Poultry Science, 91, 175-88. https://doi.org/10.3382/ps.2011-01497

Jacob, F.G., Baracho, M.D.S., Nääs, I.A., Souza, R., & Salgado, D.D.A. (2016). The use of infrared thermography in the identification of pododermatitis in broilers. Journal of the Brazilian Association of Agricultural Engineering, 36, 253-259. https://doi.org/10.1590/1809-4430-Eng.Agric.v36n2p253-259/2016

Kim, N.Y., Kim, S.J., Oh, M., Jang, S.Y., & Moon, S.H. (2021). Changes in facial surface temperature of laying hens under different thermal conditions. Animal Bioscience, 34(7), 1235-1242. https://doi.org/10.5713/ab.20.0647

Leeson, S., & Walsh, T. (2004). Feathering in commercial poultry I. Feather growth and composition. World's Poultry Science Journal, 60(1), 42-51. https://doi.org/10.1079/WPS20033

McManus, C., Tanure, C.B., Peripolli, V., Seixas, L., Fischer, V., Gabbi, A.M., Menegassi, S.R.O., Stumpf, M.T., Kolling, G.J., Dias, E., & Costa, J.B.G. (2016). Infrared thermography in animal production: an overview. Computers and Electronics in Agriculture, 123, 10-16. https://doi.org/10.1016/j.compag.2016.01.027

Nääs, I.A., Romanini, C.E.B., Neves, D.P., Nascimento, G.R., & Vercellino, R.A. (2010). Broiler surface temperature distribution of 42 day old chickens. Scientia Agricola, 67(5), 497-502. https://doi.org/10.1590/S0103-90162010000500001

Nääs, I.A., Garcia, R.G., & Caldara, F.R. (2014). Infrared thermal image for assessing animal health and welfare. Journal of Animal Behaviour and Biometeorology, 2(3), 66-72.

Nascimento, S.T., da Silva, I.J.O., Maia, A.S.C., de Castro, A.C., & Vieira, F.M.C. (2014). Mean surface temperature prediction models for broiler chickens-a study of sensible heat flow. International Journal of Biometeorology, 58, 195-201. https://doi.org/10.1007/s00484-013-0702-7

Nascimento, S.T., Maia, A.S.C., Gebremedhin, K.G., & Nascimento, C.C.N. Metabolic heat production and evaporation of poultry. Poultry Science, 96(8), 2691-2698. https://doi.org/10.3382/ps/pex094

Nikkhah, A., Plaizier, J.C., Einarson, M.S., Berry, R.J., Scott, S.L., & Kennedy, A.D. (2005). Infrared thermography and visual examination of hooves of dairy cows in two stages of lactation. Journal of Dairy Science, 88(8), 2749-2753. https://doi.org/10.3168/jds.S0022-0302(05)72954-4

Schaefer, A.L., Cook, N.J., Bench, C., Chabot, J.B., Colyn, J., Liu, T., Okine, E.K., Stewart, M., & Webster, J.R. (2012). The non-invasive and automated detection of bovine respiratory disease onset on receiver calves using infrared thermography. Research in Veterinary Science, 93(2), 928-935. https://doi.org/10.1016/j.rvsc.2011.09.021

Shinder, D., Rusal, M., Tanny, J., Druyan, S. & Yahav, S. (2007). Thermoregulatory response of chicks (*Gallus domesticus*) to low ambient temperatures at an early age. Poultry Science, 86(10), 2200-2209. https://doi.org/10.1093/ps/86.10.2200

Steenfeldt, S., Sørensen, P., & Nielsen, B.L. (2019). Effects of choice feeding and lower ambient temperature on feed intake, growth, foot health, and panting of fast- and slow-growing broiler strains. Poultry Science, 98(2), 503-513. http://dx.doi.org/10.3382/ps/pey323

Stewart, M., Stafford, K.J., Dowling, S.K., Schaefer, A.L., & Webster, J.R. (2008). Eye temperature and heart rate variability of calves disbudded with or without local anaesthetic. Physiology & Behavior, 93(4-5), 789-797. https://doi.org/10.1016/j.physbeh.2007.11.044

Tessier, M., Du Tremblay, D., Klopfenstein, C., Beauchamp, G., & Boulianne, M. (2003). Abdominal skin temperature variation in healthy broiler chickens as determined by thermography. Poultry Science, 82(5), 846-849. https://doi.org/10.1093/ps/82.5.846

Tickle, P.G., & Codd, J.R. (2019). Thermoregulation in rapid growing broiler chickens is compromised by constraints on radiative and convective cooling performance. Journal of Thermal Biology, 79, 8-14. https://doi.org/10.1016/j.jtherbio.2018.11.007

Torrey, S., Mohammadigheisar, M., dos Santos, M.N., Rothschild, D., Dawson, L.C., Liu, Z., Kiarie, E.G., Edwards, A.M., Mandell, I., Karrow, N., Tulpan, D., & Widowski, T.M. (2021). In pursuit of a better broiler: growth, efficiency, and mortality of 16 strains of broiler chickens. Poultry Science, 100(3), 100955. https://doi.org/10.1016/J.PSJ. 2020.12.052

Warriss, P.D., Pope, S.J., Brown, S.N., Wilkins, L.J., & Knowles, T.G. (2006). Estimating the body temperature of groups of pigs by thermal imaging. Veterinary Record, 158(10), 331-334. https://doi.org/10.1136/vr.158.10.331

Wecke, C., Khan, D.R., Sùnder, A., & Liebert, F. (2017). Age and gender depending growth of feathers and feather-free body in modern fast growing meat-type chickens. Open Journal of Animal Sciences, 7, 376-392. https://doi.org/10.4236/ojas.2017.74029

Weimer, S.L., Wideman, R.F., Scanes, C.G., Mauromoustakos, A., Christensen, K.D., & Vizzier-Thaxton, Y. (2019). The utility of infrared thermography for evaluating lameness attributable to bacterial chondronecrosis with osteomyelitis. Poultry Science, 98(4), 1575-1588. http://dx.doi.org/10.3382/ps/pey538

Weimer, S.L., Wideman, R.F., Scanes, C.G., Mauromoustakos, A., Christensen, K.D., & Vizzier-Thaxton, Y. (2020). Broiler stress responses to light intensity, flooring type, and leg weakness as assessed by heterophil-to-lymphocyte ratios, se-

rum corticosterone, infrared thermography, and latency to lie. Poultry Science, 99(7), 3301-3311. https://doi.org/10.1016/j.psj.2020.03.028

Wilcox, C.H., Sandilands, V., Mayasari, N., Asmara, I.Y., & Anang, A. (2024). A literature review of broiler chicken welfare, husbandry, and assessment. World's Poultry Science Journal, 80(1), 3-32. https://doi.org/10.1080/00439339.2023.2264824

Yahav, S., & Giloh, M. (2012). Infrared thermography-Applications in poultry biological research. In: Prakash RV (Ed). Infrared Thermography. (pp. 93-116). IntechOpen.

Yalcin, S., Settar, P., Ozkan, S., & Cahaner, A. (1997). Comparative evaluation of three commercial broiler stocks in hot versus temperate climates. Poultry Science, 76(7), 921-929. https://doi.org/10.1093/ps/76.7.921

Medit Vet J, 9(3): 403-409, 2024
DOI: 10.24880/meditvetj.1561120

Research Article

Pathomorphological approach on canine sebaceous tumors

Gözde Yücel Tenekeci[1], Arda Selin Tunç[1], Oya Burçin Demirtaş[1]

[1]Department of Pathology, Faculty of Veterinery Medicine, Ankara University, Ankara, Türkiye

Key Words:
canine
epithelioma
Ki-67
malignancy
sebaceous tumors

Received : 4 October 2024
Revised : 20 November2024
Accepted : 22 November 2024
Published : 31 December 2024
Article Code : 1561120

Correspondence:
G. YÜCEL TENEKECİ
(gozdeyucel@gmail.com)

ORCID
G. YÜCEL TENEKECİ : 0000-0002-2586-8346
AS. TUNÇ : 0000-0002-4813-7626
OB. DEMİRTAŞ : 0000-0003-0850-2374

ABSTRACT

Sebaceous neoplasms are among the most frequently observed skin tumors in dogs. The histological classification of sebaceous glands (including Meibomian glands) is based on the sebocyte and basaloid reserve cell components. In this study aiming to examine sebaceous tumors in detail, 28 biopsies diagnosed with sebaceous neoplasia, including Meibomian gland neoplasia, were examined and diagnosed as adenoma (n:9), epithelioma (n:12), and carcinoma (n:7). Histopathologically; cell ratios (sebaceous/basal), appearance (diffuse/multilobular), presence of ulcers, necrosis, inflammation, pleomorphism and mitosis were evaluated. Ki-67 biomarker was used immunohistochemically to assess cell division. Based on histopathological and immunohistochemical examinations, it was determined that epitheliomas would rather be classified as low-grade malignancies due to their noticeable mitotic activity and should be investigated in more detail.

INTRODUCTION

Sebaceous gland tumors originate from the sebaceous glands in dermis and are among the most frequently observed tumors of dogs. They represent the third most common type of skin tumors, accounting for 22-35% of all cutaneous epithelial tumors (Vail and Withrow, 2007). They are classified as sebaceous adenoma, sebaceous ductal adenoma, sebaceous epithelioma, and sebaceous carcinoma according to their histological appearances. In adenomas, the main tumor cells are sebocytes with fewer (>50%) basaloid reserve cells and a multilobulated appearance. In sebaceous ductal adenomas, many keratinized ducts and few sebocytes and basaloid cells are seen. Sebaceous epitheliomas are characterized by a dominant population of basaloid reserve cells with few sebocytes and ducts. This type is considered a low-grade malignancy tumor, with a high mitotic activity and minimal pleomorphism. On the other hand, carcinomas consist of sebocytes showing pleomorphism with few reserve cells and ducts and a multilobulated appearance (Hendrick, 2016; Goldschmidt and Goldschmidt, 2017).

Meibomian neoplasms arise from the tarsal glands on the inner eyelid. These glands are modified sebaceous glands and classification of their tumors is similar to sebaceous neoplasms (Goldschmidt and Goldschmidt, 2017).

Histopathological features and particularly the epithelial cell ratio (sebaceous/basaloid) are of non-negligable importance for classification of sebaceous and meibomian gland tumors. Besides, circumscription, ulcer, necrosis, inflammation, pleomorphism and mitosis are considered (Costa et al., 2020).

Ki-67 is the most commonly used marker to assess proliferation in tumors. MKI67 is a protein expressed in all nuclei during the active phases of the cell cycle. Ki-67 is used to detect MKI67. It is stated that the higher Ki-67 ratio a tumor shows, the more malignant characteristics it has. (Scholzen and Gerdes, 2000; Sun and Kaufman, 2018).

In this study, 28 cases from 25 dogs submitted to our department and diagnosed with sebaceous and meibomian gland tumors were examined, with detailed evaluation of histopathological features and cell proliferation using Ki-67.

MATERIALS and METHODS

Sections were taken from paraffin blocks prepared from 28 biopsies in total, that were brought from the animal hospital of the faculty and private clinics. Hematoxylen-Eosin (HE) and trichrome stainings were performed and epithelial cell ratio (sebaceous/basaloid), diffuse/multilobular presentation, ulcer, necrosis, presence of inflammation, pleomorphism and mitosis were evaluated.

Immunohistochemically, sections taken on adhesive (3 aminopropyltriethoxysilane [APES]) slides were treated according to the kit procedure with avidine-biotine peroxidase method. For antigen rectrieval, boiling Citrate Buffer was used in steamer for 20 minutes. Anti-ki67 (1:100) (ThermoScientific,

To cite this article:
Yücel Tenekeci G, Tunç AS, Demirtaş OB. Pathomorphological approach on canine sebaceous tumors. Medit Vet J. 2024; 9(3): 403-409.

SP6) was incubated at 37°C for 1 hour. AEC was used as chromogen, and Mayer's Hematoxylin was used for couterstaining. Nuclear positive stainings were evaluated under the light microscope.

Nuclear pleomorphism (graded as 0,1,2,3 respectively), mitotic index (graded as -, +,++,+++ respectively) and Ki-67 (graded as +,++,+++ respectively) were assessed semi-quantitatively under x400 magnification.

RESULTS

In the study, sebaceous/meibomian tumors were most commonly observed in the following breeds: Cocker spaniel (n:6), Golden Retriever (n:5), Labrador retriever (n:2), Terrier (n:2), mixed breeds (n:2), Alaska malamute (n:1), German Shepherd (n:1), and Siberian Husky (n:1). Breed information was not available for five dogs. Sebaceous/meibomian tumors were observed in dogs aged between 2 and 16 years, with an average age of 9.6 years. Twenty-eight cases were observed in 25 animals (tumors occurred in two different locations in three animals). Of these, 15 were male, 8 were female, and gender information was not provided for two. Twenty-one of 28 tumors were located on the head and neck with 14 occuring on and around the eye and 10 of them being meibomian tumors. Of the remaining 7 head-neck located tumors, 4 were on the ear region. Information about the animals, biopsies and diagnoses are given in Table 1.

Biopsies taken from the eye and the skin were evaluated together with the prefix meibomian- used for tumors originating from the eye glands, and sebaceous- used for the tumors originating from the fat glands (including periorbital region).

Table 1. Breed, gender, age, localization and diagnostic data of the cases.

Case number	Dog data	Mass data	Diagnose
1.	Alaskan malamute, Male, 8 years old	Under left eye	Sebaceous carcinoma
2.	*No information*, Male, 14 years old	Right cheek Right ear canal entrance	Sebaceous epithelioma Sebaceous epithelioma
3.	*No information*, Female, 13 years old	Behind right ear	Sebaceous epithelioma
4.	*No information*, Male, No information	No information	Sebaceous gland adenoma
5.	*No information*, Female, 10 years old	Eye	Meibomian epithelioma
6.	Golden retriever, Male, 10 years old	Left eyelid	Meibomian adenoma
7.	*No information*, Male, 7 years old	Right eyelid	Sebaceous carcinoma
8.	Cocker Spaniel, Female, 12 years old	Foot	Sebaceous gland adenoma
9.	Terrier, Female, 16 years old	Forehead	Sebaceous epithelioma
10.	Labrador retriever, Male, 10 years old	Lower eyelid	Meibomian epithelioma
11.	Golden retriever, Male, 10 years old	Left upper eyelid	Meibomian adenoma
12.	Golden retriever, D, 10 years old	Upper eyelid	Sebaceous carcinoma
13.	German shepherd, Male, 2 years old	Eyelid	Sebaceous carcinoma
14.	Cocker Spaniel, Female, 12 years old	Corner of eye Ear	Meibomian epithelioma Sebaceous epithelioma
15.	Melez, Male, 6 years old	Skin	Sebaceous gland adenoma
16.	Cocker Spaniel, Male, 10 years old	Ear	Sebaceous epithelioma
17.	Golden retriever, Male, 10 years old	Eye	Sebaceous gland adenoma
18.	Melez, *No information*, 3 years old	Nape	Sebaceous carcinoma
19.	Siberian Husky, Male, 10 years old	Right eyelid	Meibomian carcinoma
20.	Cocker Spaniel, Male, 9 years old	Left eyelid	Meibomian carcinoma
21.	Terrier, Female, 10 years old	Fossa paralumbalis	Sebaceous gland adenoma
22.	Cocker Spaniel, Female, 11 years old	Skin	Sebaceous gland adenoma
23.	Cocker Spaniel, Male, 8 years old	Skin Eye	Sebaceous gland adenoma- Meibomian epithelioma
24.	Labrador retriever, Male, 9 years old	Eyelid	Meibomian epiteliyoma
25.	Golden retriever, Female, 11 years old	Eye corner	Meibomian epithelioma

Among the 28 biopsies examined, 9 were adenomas, 12 were epitheliomas, and 7 were carcinomas. In aminals with tumors in two different regions, two dogs had the same diagnosis for both tumors, while one had epithelioma on the eye and ademona on the body.

In histopathological evaluation; based on the sebaceous/basal epithelium ratio, 5 of the sebaceous/meibomian adenomas (55.5%) were graded as 3/1, while 4 (44,4%) were graded as 3/0 (Figure 1). All of the epitheliomas except for one (n:11, 91,6%) had an epithelial ratio of 1/3 (Figure 2 and Figure 3). The ratio was 1/2 in one case (8.3%). Among carcinomas, all but one had a ratio of 3/1 (n: 6, 85.7%), (Figure 4) while one case (%14.2) had the ratio of 2/2.

When pleomorphism was considered,6 of the adenomas (n=9) 6 (66.6%) had the score of 0, and 3 (50%) had the score of 1. The score was 0 in only one of the epithelioma cases (n=12) (8.33%), while the score was 1 in 8 (66.6%) cases (Figure 2), and 2 in 3 (25%) cases (Figure 3). Six of the carcinomas (n=7) (85.7%) scored 2, while one case scored 3 (14.2%).

Cells had a multilobular pattern in all the adenomas except for one (n=8), which had a diffuse pattern. Nine of the epitheliomas presented a multilobular pattern (Figure 2 and Figure 3) while 3 had a diffuse pattern (Figure 4). Neoplastic cells presented a diffuse pattern in all cases with carcinoma (n=7).

In terms of cyst formation, 4 of the adenomas, 11 of the epitheliomas and 4 of the carcinomas had cysts. Ulceration was reported in 3 adenomas, 6 epitheliomas, and 4 carcinomas. Only one adenoma, 7 epitheliomas and 5 carcinomas had necrosis. All cases with necrosis were accompanied by ulceration and inflammation. Regardless of classification, most cases (22/28) showed inflammatory changes. Among these inflammations, neutrophils were predominant in the areas of ulceration and necrosis, while interstitial sites in tumoral region mostly contained mononuclear cells. Hemorrhage was seen in 12 cases (adenoma:1, epithelioma:7, carcinoma:4). Histopathological evaluations are given in Table 2.

Histopathologically, mitotic activity was severe (+++) (Figure 2 and Figure 3) in epithelioma, intermediate (++) in carcinoma, and rarely seen in adenomas.

Immunohistochemically, Ki-67 was moderatly positive (++) in epithelioma and carcinoma, while it was mild (+) in adenomas. (Figure 5).

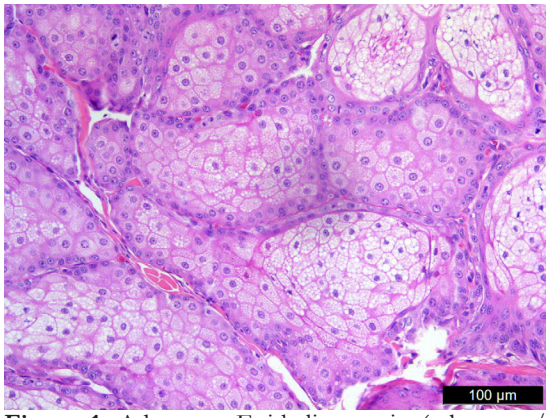

Figure 1. Adenoma. Epithelium ratio (sebaceous/basaloid): 3/0 multilobular appearance, HE.

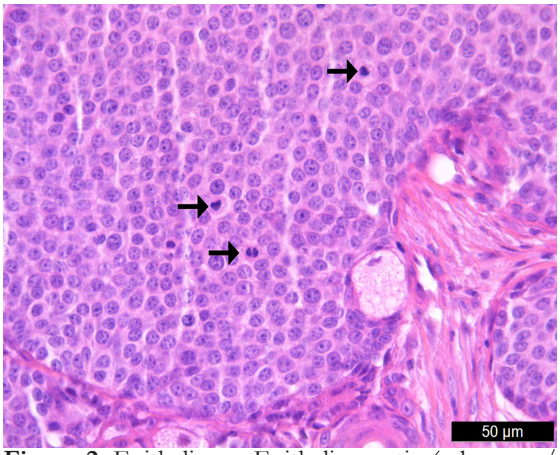

Figure 2. Epithelioma. Epithelium ratio (sebaceous/basaloid): 1/3, Nuclear pleomorphism:1, multilobular appearance, mitotic figures (+++) (arrows), HE.

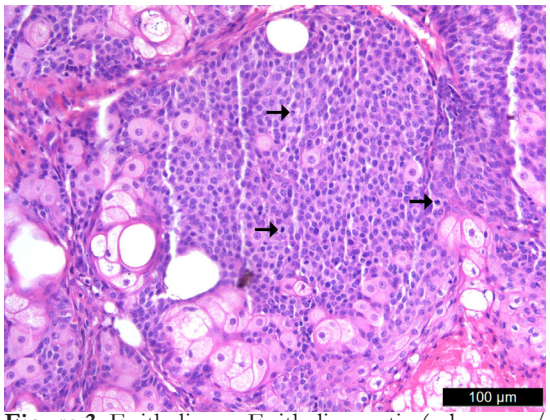

Figure 3. Epithelioma. Epithelium ratio (sebaceous/basaloid): 1/3, Nuclear pleomorphism:2, multilobular appearance, mitotic figures (+++) (arrows), HE.

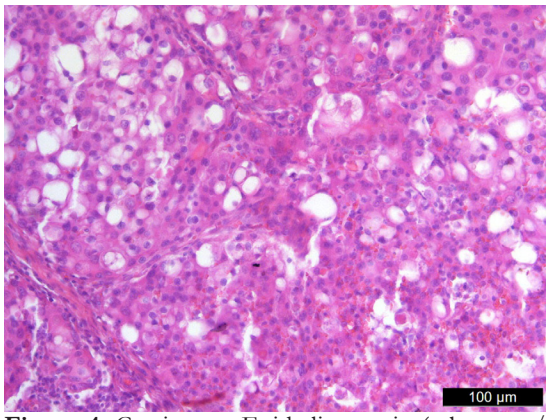

Figure 4. Carcinoma. Epithelium ratio (sebaceous/basaloid): 3/1, diffuse appearance, HE.

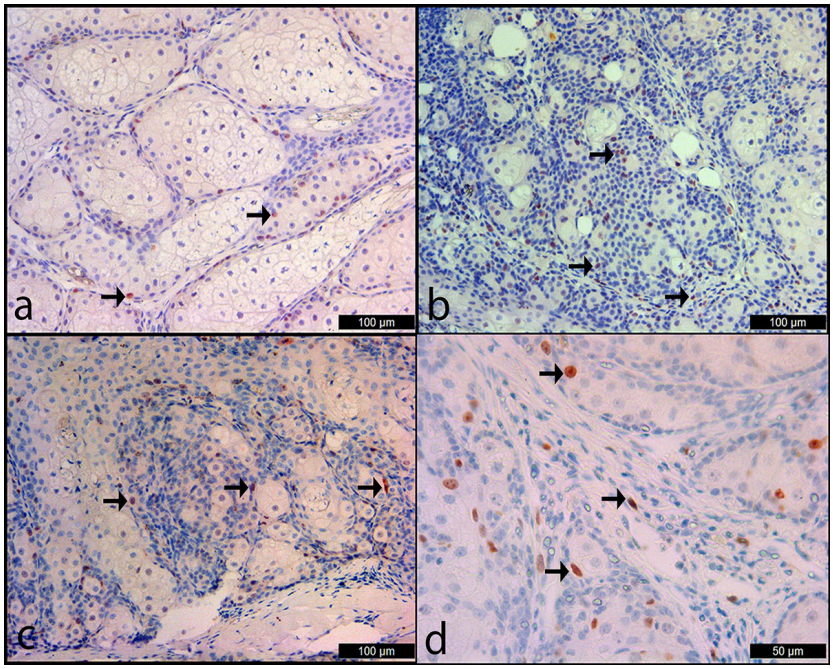

Figure 5. Immunohistochemical grading of sebaceous gland tumors for Ki-67 marker. Nuclear positivities (arrows), a) Adenoma (+), b) epithelioma (++) and c,d) carcinoma (++).

Table 2. Evaluation of criteria used in histopathological examination of the sebaceous tumors according to the cases.

No	Epithelium ratio (sebaceous/basal)	Nuclear pleomorphism (0, 1, 2, 3)	Diffuse (D) / Multilobular (ML)	Cyst(Yes/No)	Ulceration (Yes/No)	Necrosis (Yes/No)	İnflammation (Yes/No)	Hemorrhage (Yes/No)	Diagnose
1.	3/1	2	D	+	+	+	+	+	Sebaceous carcinoma
2.	1/3	0	ML	+	+	+	+	+	Sebaceous epithelioma
	1/3	2	ML	+	+	+	+	+	Sebaceous epithelioma
3.	1/3	2	ML	+	+	+	+	+	Sebaceous epithelioma
4.	3/0	0	ML	+	-	-	+	-	Sebaceous gland adenoma
5.	1/2	1	ML	-	-	-	+	-	Meibomian epithelioma
6.	3/0	1	ML	-	-	-	+	+	Meibomian adenoma
7.	2/2	2	D	+	-	-	-	-	Sebaceous carcinoma
8.	3/0	0	ML	+	+	+	+	-	Sebaceous gland adenoma
9.	1/3	2	ML	+	+	+	+	+	Sebaceous epithelioma
10.	1/3	1	ML	+	-	-	+	-	Meibomian epithelioma
11.	3/1	1	D	+	-	-	+	-	Meibomian adenoma
12.	3/1	3	D	+	+	+	+	+	Sebaceous carcinoma
13.	3/1	2	D	-	+	+	+	-	Sebaceous carcinoma
14.	1/3	1	ML	+	+	+	+	-	Meibomian epithelioma
	1/3	1	ML	+	+	+	+	-	Sebaceous epithelioma
15.	3/1	0	ML	-	-	-	-	-	Sebaceous gland adenoma
16.	1/3	1	ML	+	+	+	+	+	Sebaceous epithelioma
17.	3/1	1	ML	-	-	-	-	-	Sebaceous gland adenoma
18.	3/1	2	D	-	+	+	+	+	Sebaceous carcinoma
19.	3/1	2	D	-	+	+	+	+	Meibomian carcinoma
20.	3/1	2	D	+	-	-	+	-	Meibomian carcinoma
21.	3/0	0	ML	-	+	-	+	-	Sebaceous gland adenoma
22.	3/1	0	ML	+	+	-	+	-	Sebaceous gland adenoma
23.	3/1	0	ML	-	-	-	-	-	Sebaceous gland adenoma
	1/3	1	D	+	-	-	+	+	Meibomian epithelioma
24.	1/3	1	D	+	-	-	-	+	Meibomian epithelioma
25.	1/3	1	D	+	-	-	-	-	Meibomian epithelioma

DISCUSSION

Twenty-eight biopsy samples taken from 25 dogs in total were evaluated in this study. Cocker Spaniel is one of the breeds in which sebaceous tumors are frequently seen,as reflected in our findings. In terms of age, especially with epitheliomas being reported in dogs over 9-10 years of age, our results are consistent with previous literature (Goldschmidt and Goldschmidt, 2017). Although no general gender predisposition was previously stated, it drew attention that the tumors were mostly seen in male animals in our study. While tumor classification was made into 4 groups (sebaceous adenoma, sebaceous ductal adenoma, sebaceous epithelioma, and sebaceous carcinoma) (Goldschmidt and Goldschmidt, 2017), no ductal adenomas were encountered. Same classification was used for Meibomian gland tumors.

Sebaceous adenomas are known to be well-circumscribed nodules and are composed of large amount of typical and uniform sebaceous cells (Goldschmidt and Goldschmidt, 2017). Sebaceous carcinomas are poorly circumscribed nodules composed of large amount of atypical and pleomorphic sebaceous cells. These tumors are distinguishable by the lack of significant numbers of basaloid reserve cells (Goldschmidt and Goldschmidt, 2017). Sebaceous epitheliomas are identified by their predominant population of reserve cells, with small numbers of sebocytes (Goldschmidt and Goldschmidt, 2017). Consistent with previous research, adenomas were well-circumscribed and had a nodular/multi-nodular pattern while carcinomas mainly had a diffuse pattern. In the detailed evaluation of tumor components, the sebaceous-to-basaloid epithelium ratios were examined. The highest ratios were reported for adenomas, epitheliomas and carcinomas with 80% (3:1), 100% (1:3), and 66.7% (2:2) respectively. In a similar study by Costa et al. (2020), the ratios were reported as 55.5% (3:1) for adenoma, 91.6% (1:3) for epithelioma, and 85.7% (3:1) for carcinoma. These findings suggest that carcinomas have a notably higher ratio of sebaceous epithelium.

Necrosis is a well-known criterion to evaluate whether tumors are aggresive and fast-growing (Proskuryakov and Gabai, 2000). Inflammation can also accompany necrosis. In our study both criteria correlated with malignancy of the tumors. The presence of these histopathological criteria in epitheliomas similarly to carcinomas highlights the malignancy potential of epitheliomas as well. .

Regarding pleomorphism, parallel to a similar study (Costa et al, 2020), intermediate pleomorphism (score1 and 2) was prominent in epitheliomas. On the other hand, the presence of only one carcinoma with a pleomorphism score of 3 (the highest) drew our attention.

One of the most important malignancy criteria for tumors is without a doubt the histopathological evaluation of the mitotic activity as a high mitotic index is characteristic of malignant tumors (De Las Mulas et al, 1999; Bertram et al, 2024). In our study, mitotic activity was found to be higher in epitheliomas than in carcinomas. Ki-67 protein comes forth while evaluating the cell division phases (Gerdes et al, 1983; Scholzen and Gerdes, 2000). This protein is only expressed in the growing and dividing phases (G1, S, G2, and M) but not in the resting phase (G0). That is why Ki-67 is a good marker for aggressively proliferating tumor cells (Starborg et al, 1996; Li et al, 2015). Our data suggest that, both epithelioma and carcinoma had moderate ki-67 expression. The conventional criteria for differentiating sebaceous adenoma from epithelioma are not appropriate. Similarly, a study by Keleş et al. (2024) on dogs showed that epitheliomas are potentially malignant. Kim et al. (2024) have also named epithelioma as carcinoma.

CONCLUSION

As a result, prominent changes in subtypes were revealed through detailed histopathological examinations. Furthermore, we suggest that the prognosis of epitheliomas should be examined in more detail due to the fact that they are a frequently observed tumor with low-grade malignancy. Given the findings on low-grade malignancy potential in epitheliomas, future prognostic studies specifically targeting these tumor types would be beneficial.

DECLARATIONS

Ethics Approval

Not applicable.

Conflict of Interest

The authors stated that they have no conflict of interest.

Consent for Publication

Not applicable.

Author contribution

Idea, concept and design: GYT

Data collection and analysis: GYT, AST, OBD

Drafting of the manuscript: GYT, AST, OBD

Critical review: GYT, AST

Data Availability

Not applicable

Acknowledgements

We would like to thank the members of the Pathology Department for their contributions to the diagnosis of sebaceous gland tumors and the faculty hospital and private institutions for the supply of materials.

REFERENCES

Bertram, C. A., Donovan, T. A., & Bartel, A. (2024). Mitotic activity: A systematic literature review of the assessment methodology and prognostic value in canine tumors. Veterinary pathology, 27;61(5):752–764. https://doi.org/10.1177/03009858241239565

Costa, F. B., da Silva, K. V. G. C., da Silva Leite, J., Silva, F. B. F., dos Santos Batista, B. P., de Melo, J. F., & Ferreira, A. M. R. (2020). Histopathological study of canine sebaceous tumors and their association with PCNA expression by immunohistochemistry. Revista Brasileira de Ciência Veterinária, 27(3). https://doi.org/10.4322/rbcv.2020.027

De Las Mulas, J. M., Millan, Y., Ruiz-Villamor, E., Bautista, M. J., Rollon, E., & De Los Monteros, A. E. (1999). Apoptosis and mitosis in tumours of the skin and subcutaneous tissues of the dog. Research in veterinary science, 66(2), 139-146. https://doi.org/10.1053/rvsc.1998.0260

Gerdes, J., Schwab, U., Lemke, H., & Stein, H. (1983). Production of a mouse monoclonal antibody reactive with a human nuclear antigen associated with cell proliferation. International journal of cancer, 31(1), 13-20. https://doi.org/10.1002/ijc.2910310104

Goldschmidt M.H., Goldschmidt K.H. (2017). Epithelial and Melanocytic Tumors of the Skin. In: D. J. Meuten (Ed.). Tumors in Domestic Animals (pp. 88-141). Iowa State Press. https://doi.org/10.1002/9781119181200.ch4

Hendrick, M.J. (2016). Mesenchymal tumors of the skin and soft tissues. Tumors in domestic animals (pp. 142-175). https://doi.org/10.1002/9781119181200.ch5

Keleş, Ö. F., Kuşçu, Y., Kayıkçı, C., & Çiçek, H. A. (2024). Sebaceous gland epithelioma with potential malignancy in a dog. Mediterranean Veterinary Journal, 9(2), 333-336. https://doi.org/10.24880/meditvetj.1541593

Kim, S., Chaudhary, P. K., Upadhayaya, S., Seo, K. W., & Kim, S. (2024). Histopathological and Immunohistochemical Characterization of Sebaceous Adenoma and Epithelioma in Dogs. Animals, 14(10), 1457. https://doi.org/10.3390/ani14101457

Li, L. T., Jiang, G., Chen, Q., & Zheng, J. N. (2015). Ki67 is a promising molecular target in the diagnosis of cancer. Molecular medicine reports, 11(3), 1566-1572. https://doi.org/10.3892/mmr.2014.2914

Proskuryakov, S. Y., & Gabai, V. L. (2010). Mechanisms of tumor cell necrosis. Current pharmaceutical design, 16(1), 56-68. https://doi.org/10.2174/138161210789941793

Scholzen, T., & Gerdes, J. (2000). The Ki□ 67 protein: from the known and the unknown. Journal of cellular physiology, 182(3), 311-322. https://doi.org/10.1002/(SICI)1097-4652

Starborg, M., Gell, K., Brundell, E., & Höög, C. (1996). The murine Ki-67 cell proliferation antigen accumulates in the nucleolar and heterochromatic regions of interphase cells and at the periphery of the mitotic chromosomes in a process essential for cell cycle progression. Journal of cell science, 109(1), 143-153. https://doi.org/10.1242/jcs.109.1.143

Sun, X., & Kaufman, P. D. (2018). Ki-67: more than a proliferation marker. Chromosoma, 127, 175-186. https://doi.org/10.1007/s00412-018-0659-8

Vail, D. M., & Withrow, S. J. (2007). Tumors of the skin and subcutaneous tissues. Withrow, SJ; Macewen, EG Small animal clinical oncology, 4, 375-401.